PhD Thesis

Design and Synthesis of Biomolecular Amphiphiles for Effective and Stimuli Responsive Delivery of Anti-Tumor Agents

A Dissertation
Submitted in partial fulfilment of the
Requirements for the Degree of
Doctor of Philosophy

by

Soumi Das

Department of Chemistry
Indian Institute of Technology Guwahati
Guwahati-781039
Assam

August 2019

Dedicated

to

My Family

INDIAN INSTITUTE OF TECHNOLOGY GUWAHATI

Department of Chemistry

Statement

This thesis entitled **"Design and Synthesis of Biomolecular Amphiphiles for Effective and Stimuli Responsive Delivery of Anti-Tumor Agents"** is a work of research and investigation carried out by me under the supervision of Dr. Lal Mohan Kundu, Associate Professor, Department of Chemistry, Indian Institute of Technology Guwahati. This thesis has been submitted by me to the Department of Chemistry, Indian Institute of Technology Guwahati for the award of the degree of Doctor of Philosophy. I further declare that this work has not been submitted anywhere else for any degree, diploma, associateship or membership etc. of any Institute or University to the best of my knowledge.

_____

Soumi Das
Roll No: 146122025
Department of Chemistry
IIT Guwahati,
Guwahati-781039, Assam
India
Date:
Place: Guwahati, Assam

INDIAN INSTITUTE OF TECHNOLOGY GUWAHATI

Department of Chemistry

Certificate

It is certified that the thesis entitled **"Design and Synthesis of Biomolecular Amphiphiles for Effective and Stimuli Responsive Delivery of Anti-Tumor Agents"** being submitted to the Indian Institute of Technology Guwahati by Soumi Das (Roll. No. 146122025) for the award of the degree of Doctor of Philosophy in Chemistry, is a bonafide record of research work carried out by her. The information and data reported by her are solely the results of her original findings. She has diligently carried out the investigations and followed the guidelines of the laboratory. This work has not been submitted elsewhere for any degree or diploma.

_____

Dr. Lal Mohan Kundu
Thesis Supervisor
Associate Professor,
Department of Chemistry,
IIT Guwahati,
Guwahati-781039, Assam,
India.
Date:
Place: Guwahati, Assam

Acknowledgements

My Ph.D endeavour will remain incomplete without acknowledging the contributions of few people. First and foremost, it is a genuine pleasure to convey my heartfelt gratitude to Dr. Lal Mohan Kundu, my phD supervisor who not only introduced me to the splendid world of Science but also enlighten me with his precious guidance and expert advice to pursue scientific goals. Along with his precious counsel, his continuous motivation and support also helped me to grow further. I am fortunate enough to have him as my mentor and be a part of his vibrant research group. Thank you Sir.

Besides my advisor, I would also like to thank my doctoral committee members Dr. Bhubaneshwar Mondal, Prof. Gopal Das and Dr. A. S. Achalkumar for their continuous encouragement and valuable suggestions regarding my research works. Also, I would like to express my deep sense of thanks to all the faculty and staff members of Department of Chemistry and CIF for their continuous assistance.

In this note of acknowledgement, IIT Guwahati will certainly be a special mention for providing me the scholarship and a healthy atmosphere. For all the instrumental facilities required for my research work, I am truly thankful to Department of Chemistry and CIF (IIT Guwahati)

I would like to express my sincere to all my collaborators for their support and valuable discussions. I would also like to acknowledge all my past and present lab members including Dr. Laxman Burgulla, Dr. K. Radhakrishnan, Ms Kameli Gogoi, Ms. Nibedita Ghosh, Ms. Himali Horo and Mr. Gourav Bhattacharya for their cooperation and providing a friendly atmosphere in the lab. My special acknowledgement will be for Dr. Upasi Goswami, Mr. Kamlesh verma and Mr. Krishan Kumar Thakur for their assistance in biological evaluation of my works.

Next, I extend my sincere thanks to all of my friends inside and outside IITG for their constant support and encouragement.

Finally, I want to thank my parents (Mr. Narayan Chandra Das and Mrs. Gouri Das), my brother Shouvik Das and specially Dr. Subhankar Panda for their endless support, tolerance and unconditional love and care.

Thanks for being in my life

Soumi

Table of Contents

Abbreviation

WHO	World Health Organisation
DNA	Deoxyribonucleic acid
5-Fu	5-Fluorouracil
FdUMP	Fluorodeoxyuridine monophosphate
TS	Thymidylate synthase
FdUTP	Fluorodeoxyuridine triphosphate
FUTP	Fluorouridine triphosphate
RNA	Ribonucleic acid
5-FuH_2	5,6-dihydro-5-fluorouracil
DPD	Dihydropyrimidine dehydrogenase
DDS	Drug delivery system
siRNA	Small interfering RNA
CRS	Controlled release systems
EPR	Enhanced permeability retention
PEG	Polyethylene glycol
mAb	Monoclonal antibody
ADC	Antibody drug conjugate
DOX	Doxorubicin
NHL	Non-Hodgkin's lymphoma
PEM	Polymorphic epithelial mucin
FDA	Food and Drug Administration
ApDC	Aptamer drug conjugates
PTK7	Protein-tyrosine kinase-7
PSMA	Prostate-specific membrane antigen
HER3	Human epidermal growth factor receptor
SMDC	Small molecule drug conjugates
PepDC	Peptide drug conjugates
RGD	Arginylglycylaspartic acid
TAT	Trans-Activator of Transcription
CPP	Cell-penetrating peptides
CTP	Cell targeting peptides
CPT	Camptothecin
buSS	Disulfylbutyrate
PTX	Paclitaxel
GSH	Glutathione
UV	Ultraviolet
ADDC	Amphiphilic drug-drug conjugate
Ir	Irinotecan
Cb	Chlorumbucil
GCT	Gemcitabine
Cys	Cysteine
FF	Phenylalanine-phenylalanine
o	*Ortho*

HBTU	*N,N,N′,N′*-Tetramethyl-O-(1H-benzotriazol-1-yl)uronium hexafluorophosphate
DIPEA	*N*, *N*-Diisopropylethylamine
TFA	Trifluoroacetic acid
µM	Micromolar
Min	Minutes
h	Hours
T_g	Sol-gel transition temperature
^oC	Degree Celsius
FESEM	Field emission scanning electron microscope
nm	Nanometre
µm	Micrometer
DMSO	Dimethylsulphoxide
DMF	*N*,*N*-Dimethylformamide
LVR	Linear viscoelastic region
G´	Storage modulus
G´´	Loss modulus
CD	Circular dichroism
FTIR	Fourier transform infrared spectroscopy
HPLC	High-performance liquid chromatography
HRMS	High resolution mass spectroscopy
NMR	Nuclear magnetic resonance
δ	Chemical shift or delta
ppm	Parts per million
MTT	3-(4,5-Dimethylthiazol-2-yl)-2,5-Diphenyltetrazolium Bromide
µL	Microliter
µM	Micromolar
µg	Microgram
mL	Milliliter
NCCS	National Centre for Cell Science
TLC	Thin-layer chromatography
mg	Milligram
mmol	Milimole
Mp	Melting point
mM	Millimolar
TMS	Tetramethylsilane
q	Quartet
rt	Room temperature
s	Singlet
br	Broad
h	Hours
Hz	Hertz
J	Coupling constant

m	Multiplet
g	Grams
ESI	Electrospray ionization
THF	Tetrahydrofuran
HCl	Hydrochloric acid
TFA	Trifluoroacetic acid
DCM	Dichloromethane
NaOH	Sodium hydroxide
tert	Tertiary
KBr	Potassium bromide
LED	Light Emitting Diode
PBS	Phosphate-buffered saline
DMEM	Dulbecco's modified Eagle's medium
A	Absorbance/Absorption
OD	Optical density
PDC	Peptide drug conjugate
DLS	Dynamic light scattering
Vis	Visible
NP	Nanoparticle
EE	Entrapment efficiency
rpm	Revolutions per minute
MWCO	Molecular weight cut-off
CAC	Critical aggregation constant
LMWG	Low molecular weight hydrogelators
MGC	Minimum gelation concentration
IC_{50}	Half maximal inhibitory concentration
MeOH	Methanol
$CHCl_3$	Chloroform
MALDI	Matrix-assisted laser desorption ionization
TOF	Time-of-flight

Abstract

The substance in this thesis bearing the title "**Design and Synthesis of Biomolecular Amphiphiles for Effective and Stimuli-Responsive Delivery of Anti-Tumor Agents"** is compiled in five chapters based on the outcome of experimental results, performed during my Ph.D. tenure.

The first chapter (**Chapter 1**) presents a brief introduction about anticancer drug delivery systems (DDS), especially where the therapeutic molecules are covalently conjugated to DDS. The necessity of DDS in anticancer research and its evolution during the last few decades is discussed elaborately in this chapter. The significance of chemistry in bioconjugation of drugs, synthesis and designing versatile molecules for drug delivery is reviewed. Along with this, the generation of various nanostructures due to the self-assembly properties of this kind of drug conjugates is also explored extensively.

C**hapter 2** describes the design and synthesis of a peptide 5-Fluorouracil (5-Fu) conjugate that can self-assemble to form hydrogel. A photolabile *o*-nitrobenzyl linker was utilized to accomplish a photo-controlled release of hydrophilic 5-Fu from the peptide-5-Fu conjugate. With a careful choice of the peptide sequence, the peptide-drug conjugate was able to form a hydrogel within a narrow pH window (pH 6.0 - 8.0). MTT assay of the peptide-drug conjugate in HeLa cells inferred almost no cytotoxicity up to a high concentration of 110 μM. The gelator prodrug releases 5-fluorouracil in a controlled, dose-dependent manner under irradiation. The formulation and synthesis of the drug-amphiphile with a cleavable linker, solvent dependent behavior of the amphiphile, physical characteristics and properties of the gel were elaborately studied using NMR, FTIR, CD, HPLC and FESEM. Radiation-induced, controlled release of the therapeutic agent, cytotoxicity in tumor cell lines were also validated.

Chapter 3 demonstrates the procedure of fabrication of nanoparticles from the 5-Fu conjugated peptide amphiphile synthesized in chapter **1**. The covalent conjugation of 5-Fu with the peptide provided better control over the release of 5-Fu and also dramatically reduces the possibility of leaching of the drug. The prepared nanoparticles were also made efficient for passive targeting by PEG 6000 coating on its surface. Successful encapsulation of a second therapeutic agent, camptothecin (CPT), within the nanoparticles was also achieved. The stimuli-responsive release of 5-Fu was carefully

monitored by HPLC, NMR, and UV-visible spectroscopy. On the other hand, the release of the hydrophobic drug CPT from the nanoparticles was determined to be in a diffusion-controlled fashion. The cytotoxicity of the nanoparticles due to the release of two drugs was monitored minutely.

Chapter 4 introduced the design and synthesis of dual-responsive, dual drug carrier nanoparticles. Chemically modified palmitic acid containing a disulfide bond, was covalently tethered to 5-Fu through the cleavable linker. Nanoparticle formulation from the self-assembly of the molecule was carried out by the nanoprecipitation method. The novelty of the new amphiphile is that, its self-assembly property can be disrupted by cleaving the disulfide bond in presence of glutathione (GSH), an enzyme, overexpressed In tumor cells. Hydrophobic drug camptothecin was efficiently encapsulated in the nanoparticles. The release of 5-Fu was monitored in a photoresponsive manner, whereas, the non-covalently bound camptothecin could be released from the nanoparticles by the action of GSH. The synthesized amphiphile was proved to be fairly nontoxic in HeLa cell lines up to a very high concentration of 1.1 mM.

Chapter 5, the design of a low molecular weight hydrgelator containing a biomarker biotin covalently tethered to 5-Fu is demonstrated for targeted delivery of 5-Fu. The synthesized molecule formed hydrogel at pH 7. The hydrogel also can effectively entrap another water-soluble chemotherapeutic agent doxorubicin hydrochloride (DOX). The release of 5-Fu was observed in a light-dependent manner, whereas sustained-release of DOX was recorded from the hydrogel. The controlled and sustained release of both the drugs were monitored by UV-Vis, fluorescence spectroscopy and ^{1}H NMR study. The hydrogel properties and the factors responsible for self-assembly were also identified. The 5-Fu conjugate was also proved to be non-toxic up to a high concentration such as 80 µM.

Chapter 6 represented the conclusion and future perspective of the thesis**.**

Every chapter contains a brief introduction of related works in literature, description of the current result and discussions, experimental section, required references, along with all characterization data of the synthesized compounds.

Chapter 1

Introduction to Bioconjugates and Drug Delivery Systems

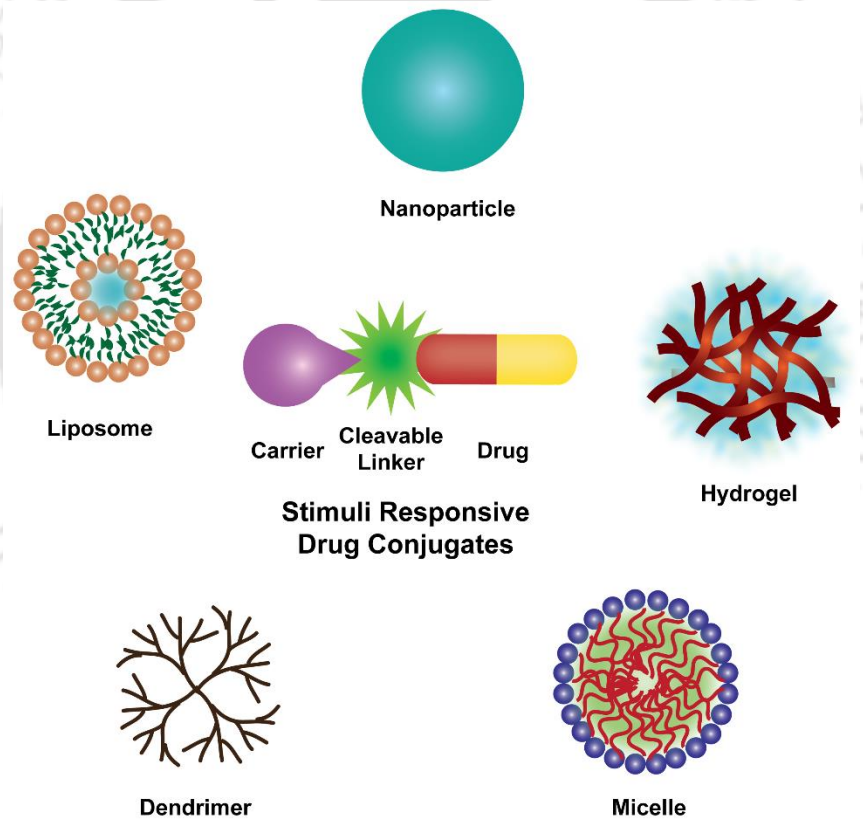

1.1 Cancer and some important anticancer agents

Cancer is the second most common reason of death, according to the reports published by World Health Organization (WHO). It is the uncontrolled growth of living cells (Figure 1.1). In broader view, cancer is a large group of diseases that involve generation of abnormal cells by rapid cell division and can grow beyond their usual boundary. Such a group or set of cells having undergone uncontrolled growth can be termed as tumors.

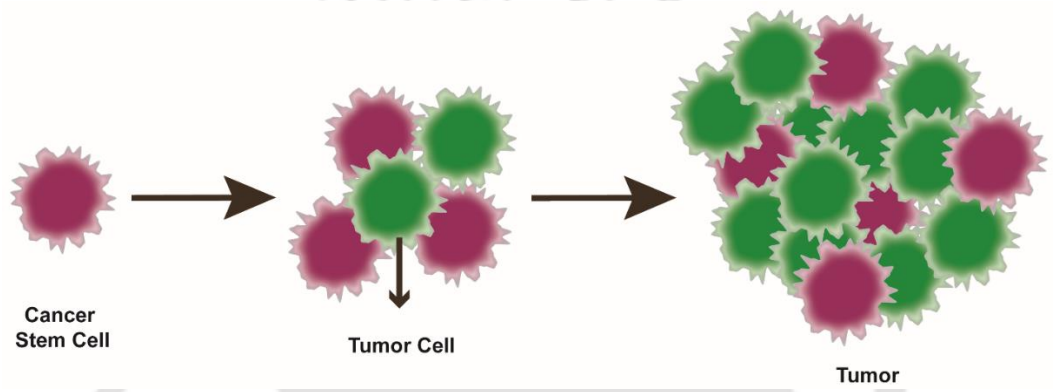

Figure 1.1 Progression of tumor.

There are more than 100 different types of cancers and each one is unique in nature except some common features. Even after treatment, the hardest issue is to get rid of all cancer cells from a body and if a few of them remain, they can proliferate again to produce a regeneration of the disease. Based on the types of cancer, it is treated in mainly three ways at present

- Surgery
- Chemotherapy
- Radiotherapy.

Among these three, chemotherapy is the treatment which uses chemical substance, specially one or a combination of anticancer drugs to treat cancer. Approximately, there are more than 200 drugs approved for cancer treatment with more in clinical trials. These drugs are divided into groups according to their chemical or physiological functionality as given in Table 1.1

Table 1.1 Types of cancer drugs

Types of Antitumor Agents	Examples
Alkylating agents	Chlorumbucil, Melphalan, Thiotepa etc.
Antimetabolite agents	Flurouracil, Gemcitabine, Methotrexate, Floxuridine etc.
DNA Cutters	Bleomycin
Topoisomerase I Poisons	Camptothecin, Topotecan, Irinothecan
Topoisomerase II Poisons	Daunorubicin

The chemical structures of some very popular anticancer drugs are presented in figure 1.2

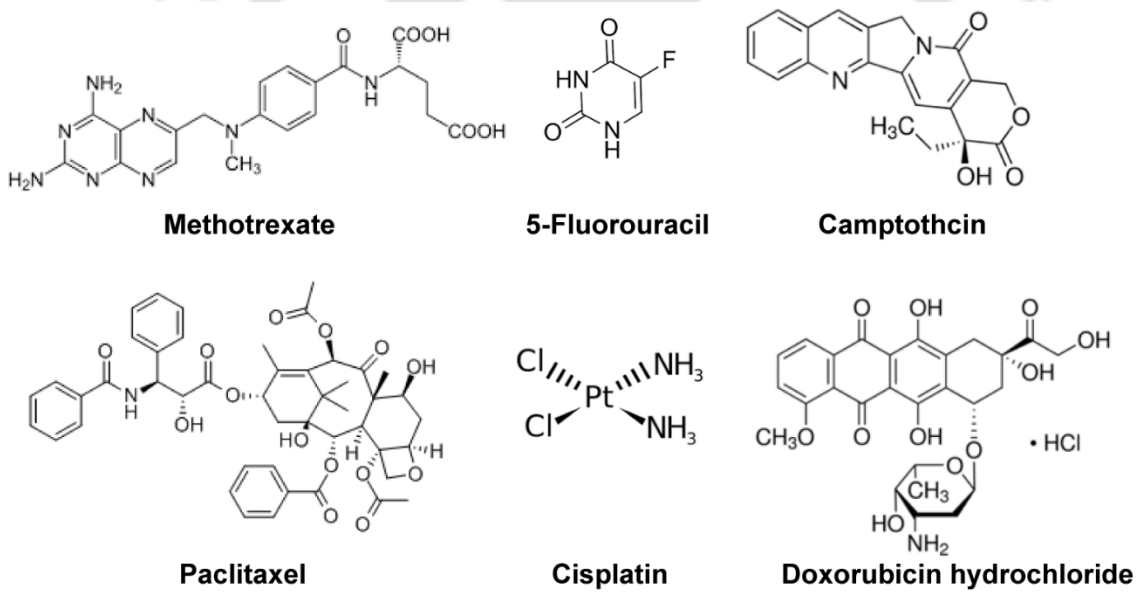

Figure 1.2 Chemical structure of some anticancer agents.

However, among these, 5-Fluorouracil is one of the extensively used drug in anticancer therapy due to its high efficacy against different types of cancer.

Since 1957, 5-Fluorouracil has found wide application for treating mainly solid tumors like malignancies in gastrointestinal tract, breast, head and neck as well as other areas. It is mostly prescribed for treating colorectal, cervical cancer. The mechanism of action of 5-Fu as an anticancer agent[1-2] is presented in figure 1.3.

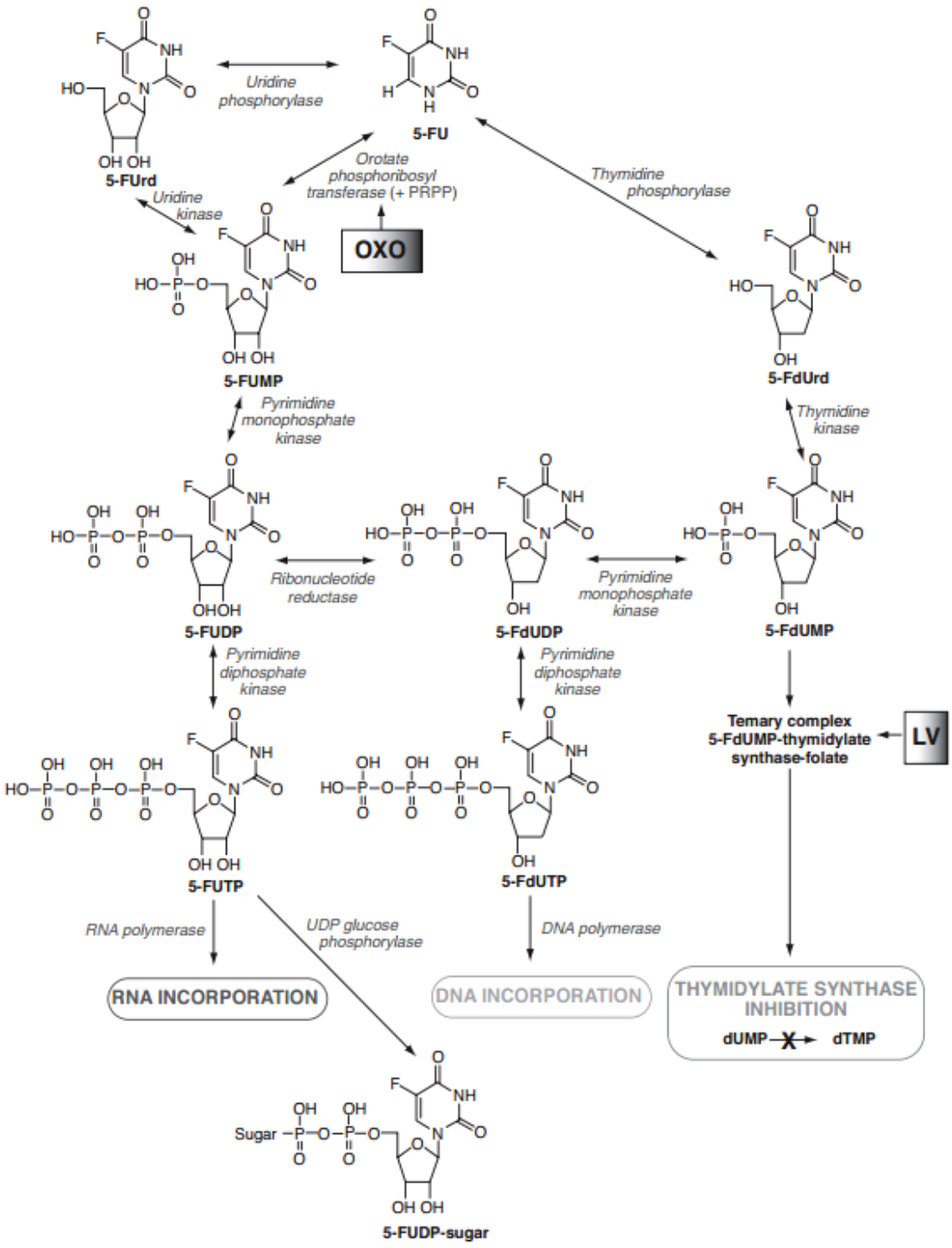

Figure 1.3 Mechanism of metabolism of 5-Fu inside body.[3]

5-Fu is converted to three major active metabolites through the following pathways

Fluorodeoxyuridine monophosphate (FdUMP): This acts as an inhibitor of thymidylate synthase (TS) which is essential in DNA synthesis. Because of this DNA replication and repair process was stopped, thus activating programmed cell death.

Fluorodeoxyuridine triphosphate(FdUTP) & Fluorouridine triphosphate (FUTP): FUTP and FdUTP both shows cytotoxicity through their incorporation into all types of RNA and thus modifying them

Despite this, the use of 5-Fu was also having several limitations[2] such as,

5-Fu undergoes rapid degradation into 5-FuH_2 by the very first enzyme in the catabolic cycle of 5-Fu, Dihydropyrimidine dehydrogenase (DPD). Therefore, the bioavailability of the drug *i.e.* amount of drug left for anabolism decreases.

The drug itself does not have any selectivity towards cancer cells. As a result, along with cancer cells, 5-Fu also invades into the normal cells, causing cell death.

Not only 5-Fu, almost all anticancer drugs have similar impediment to achieve utmost efficacy. Along with loss of bioavailability and lack of selectivity, anticancer drugs also have many more complications like poor water solubility, poor drug encapsulation capacity, stability of the drug, uncontrolled rate of release of the drug inside the cells etc.[4] All these difficulties diminish the efficiency of a drug by affecting its therapeutic concentration and activity towards the diseased cells and increasing the side effects towards normal cells. Thus, obliteration of these constrains had become as essential as the discovery of a new drug against the battle with cancer.

1.2 Synthetic Biomolecules as therapeutics and delivery vehicles

To achieve bioavailability, controlled release, target specificity and cellular uptake, therapeutic agents are often associated with delivery vehicles. Drug delivery system (DDS) is an approach to originate a formulation of the existing drugs for procuring its uttermost efficacy from the perception of its pharmacodynamics and pharmacokinetics.[5] In general, a DDS attains the maximum effect of a drug by controlling and localizing its dose, improving its target specificity and stabilizing them *in vivo*. With the rapid progression in

the field of synthetic and conjugate chemistry, material science, nanotechnology and medicinal chemistry, there is an upsurge of different designs for the development of DDS. Some of them with better controlling of the drug release whereas some introduced the techniques for targeted delivery of the drug. Overall, the medicinal world is expanding and transforming by each passing day with the invention and modification of a vast array of ideas in therapeutic research. Designing of a delivery vehicle for a drug requires sound knowledge about the basics components of a DDS. The main factors upon which the design of a DDS, are shown in figure 1.4.

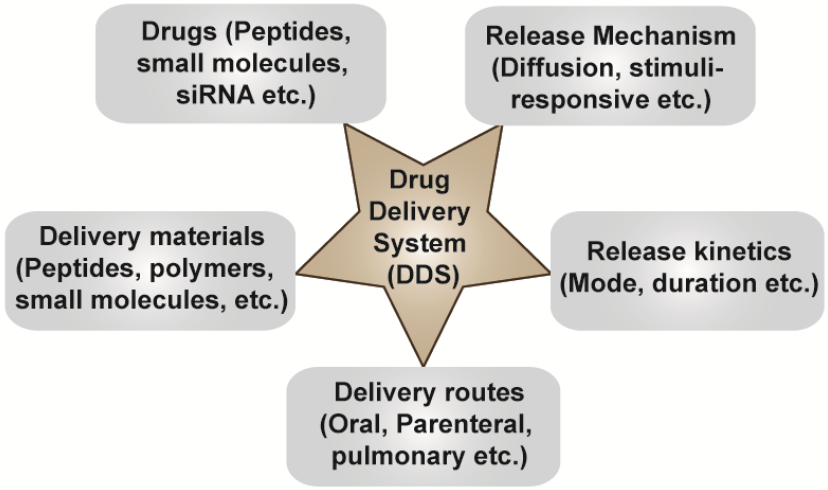

Figure 1.4 Basic constituents for designing of a DDS.

Based on the factors mentioned in figure 1.4, various delivery systems were designed to achieve a better-controlled and targeted release of drugs for gaining the optimum benefit of it.

1.2.1 Controlled drug delivery

Controlled drug delivery was invented for the sustained release of a drug at a predetermined rate to the affected cells. The concept of controlled release was first introduced back in 1952 by Smith Klein Beecham through their sustained release formulation which achieved a 12 hour efficacy in drug release kinetics.[6] Ever since, controlled delivery has gained immense popularity due to its various advantages: (a) control over the drug release rate and thus maintaining the desired drug concentration, (b)

reducing the side effects associated with overdose of the drug, (c) localising the drug in the desired place and thereby eradicating the off-target effects etc.[7]

The fundamental understanding of the drug release mechanism for a controlled release system was observed in between 1950-1980s. Diffusion, osmosis, dissolution, ion exchange etc. were used as the principal techniques for controlling the release of active drug during this period.[7] Later on 'smart' polymers, hydrogels were introduced as drug carrier and some of them were designed to control the drug release in stimuli (temperature, pH, light, glucose level) responsive manner.[8] Implants,[9] microparticles,[10] *in situ* gel-forming implants[11] have also emerged as controlled delivery vehicle. More recently, nanoparticles have grabbed the major attention in the field of DDS as well as controlled release systems (CRS).[12-13] Some of the major techniques evolved as a CRS were shown in figure 1.5

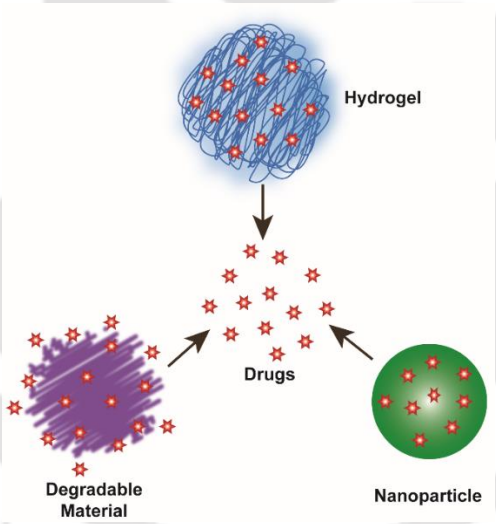

Figure 1.5 Some of the controlled release system.

Since the advent of anticancer research, several CRS were contrived for the treatment of cancers. Among them, hydrogels, degradable materials, nanoparticles have gained immense popularity. Initially, biodegradable polymers constructed most of these materials but later on small molecule based materials have also earned substantial significance. Along with small molecules, inorganic nanoparticles, proteins, lipids have also emerged as an excellent transporter of anticancer agents.[14-16] The initial success of nanoparticles in anticancer drug delivery pioneered the field of nanocarriers based drug delivery. Sundry

nanocarriers such as dendrimers, carbon dot, mesoporous silica nanoparticles, liposomes, micelles, hydrogel nanoparticles were innovated for preparing multiple CRS.

1.2.2 Targeted drug delivery

With the advancement in developing controlled release system, an urgent requirement of site-specific drug delivery was inevitably perceived as the non-specific absorption of the drug by healthy cells resulted in aggravated side effects along with substandard efficacy. Needful efforts were employed by the researchers to materialize the purpose of targeting the diseased cells keeping the healthy cells unaffected.

In case of therapeutic research, several exogenous and endogenous factors were also utilized for targeting the diseased site passively. Such factors include a change in pH, temperature between the normal and pathogenic cells, overexpression of an enzyme (such as Cathepsin B, glutathione are overexpressed in tumor cells) inside the diseased cells compared to the normal cells. Nevertheless, in many instances, the target site may not differ much from the normal cells and thus for those cases, such modes of delivery cannot provide any targeting efficiency. External stimulus like magnetic field was also applied to guide the delivery vehicle towards the specific site of action. To design such a system, drugs were attached to a ferromagnetic carrier. However, magnetic targeting is limited due to its dependence on the rate of blood flow in the target cells and for deep tissues, it becomes ineffective. Another strategy was also devised for the passive accumulation of drugs by the enhanced permeability retention (EPR) effect (extravasation across the leaky vasculature).[17] This kind of passive targeting can be achieved by making the DDS long circulating in the blood for the sufficient accumulation of the drug or the DDS in the targeted site. An easy route for attaining such feature was established by masking them with surface modification of water-soluble and well-solvated polymers. This perspective was widely used to develop a number of liposomal and micellar DDS. Although passive targeting is also restricted conditions where the vascular endothelium integrity remains uninfluenced.

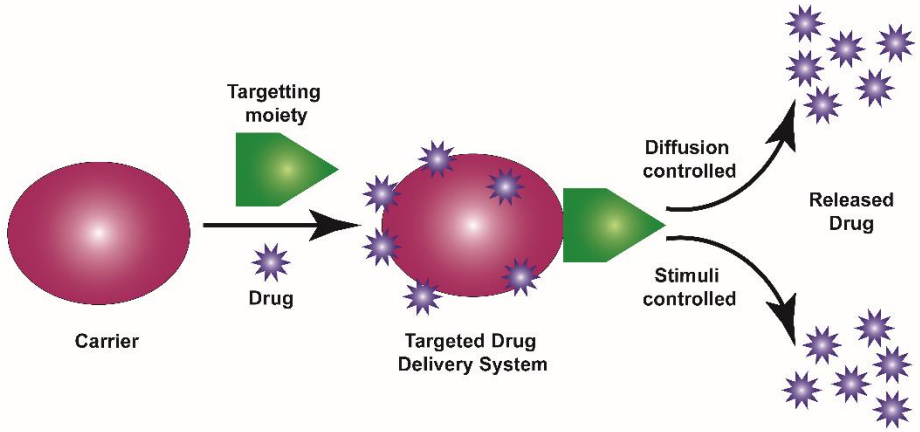

Figure 1.6 Schematic presentation of targeted drug delivery system.

The most interesting approach to accomplish effective targeting was by attaching a therapeutic agent with a targeting ligand (Figure 1.6), which can selectively deliver the cargo at the site of requirement. This is known as active targeting approach.[17] For anticancer drug delivery, several peptides, antibodies, aptamers, small molecules were identified as the targeting ligand which can recognize and bind to the receptors specifically present or overexpressed in the cancer cells.[18]

1.3 Role of bio-conjugation in anticancer drug delivery

In the present era of anticancer drug delivery, targeted drug delivery had already outperformed the non-targeted mode of delivery. However, it soon became clear that optimal delivery would not be possible by mere targeting the cancer cells. Along with targeting, attention should also be given towards the controlled release of the active drug in adequate dose. Several groups attempted delivery of a drug by physically encapsulating it within the carrier conjugated to the targeting moiety. However, the success rate was barely incremental. Usually, after the administration of a drug inside the body, a lot more factors need to be considered, such as (i) disposal of the drug-loaded carrier into the circulation system, (ii) placement of it toward the required site of action by crossing the blood vessel wall, (iii) diffusion of it around the interstitial sites of the cancer tissues, (iv) internalization of it inside the affected cells, (v) release of drugs from the carrier. In between the occurrence of the above-mentioned process ample probabilities are there for the drug being outflowed by a number of pathways like p-glycoprotein, excretory organ,

immune system etc. mediated efflux from the body. Excluding these factors, physical encapsulation system of a drug also suffers from leaching of drugs throughout the above course of endocytosis process. This, in turn, reduces the drug amount inside the delivery system and become insufficient to stop the growth of the cancer cells.

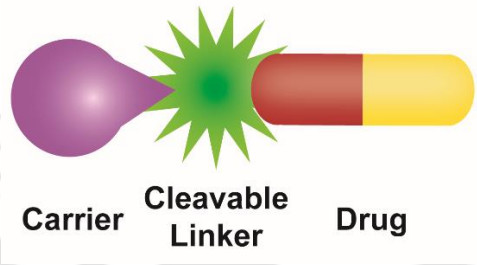

Figure 1.7 Schematic presentation of a covalently conjugated DDS.

In order to avoid these problems, researchers have introduced the idea of covalent conjugation of the drug with the carrier. Figure 1.7 represents an ideal covalently conjugated DDS. Issues of drug leakage from the system were immediately solved by means of covalent attachment of the drug. Moreover, the drug conjugation was done in such a way that it can escape the efflux mechanism of our body. Various fields were originated from this proposal depending on the targeting ligands and the nature of the carrier. Some of the important ones are discussed herein.

1.3.1 Polymer drug conjugates

Polymer drug conjugates are a macromolecular construct containing the pharmacologically active drug covalently bound to the polymer itself. It was introduced way back in 1955 by Jatzkewitz for the controlled delivery of mescaline by conjugating it with a copolymer comprising of *N*- vinylpyrrolidone and acrylic acid.[19] However, the concept of conjugating an anti-tumor agent with a polymer was pioneered by Ringsdorf in 1970s.[20] This marked a revolutionary advancement in the field of anticancer drug delivery. Today a substantial number of polymer-drug conjugates have proved to have great potential as chemotherapeutic agent and some of them are already marketed for cancer treatment. A considerable number of polymer-drug conjugates are also in clinical trial. Some of the notable chemotherapeutics consisting of polymer-drug conjugates are mentioned in Table 1.2

Table 1.2 Polymer drug conjugates based chemotherapeutics

Name	Polymer carrier	Drug	Indication(s)	Status	Ref.
Oncaspar	PEG	l-Asparaginase	Acute lymphoblastic leukaemia	Marketed in 1994	[21]
Pegilodecakin (ARMO BioSciences)	PEG	IL-10	Pancreatic cancer	Phase III (NCT02923921)	[22]
Opaxio	Polyglutamic acid	Paclitaxel	Peritoneal cancer, ovarian cancer, fallopian tube cancer	Phase III (NCT00108745)	[23]
CRLX101	Cyclodextrin-PEG	Camptothecin	Peritoneal cancer, ovarian cancer, fallopian tube cancer	Phase II (NCT01652079)	[24]
Somadex	Dextran	Somatostatin	Neuroendocrine tumours	Phase II	[25]
ProLindac™ (AP5346)	Hydroxypropy lmethacrylamide (HPMA)	oxaliplatin	Solid tumors, ovarian cancer	Phase II	[26]

1.3.2 Antibody-drug conjugate

Monoclonal antibody (mAb) based anticancer therapy has gained immense popularity over the time for its exceptional targeting efficiency. Several mAbs, which can recognize specific antigens overexpressed or present in the cancer cells, were developed so far. These antigens usually are glycoproteins, carbohydrates and cell surface proteins, which are critically involved in tumor growth and progression. Depending upon the type of antigens, mAbs can not only target cancer cells but also can effectively kill them. The lack of therapeutic activity of most of the antibodies was ameliorated by conjugating them with an already known cytotoxic agent (drug), initiating a prospective area of antibody-drug conjugate (ADC) in anticancer research world.

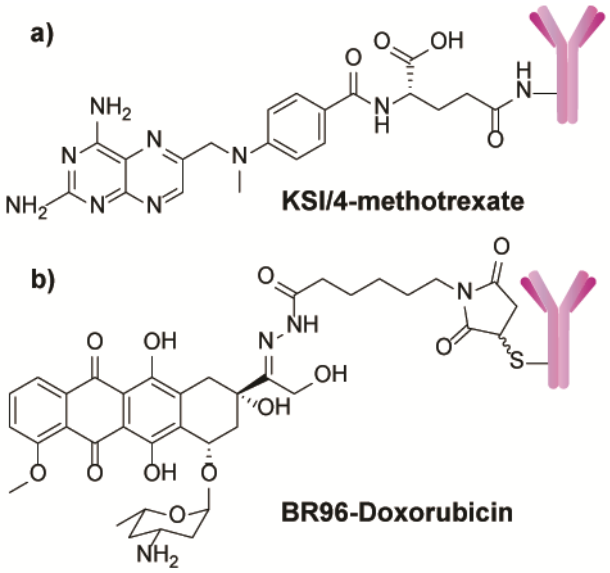

Figure 1.8 Structures of some ADCs.

The very first human clinical trial of mAb (named as Ab 89 which was specific for a lymphoma associated antigen) was performed in 1980 on a lymphoma patient.[27] Later on, a lot more antibodies were developed having greater efficiency to bind to the cancer cell-specific antigens. With the furtherance of the library of tumor homing mAbs, various anticancer agents were covalently linked with them to achieve the optimal potency of that drug. Methotrexate, a popular anticancer agent was conjugated with a murine KS1/4 antibody via an amide bond (Figure 1.8a) and the system was evidenced of having tumor-specific localization after the phase I clinical trial evaluation.[28] Similarly doxorubicin-antibody conjugate BR96-Dox (Figure 1.8b) have furthered into phase II clinical trial.[29] Table 1.3 describes some other ADCs approved for anticancer treatment.[30]

Table 1.3 Description of Antibody-drug conjugates in clinical trial.

Antibody	**Antigen**	**Disease**	**Clinical trial status**
Tositumomab[31]	CD20	NHL	Approved by FDA
Ibritumomab tiuxetan (Zevalin)[32]	CD20	NHL	Approved by FDA (Phase IV)
Epratuzumab[33]	CD22	NHL	Phase III

chTNT-1/B[34]	DNA	anaplastic astrocytoma, glioblastoma multiforme		Phase III
Pemtumomab[35]	PEM	Gastric, carcinoma	ovarian	Phase III

NHL, non-Hodgkin's lymphoma; PEM, polymorphic epithelial mucin

1.3.3 Aptamer-drug conjugate

After antibody, aptamers have attracted the greatest attention for targeted anticancer drug delivery. It is a single-stranded oligonucleotide, which is able to specifically recognize the tumor cells. Aptamers have several advantages over antibodies like (i) easy cost-effective synthesis and chemical modifications, (ii) low immunogenicity, (iii) its screening can be done for a vast array of molecular targets including for those, which are difficult to prepare antibodies against, (iv) strong binding capability with the target compared to the other ligands.[36] Several other groups have employed aptamers in designing various aptamer drug conjugates (ApDC) for targeted delivery of the corresponding drugs including anticancer ones. The following Table 1.4 discusses some of the ApDCs utilized in anticancer treatment.

Table 1.4 Aptamer drug conjugates used in chemotherapy

Aptamers	**Therapeutic agent**	**Molecular target**	**Ref.**
AS1411	Chemotherapeutics, photosensitizers	Nucleolin	37
sgc8	Immunotherapeutics, photosensitizers, chemotherapeutics etc.	PTK7	38
A9, A10	siRNA, chemotherapeutics etc.	PSMA	39
AptA, AptB	Chemotherapeutics	Mucin 1	40
A30	Chemotherapeutics	HER3	41

PTK7: protein tyrosine kinase 7, PSMA: prostate-specific membrane antigen, HER: human epidermal growth factor receptor.

Initially, ApDCs were synthesized in 1:1 ratio of drug: aptamer. For example, doxorubicin (dox) was conjugated with sgc8 aptamer *via* an acid cleavable linker. This system provided highly selective apoptosis of various cancer cells through sgc8 mediated targeting.[42] In spite of the initial success to treat cancer with this kind of ApDCs, it was suffering from having low amount of drug carried by each aptamer. Nevertheless, this problem was soon resolved by designing ApDCs where the drug was conjugated with an aptamer in 1: n ratio of aptamer: drug. This novel designing principle was used by several research groups like Tan and his co-workers had conjugated multiple copies of 5-Fu with sgc8 aptamer.[43] The synthesis was carried out by synthesizing phosphoramidite D, a therapeutic module comprised of 5-Fu, solid-phase synthesis functionality and a photocleavable linker in between them. This module then integrated with the aptamer by automated solid-phase synthesis. This system was shown to have specific binding affinity and internalization and subsequent cytotoxic effect towards the targeted cancer cells.

1.3.4 Small molecule drug conjugate

Numerous small molecule-targeting agents were developed and utilized in anticancer drug delivery. Apart from peptides, which is discussed in detail later, other such notable ligands (Figure 1.9) are folic acid (binds to the folate receptors)[44], biotin (binds to the biotin receptors)[45], glutamic acid urea derivatives (binds to the PSMA receptors)[46], aromatic sulphonamides[47] (binds to carbonic anhydrase IX, specifically present in renal carcinoma and also, a marker for hypoxia).

So far, a number of folate-vinca alkaloids were developed and undergone clinical trials. Some of these folate-vinca SMDCs are vintafolide (EC145 and MK-8109), vinorelbine (EC1041), vindesine (EC192), vinflunine (EC1044). Among them, vintafolides gained popularity. Vintafolides are comprised of folic acid as targeting ligand, desacetyl vinblastine as the cytotoxic payload and a disulfide linker for controlling the release of the drug.[48] Again maytansinoid DM1, a popular cytotoxic agent was conjugated with a bivalent ligand against carbonic anhydrase IX.[49] To prepare biotin guided SMDCs different anticancer agents like doxorubicin,[50] gemcitabine,[51] SBT-1214[52] were conjugated with biotin via photo cleavable *o*-nitro benzyl and reduction cleavable disulfide linkers.

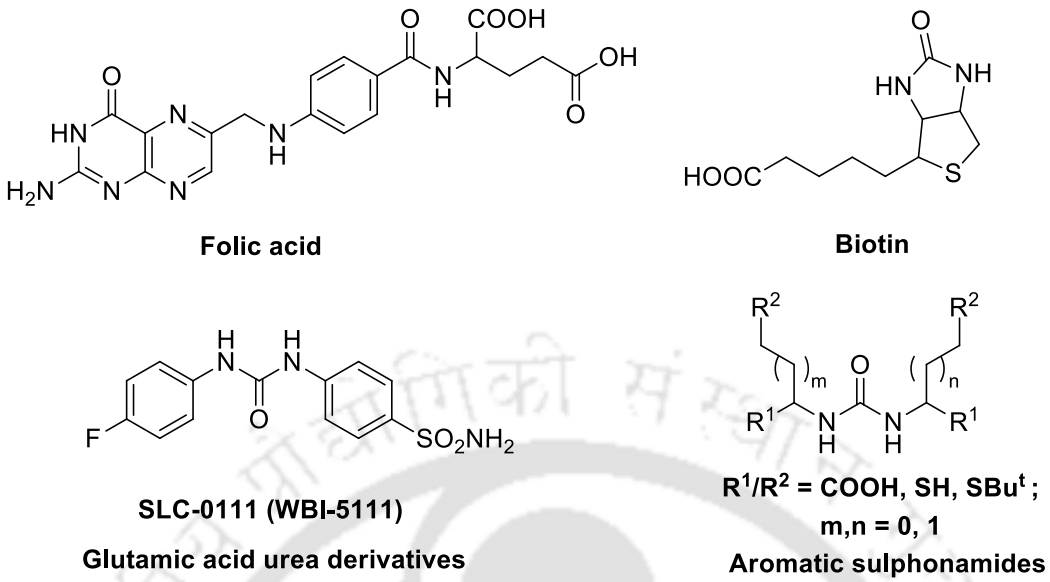

Figure 1.9 Chemical structures of some small-molecule cancer-targeting agent.

1.3.5 Peptide drug conjugate

Peptide drug conjugates (PepDC) were one of the SMDCs developed for targeted drug delivery. The basic design of a PepDC consists of the drug, peptide and a linker as a connector between the two. Depending upon the peptide nature, PepDCs can be made useful for various purposes. For example, a tumor homing peptide can render a PepDC target efficiency for cancer treatment. Similarly, attachment of a cell-penetrating peptide sequence with a DDS provides it peptide-aided endocytosis, overcoming all the barriers. PepDCs have a number of advantages over ADCs like (i) their low molecular weight enhances the penetrability into solid tissues and also increases the drug loading efficiency, (ii) their synthesis procedures are economically more viable compared to ADCs, (iii) they are highly biodegradable and do not induce any immunogenic response *in vivo*.[53-54]

Cell targeting peptides have specific binding affinity towards specific receptors, which are either overexpressed or present in those target cells. Integrin is among such receptors which has long been identified as overexpressed in cancer cells due to their eminent involvement in the pathological process of the disease progression. A lot of integrin targeting peptides were designed and incorporated into the delivery system for a therapeutic cargo. For instance, the shortest peptide used for tumor targeting is RGD

having the sequence Arg-Gly-Asp. Paclitaxel was conjugated with dimeric RGD peptide through a succinate linker (Figure 1.10).[55]

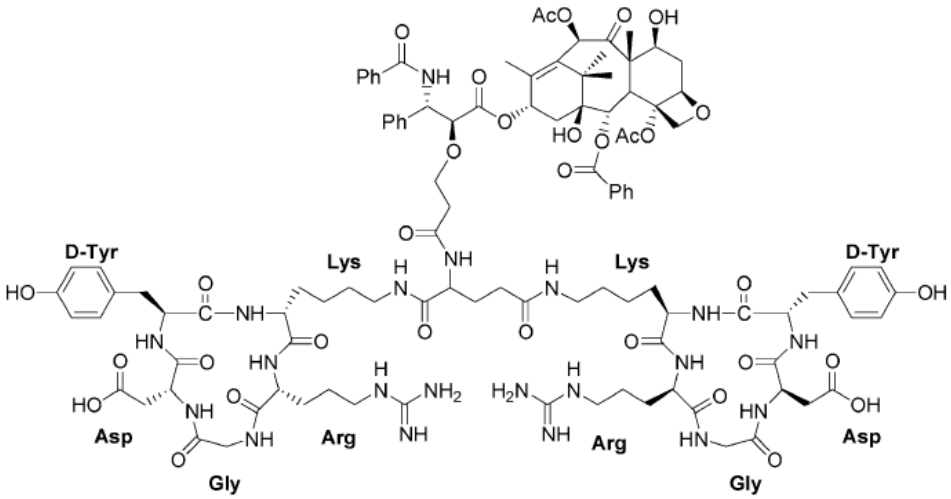

Figure 1.10 Structure of paclitaxel-RGD conjugate

Recently rapid technological evolution such as solid-phase peptide synthesis, proteomics etc. promoted the identification as well as logical design of new class of targeting peptides. With such improvement in peptide designing and identification, the field of PepDCs has also progressed in fast pace. Already some PepDCs have been marketed and a prodigious number of them have been undergoing clinical trial. Table 1.8 provides information about some of such PepDCs and their status in clinical phase.

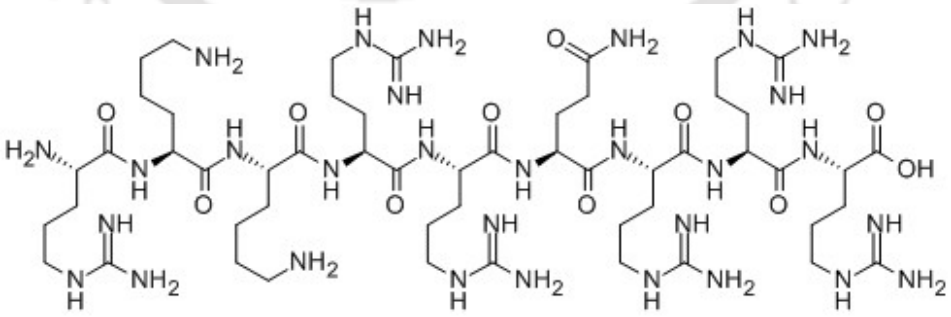

Figure 1.11 Structure of protein derived cell penetrating TAT peptide

Peptides were not only designed to target the diseased cells but also made to cross the cell membrane, which are called cell-penetrating peptides (CPP). Proper cellular uptake of drugs has always been a major hindrance in drug delivery. A smooth transit of drugs

through the cell membrane can reduce the amount of drug to be administered to achieve the required effect, thus reducing the side effects associated with excess drug absorption by the healthy cells. CPPs introduced in a DDS for its significant role in the smooth passing of the drug across the cell membrane. CPPs are short peptides, which commonly have positive charges or amphipathicity. For anticancer drug delivery, chemotherapeutics were usually attached with a CPP such as TAT (Figure 1.11), a protein derived peptide, MAP, 8-lysines etc. For instance, DOX was coupled with TAT attached elastin-like peptide via a lysosomally cleavable tetrapeptide for the thermally targeted dox delivery.[56] CPPs were also attached with nanocarriers such as liposomes,[57] micelles,[58] gold nanoparticles,[59] mesoporous silica nanoparticles[60] for drug or gene delivery to the cancer cells.

Table 1.5 Peptide drug conjugates used in cancer therapy

Peptides in cancer drug delivery	**Peptide sequence**	**Role of the peptide**	**Ref.**
RGD peptides	RGD c(RGDfK)	Targeting integrin $\alpha_v\beta_3$ which is overexpressed or highly selectively expressed on some cancer cell surface	61-63
Low density lipoprotein peptides	CEKLKEAFRLTRKRGLKLA	Targeting low density lipoprotein (LDL) receptors. LDL is overexpressed in many cancer cells.	64
MMP-2200	H_2N–l-Tyr-d-Thr-Gly-l-Phe-l-Leu-l-Ser–O–β-d-lactose–$CONH_2$	Helps to cross blood brain barrier	65
LHRH Analog peptides	GlpHWSYKLRPG-NH2 (Glp = Pyroglutamic acid)	luteinizing hormone-releasing hormone (LHRH) receptors	66
HIV-1 TAT protein	GRKKRRQRRRPPQ	A cationic peptide, helps in cell penetration	67
Bombesin Analog peptides	QWAVGHLM	Targeting bombesin Receptor, overexpressed in many cancer cells	68
MAP	KLALKLALKALKAALKLA	An amphipatic cell penetrating peptide	69

Besides CPPs and CTPs self-assembling peptide, drug conjugates have also emerged as a potential subset of PepDCs. This novel approach utilized the drug as a building block of a supramolecular architecture for its self-delivery. This kind of PepDCs have gained significant attention for the past few years due to its unique features like (i) a fixed and higher drug loading content, (ii) avoidance of premature degradation and rapid clearance, (iii) retaining of inherent activity of the drug upon release from the conjugate. Several research groups have designed such PepDCs by conjugating a hydrophilic peptide to a hydrophobic drug and vice versa. Such a strategy was followed by Cui and co-workers at the time of developing a supramolecular filament comprised of camptothecin (CPT) (Figure 1.12), a widely used anticancer drug.[70] They have conjugated CPT, a hydrophobic drug to a hydrophilic and β sheet forming peptide sequence derived from Tau protein through a reduction cleavable disulfylbutyrate (buSS) linker. By using the two amino group of lysine a branching point was created inside the molecule so that one, two even four CPT molecule can be attached with the whole system. All the molecules formed filamentous structure in water. They have also showed the controlled and steady release of bioactive CPT in glutathione responsive manner.

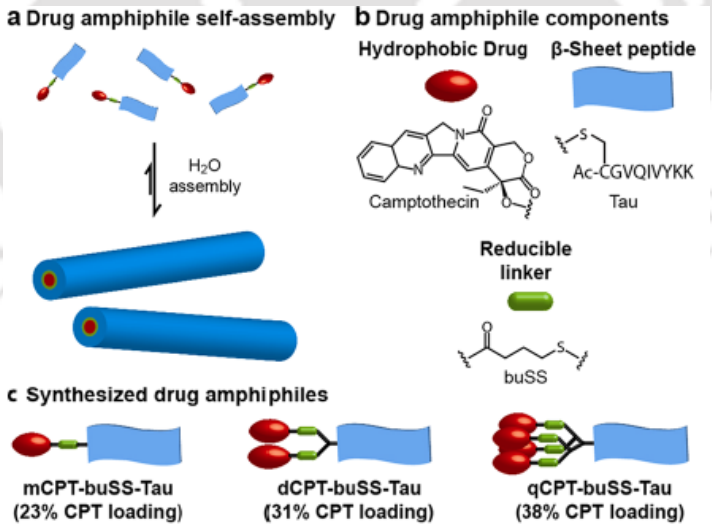

Figure 1.12 Design of a camptothecin peptide conjugate and its self-assembly mechanism.

1.4 Self-assembly of drug conjugates

As described earlier nanomaterials gained profound importance in the field of drug delivery since the emergence of this concept. Initial attempts were made by physically encapsulating the drug inside or on the surface of the nanocarriers. However later on the origination of covalent conjugation of drug with the carrier was able to tackle the drawbacks associated with physical encapsulation. Lately, researchers have combined the advantage of both nanosystems, drug conjugation by designing discrete amphiphiles with the conjugation of drugs with polymers, peptides, oligonucleotides, targeting agent, and sometimes even with another drugs. The basic idea of designing this kind of amphiphiles was to use the drug as a building block to generate diverse supramolecular structures. In this concept, instead of attaching or physically encapsulating the drug with the nanoparticles, it was used to create molecular building block, which can self-assemble by non-covalent forces, generating the nanostructure for its self-delivery. For example, Cui and his group conjugated the hydrophobic anticancer agent paclitaxel (PTX) with a β-sheet forming peptide to prepare the drug amphiphile which can self-assemble into filamentous nanostructures[71] (Figure 1.13). 4-(pyridin-2-yl-disulfanyl)butyrate (buSS) was used as a connector between the drug and the peptide owing to its degradability in presence of glutathione (GSH), an enzyme known to be overexpressed in many cancer cells. This system provided quite a high 41% fixed loading of PTX, markedly improving it's loading efficiency of the previously reported delivery systems. In addition, the conjugate was shown to have gained more stability due to its self-assembly into supramolecular architecture. In this report, it was also shown that the cytotoxic effect of the filaments remained comparable with the free PTX against a variety of cancer cell lines.

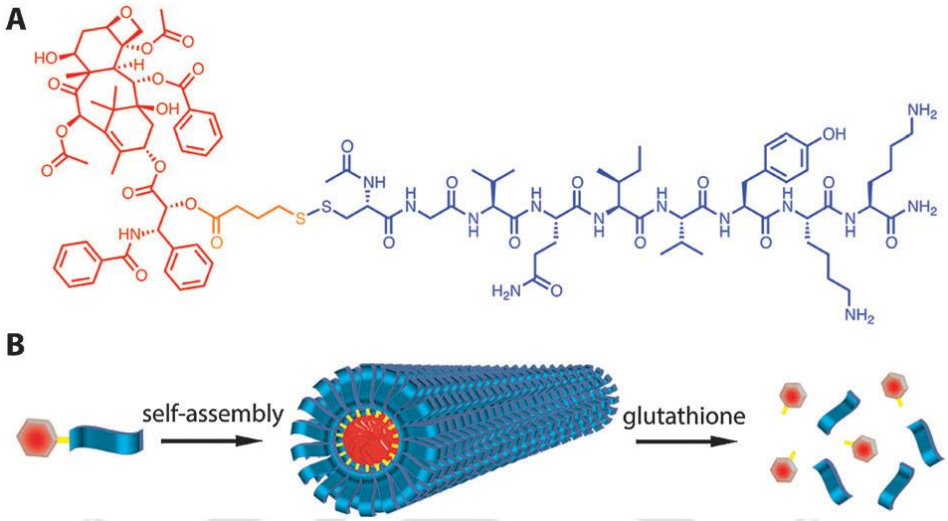

Figure 1.13 (A) Chemical structure of PTX-Tau drug amphiphile, (B) schematic presentation of its self-assembly into filamentous nanostructures.

Similarly, Agarwal and her group has also demonstrated a photo controlled biocompatible DDS based on coumarin functionalized block copolymers.[72] A micelle forming drug conjugate was made by a covalent attachment of 5-Fu with the coumarin functionalized block co-polymers by photoirradiation at > 310nm (Figure 1.14). The controlled release of 5-Fu from the micelle was shown by *in vitro* drug release experiment under UV irradiation of 254 nm.

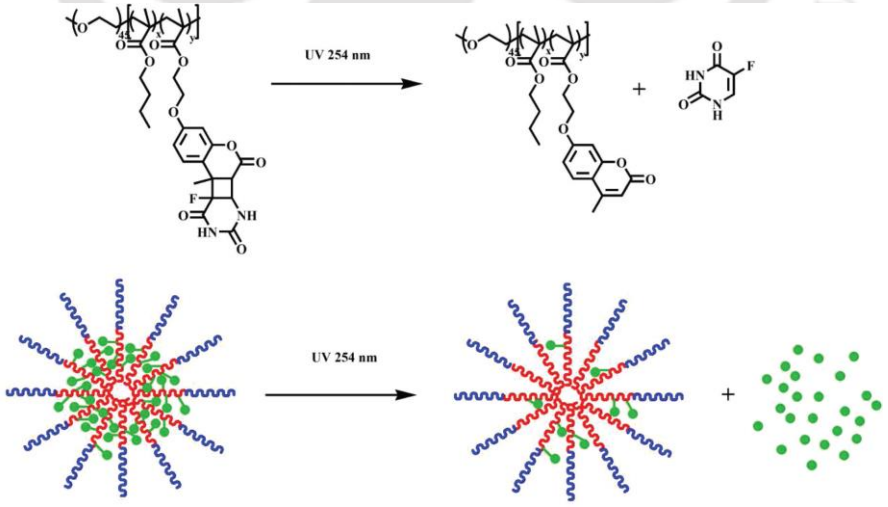

Figure 1.14 Schematic illustration of photo-controlled release of 5-Fu from the micelle comprised of the polymer 5-Fu conjugate.

Apart from polymers peptides drug amphiphiles were also designed by conjugation of oligonucleotides with it. Zhang and his group designed a camptothecin (CPT) oligonucleotide amphiphile by connecting three CPT molecules with DNA strands via a self-immolative and a photolabile *o*-nitrobenzyl linker.[73] Depending on the DNA size and assembly condition, the synthesized amphiphiles were able to form micellar structures with different morphology (Figure 1.15).

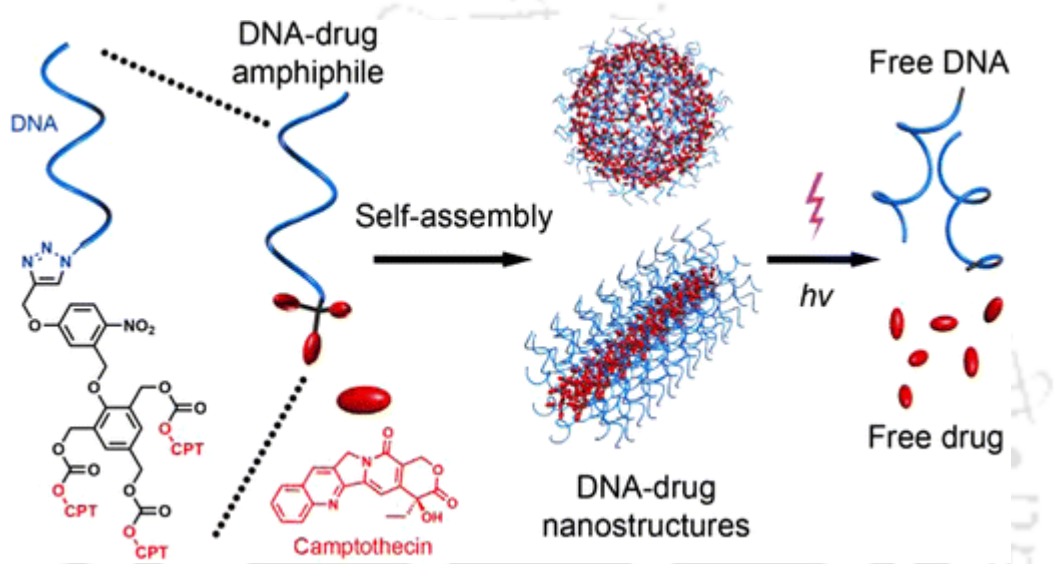

Figure 1.15 Graphical presentation of nanostructure formed by the self-assembly of DNA-CPT conjugate and photo-induced release of free CPT from it.

The DNA-CPT conjugate was shown to have light controlled localized cytotoxicity. Drug amphiphiles were not only designed by conjugating drug with polymers, peptides or oligonucleotides. Depending upon the inherent hydrophilic or hydrophobic nature of the drug itself, two of them was also combined to originate amphiphilic drug-drug conjugate (ADDC) (Figure 1.16). This novel and highly promising strategy was very recently pioneered by Yan and his group aiming at the development of carrier-free delivery system.[74]

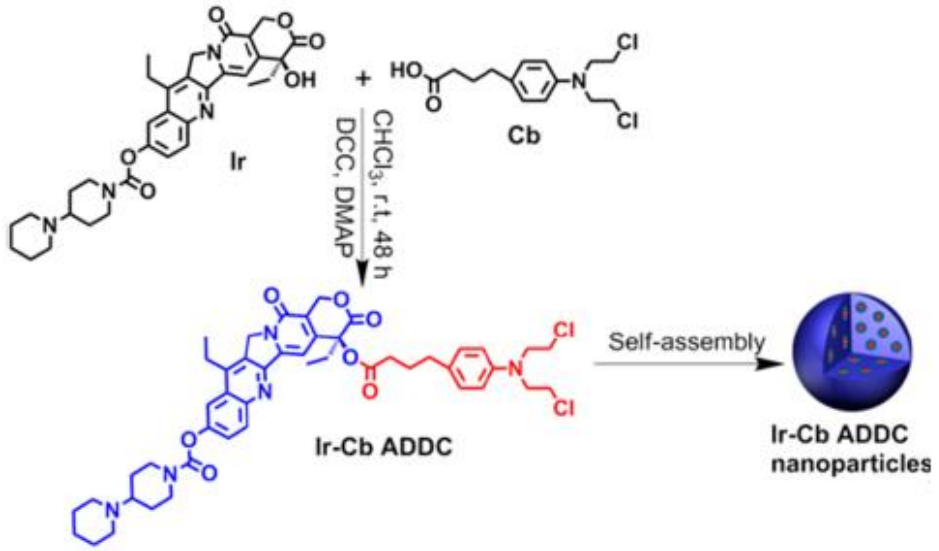

Figure 1.16 Schematic presentation of the amphiphilic drug-drug conjugate (ADDC) and its self-assembly into nanoparticles.

They have attached irinotecan (Ir) and Chlorumbucil (Cb), two renowned anticancer drugs by an ester linkage.[74] The hydrophilic nature of Ir and the hydrophobic nature of Cb provided the whole molecule an amphiphilic structure. This ADDC was shown to self-assemble into nanoparticles (Figure 1.8) in water providing longer retention time, which facilitates their accumulation inside tumor cells. Both the drugs exhibited synergetic cytotoxicity to the cancer cells leading to higher apoptosis compared to the free drugs. Lately, a number of ADDCs were developed by this group with the combination of various anticancer drugs.[75-76]

1.5 Importance of cleavable linkers in drug conjugation

As evident from the previous discussions, physical encapsulation of an anticancer drug within the carrier leads to its low bioavailability and results in poor effectiveness. To avoid these limitations, the concept of covalent conjugation of the drug with the carrier was introduced. Various conjugation strategies to achieve diverse goals have already been discussed in the previous sections. However, one important consideration during the design of a covalent conjugation strategy is the choice of the linker, through which the drug will be connected with the carrier. Several chemical moieties were engineered to obtain a specific stimuli-responsive release of the drug at the targeted site.

The linker design varied from a simple hydrolyzable bond to a specific one, which can be broken in response to a change in environment such as pH, specific enzymes or excess reducing agents. Disulfide linker was one of such kind, which has been extensively explored in drug delivery applications due to its easy conjugation chemistry and also the excess intracellular concentration of reducing agents like glutathione, cysteine.[77] Kong and his co-workers have designed doxorubicin–disulfide–methoxy polyethylene glycol conjugate, which can self-assemble to generate micelles.[78] The hydrophobic unit of the design was prepared by polymerizing doxorubicin (DOX) with disulfide-based diacrylate so that glutathione responsive cleavage of the disulfide bond will trigger the release of DOX from the micelles. Their results also demonstrated the sustained release of DOX from the micelles in presence of high concentration of glutathione.

Apart from these internal stimuli, some external stimuli like UV-light, near-infrared light, ultrasound, magnetic field etc. also gained much popularity for drug delivery. Several linkers were also designed to be cleavable by these kinds of external stimuli. Some of the linkers developed for drug delivery are listed in Table 1.6.

Table 1.6 Description of some cleavable linkers.

Cleavage condition	Cleavable group	Ref
Photo-responsive	o-nitrobenzyl based linker (cleavage at 300-365 nm)	79
	6-bromo 7-alkoxycoumarin-4-ylmethoxycarbonyl (Cleavable at 330 nm)	52
Enzyme	Val-Cit, Phe-Lys peptide (Cathepsin B), Ester (Esterase)	80
Reduction cleavable	Disulfide (Glutathione)	81
pH sensitive	Hydrazone (acid), Ester (acid)	82-83
Reactive oxygen	Poly (amino thioketal)	84
	Vinyldithioether	85

Among them, the progression in the development of light-responsive drug delivery was noteworthy.[86] Various photo-labile chemical units were designed and applied successfully for drug conjugation as well as to prepare nano vehicles. *o*-nitrobenzyl is such a kind of

photo-cleavable linker which has been explored most extensively for drug delivery. It can uncage the cargo upon irradiation under 365 nm UV-light which falls under relatively harmless UV-A region.[87] For example, Wang developed a modular aptamer drug conjugates (ApDC) where a phosphoramidite unit was designed and synthesized to carry 5-Fu.[43]

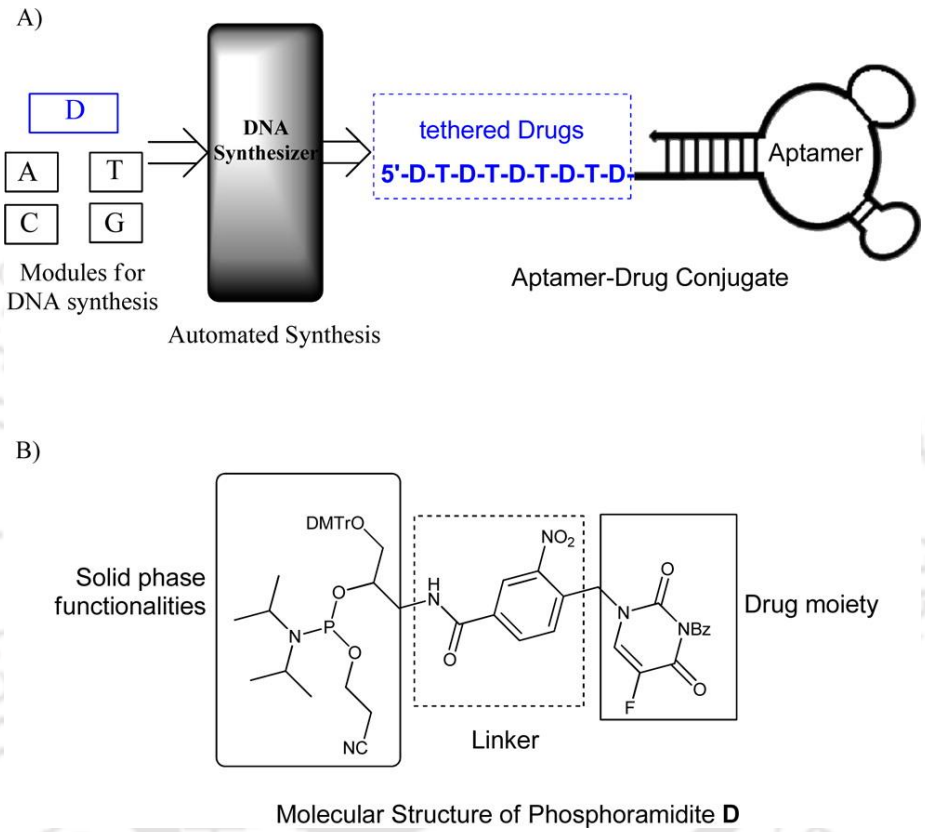

Figure 1.17 Schematic diagram of the aptamer 5-Fu conjugate.

The attachment of 5-FU with that aptamer was made through a photocleavable linker to obtain the spatiotemporal control over drug release (Figure 1.17). Then this phosphoramidite moiety serves as a building block that can be conjugated with a DNA aptamer, sgc8 by using an automated DNA synthesizer. The DNA aptamer sgc8 can selectively target protein tyrosine kinase 7 (PTK7) which is overexpressed in various cancer cells. This system was proven to deliver 5-Fu specifically to HCT116 cell line overexpressed with PTK7 in a photo-controlled and dose-dependent manner.

Not only drug conjugation *o*-nitrobenzyl moiety was also used to design nanocarriers as well as materials. Like Liu and his group have developed a Photo- and thermo-responsive

hydrogel comprised of a amphiphilic triblock copolymers, poly(N-isopropylacrylamide)-b-poly(4- acryloylmorpholine)-b-poly(2-((((2-nitrobenzyl)oxy)carbonyl)amino) ethyl methacrylate) (PNIPAM-b-PNAM-b-PNBOC).[88] The hydrogel was able to encapsulate water-soluble gemcitabine (GCT) and water-insoluble DOX drugs concomitantly. The co-release of both the drugs was regulated by either UV irradiation or temperature variations.

1.6 Conclusion

Short, synthesized peptides and other small molecule-based materials are rapidly emerging as powerful biomolecules that escalated its application widely, including in therapeutic research, due to their excellent biocompatibility and biodegradability. Self-assembly of peptides and amphiphiles has been explored largely to prepare various nanostructures. Synthesized amphiphilic biomolecules are also remarkably popular as theranostics and drug delivery systems (DDS).

Very recently, nanomedicines have gained ardent recognition in the chemotherapeutic world. Several nanomaterial-based chemotherapeutics have already found its utilization in clinical purposes. Lately, one component nanomedicines constructed with self-assembling drug conjugates have emerged as exceptionally beneficial to be used in chemotherapy. They have all the combined advantages of a nanomaterial and a drug conjugates such as (i) a fixed and higher drug loading content, (ii) avoidance of premature degradation and rapid clearance, (iii) retaining of inherent activity of the drug upon release from the conjugate, (iv) stimuli-responsive release of the drug, (v) targeted and controlled release of the drug etc. Many of them are also in clinical trial phases.

1.7 Objective of research work

The aim of this thesis is to synthesize peptide and other biomolecules, including drug conjugates to study their self-assembly properties as well as to explore their potential as controlled and targeted delivery systems.

Aiming the above, the following objectives have been formulated

a) Synthesis of peptide conjugated 5-Fu as nontoxic prodrug hydrogelator for controlled delivery of active 5-Fu. Covalent attachment of 5-Fu containing a

cleavable linker is expected to reduce the cytotoxicity and increase the stability of 5-Fu and thereby minimizing its side effects. Peptide 5-Fu conjugate is also designed to act as an amphiphile which can self-assemble to form hydrogel.

b) Originate a method to control the self-assembly of the previously synthesized 5-Fu peptide conjugate and forming nanoparticles from it. Due to the presence of hydrophobic phenylalanine moiety, the nanoparticles are also expected to entrap another hydrophobic anticancer agent. Thus the system will act as a dual drug delivery system.

c) Development of a dual responsive, dual drug carrier. Synthesis of an amphiphilic palmitic acid 5-Fu conjugate, which may display self-assembly characteristic to generate nanoparticles. The hydrophobic region of the molecule is also expected to carry a hydrophobic antitumor agent along with 5-Fu which is attached via a photo-cleavable linker. Moreover, the design of the molecule was made in such a way that its self-assembly could be broken in presence of an enzyme, overexpressed in certain cancer cells. Thus release of the hydrophobic agent is expected to occure specifically in the cancer cells in presence of excess GSH.

d) Synthesis of biotin 5-Fu conjugate to generate self-assembled nanostructures from it by utilizing its extensive hydrogen bonding capability. Methods to prepare hydrogel from it and also exploring the capacity of loading another water-soluble drug inside the hydrogel network. The molecule possesses all the advantages of covalent conjugation of drug. Additionally, the hydrogel is expected to behave as a dual drug delivery vehicle which will be able to release the drugs individually.

1.8 References

1. Panczyk, M., Pharmacogenetics research on chemotherapy resistance in colorectal cancer over the last 20 years. *World J. Gastroenterol.* **2014,** *20* (29), 9775-9827.

2. Malet-Martino, M.; Martino, R., Clinical studies of three oral prodrugs of 5-fluorouracil (capecitabine, UFT, S-1): a review. *The oncologist* **2002,** *7* (4), 288-323.

3. Pratt, S.; Shepard, R. L.; Kandasamy, R. A.; Johnston, P. A.; Perry, W.; Dantzig, A. H., The multidrug resistance protein 5 (ABCC5) confers resistance to 5-fluorouracil and transports its monophosphorylated metabolites. *Mol. Cancer Ther.* **2005,** *4* (5), 855-863.

4. Kamb, A.; Wee, S.; Lengauer, C., Why is cancer drug discovery so difficult? *Nat. Rev. Drug Discov.* **2007,** *6* (2), 115-120.

5. Allen, T. M.; Cullis, P. R., Drug delivery systems: entering the mainstream. *Science* **2004,** *303* (5665), 1818-1822.

6. Lee, P. I.; Li, J. X., Evolution of oral controlled release dosage forms. *Oral Controlled Release Formulation Design and Drug Delivery. John Wiley & Sons, Inc* **2010**, 21-31.

7. Tibbitt, M. W.; Dahlman, J. E.; Langer, R., Emerging frontiers in drug delivery. *J. Am. Chem. Soc.* **2016,** *138* (3), 704-717.

8. Mura, S.; Nicolas, J.; Couvreur, P., Stimuli-responsive nanocarriers for drug delivery. *Nat. Mater.* **2013,** *12* (11), 991-1003.

9. Fung, L. K.; Saltzman, W. M., Polymeric implants for cancer chemotherapy. *Adv. Drug Delivery Rev.* **1997,** *26* (2-3), 209-230.

10. Freiberg, S.; Zhu, X., Polymer microspheres for controlled drug release. *Int. J. Pharm.* **2004,** *282* (1-2), 1-18.

11. Kempe, S.; Mäder, K., In situ forming implants—an attractive formulation principle for parenteral depot formulations. *J. Control. Release* **2012,** *161* (2), 668-679.

12. Brannon-Peppas, L.; Blanchette, J. O., Nanoparticle and targeted systems for cancer therapy. *Adv. Drug Delivery Rev.* **2012,** *64*, 206-212.

13. Kalaydina, R.-V.; Bajwa, K.; Qorri, B.; Decarlo, A.; Szewczuk, M. R., Recent advances in "smart" delivery systems for extended drug release in cancer therapy. *Int. J. Nanomed.* **2018,** *13*, 4727-4745.

14. Huang, H.-C.; Barua, S.; Sharma, G.; Dey, S. K.; Rege, K., Inorganic nanoparticles for cancer imaging and therapy. *J. Control. Release* **2011,** *155* (3), 344-357.

15. Elzoghby, A. O.; Samy, W. M.; Elgindy, N. A., Protein-based nanocarriers as promising drug and gene delivery systems. *J. Control. Release* **2012,** *161* (1), 38-49.

16. Namiki, Y.; Fuchigami, T.; Tada, N.; Kawamura, R.; Matsunuma, S.; Kitamoto, Y.; Nakagawa, M., Nanomedicine for cancer: lipid-based nanostructures for drug delivery and monitoring. *Acc. Chem. Res.* **2011,** *44* (10), 1080-1093.

17. Dai, L.; Liu, J.; Luo, Z.; Li, M.; Cai, K., Tumor therapy: targeted drug delivery systems. *J. Mater. Chem. B* **2016,** *4* (42), 6758-6772.

18. Srinivasarao, M.; Low, P. S., Ligand-targeted drug delivery. *Chem. Rev.* **2017,** *117* (19), 12133-12164.

19. Jatzkewitz, H., Peptamin (glycyl-L-leucyl-mescaline) bound to blood plasma expander (polyvinylpyrrolidone) as a new depot form of a biologically active primary amine (mescaline). *Z. Naturforsch* **1955,** *10*, 27-31.

20. Ringsdorf, H. In Structure and properties of pharmacologically active polymers, *J. Polym. Sci., Polym. Symp.* **1975**, 35-153.

21. Graham, M. L., Pegaspargase: a review of clinical studies. *Adv. Drug Delivery Rev.* **2003,** *55* (10), 1293-1302.

22. Naing, A.; Papadopoulos, K. P.; Autio, K. A.; Ott, P. A.; Patel, M. R.; Wong, D. J.; Falchook, G. S.; Pant, S.; Whiteside, M.; Rasco, D. R., Safety, antitumor activity, and immune activation of pegylated recombinant human interleukin-10 (AM0010) in patients with advanced solid tumors. *J. Clin. Oncol.* **2016,** *34* (29), 3562-3569.

23. Paz-Ares, L.; Ross, H.; O'brien, M.; Riviere, A.; Gatzemeier, U.; Von Pawel, J.; Kaukel, E.; Freitag, L.; Digel, W.; Bischoff, H., Phase III trial comparing paclitaxel

poliglumex vs docetaxel in the second-line treatment of non-small-cell lung cancer. *Br. J. Cancer* **2008,** *98* (10), 1608-1613.

24. Pham, E.; Birrer, M. J.; Eliasof, S.; Garmey, E. G.; Lazarus, D.; Lee, C. R.; Man, S.; Matulonis, U. A.; Peters, C. G.; Xu, P., Translational impact of nanoparticle–drug conjugate CRLX101 with or without bevacizumab in advanced ovarian cancer. *Clin. Cancer Res.* **2015,** *21* (4), 808-818.

25. Liu, Z.; Marquez, M.; Nilsson, S.; Holmberg, A. R., Incubation with somatostatin, 5-aza decitabine and trichostatin up-regulates somatostatin receptor expression in prostate cancer cells. *Oncol. Rep.* **2008,** *20* (1), 151-154.

26. Nowotnik, D. P.; Cvitkovic, E., ProLindac™(AP5346): a review of the development of an HPMA DACH platinum polymer therapeutic. *Adv. Drug Delivery Rev.* **2009,** *61* (13), 1214-1219.

27. Nadler, L. M.; Stashenko, P.; Hardy, R.; Kaplan, W. D.; Button, L. N.; Kufe, D. W.; Antman, K. H.; Schlossman, S. F., Serotherapy of a patient with a monoclonal antibody directed against a human lymphoma-associated antigen. *Cancer Res.* **1980,** *40* (9), 3147-3154.

28. Elias, D. J.; Kline, L. E.; Robbins, B. A.; Johnson Jr, H.; Pekny, K.; Benz, M.; Robb, J. A.; Walker, L. E.; Kosty, M.; Dillman, R. O., Monoclonal antibody KS1/4-methotrexate immunoconjugate studies in non-small cell lung carcinoma. *Am. J. Respir. Crit. Care Med.* **1994,** *150* (4), 1114-1122.

29. Tolcher, A. W.; Sugarman, S.; Gelmon, K. A.; Cohen, R.; Saleh, M.; Isaacs, C.; Young, L.; Healey, D.; Onetto, N.; Slichenmyer, W., Randomized phase II study of BR96-doxorubicin conjugate in patients with metastatic breast cancer. *J. Clin. Oncol.* **1999,** *17* (2), 478-478.

30. Milenic, D. E.; Brady, E. D.; Brechbiel, M. W., Antibody-targeted radiation cancer therapy. *Nat. Rev. Drug Discov.* **2004,** *3* (6), 488-499.

31. Dewaraja, Y. K.; Schipper, M. J.; Roberson, P. L.; Wilderman, S. J.; Amro, H.; Regan, D. D.; Koral, K. F.; Kaminski, M. S.; Avram, A. M., 131I-tositumomab

radioimmunotherapy: Initial tumor dose–response results using 3-dimensional dosimetry including radiobiologic modeling. *J. Nucl. Med.* **2010,** *51* (7), 1155-1162.

32. Shimoni, A.; Avivi, I.; Rowe, J. M.; Yeshurun, M.; Levi, I.; Or, R.; Patachenko, P.; Avigdor, A.; Zwas, T.; Nagler, A., A randomized study comparing yttrium-90 ibritumomab tiuxetan (Zevalin) and high-dose BEAM chemotherapy versus BEAM alone as the conditioning regimen before autologous stem cell transplantation in patients with aggressive lymphoma. *Cancer* **2012,** *118* (19), 4706-4714.

33. Sharkey, R. M.; Govindan, S. V.; Cardillo, T. M.; Goldenberg, D. M., Epratuzumab–SN-38: a new antibody–drug conjugate for the therapy of hematologic malignancies. *Mol. Cancer Ther.* **2012,** *11* (1), 224-234.

34. Street, H. H.; Goris, M. L.; Fisher, G. A.; Wessels, B. W.; Cho, C.; Hernandez, C.; Zhu, H. J.; Zhang, Y.; Nangiana, J. S.; Shan, J. S., Phase I study of 131I-chimeric (ch) TNT-1/B monoclonal antibody for the treatment of advanced colon cancer. *Cancer Biother. Radiopharm.* **2006,** *21* (3), 243-256.

35. Trikha, M.; Yan, L.; Nakada, M. T., Monoclonal antibodies as therapeutics in oncology. *Curr. Opin. Biotechnol.* **2002,** *13* (6), 609-614.

36. Zhu, G.; Chen, X., Aptamer-based targeted therapy. *Adv. Drug Delivery Rev.* **2018**, *134*, 65-78.

37. Bates, P. J.; Reyes-Reyes, E. M.; Malik, M. T.; Murphy, E. M.; O'toole, M. G.; Trent, J. O., G-quadruplex oligonucleotide AS1411 as a cancer-targeting agent: Uses and mechanisms. *Biochim. Biophys. Acta* **2017,** *1861* (5), 1414-1428.

38. Wu, C.; Han, D.; Chen, T.; Peng, L.; Zhu, G.; You, M.; Qiu, L.; Sefah, K.; Zhang, X.; Tan, W., Building a multifunctional aptamer-based DNA nanoassembly for targeted cancer therapy. *J. Am. Chem. Soc.* **2013,** *135* (49), 18644-18650.

39. Lupold, S. E.; Hicke, B. J.; Lin, Y.; Coffey, D. S., Identification and characterization of nuclease-stabilized RNA molecules that bind human prostate cancer cells via the prostate-specific membrane antigen. *Cancer Res.* **2002,** *62* (14), 4029-4033.

40. Ferreira, C.; Matthews, C.; Missailidis, S., DNA aptamers that bind to MUC1 tumour marker: design and characterization of MUC1-binding single-stranded DNA aptamers. *Tumor Biol.* **2006,** *27* (6), 289-301.

41. Chi-hong, B. C.; Chernis, G. A.; Hoang, V. Q.; Landgraf, R., Inhibition of heregulin signaling by an aptamer that preferentially binds to the oligomeric form of human epidermal growth factor receptor-3. *Proc. Natl. Acad. Sci. U.S.A.* **2003,** *100* (16), 9226-9231.

42. Huang, Y. F.; Shangguan, D.; Liu, H.; Phillips, J. A.; Zhang, X.; Chen, Y.; Tan, W., Molecular assembly of an aptamer–drug conjugate for targeted drug delivery to tumor cells. *ChemBioChem* **2009,** *10* (5), 862-868.

43. Wang, R.; Zhu, G.; Mei, L.; Xie, Y.; Ma, H.; Ye, M.; Qing, F.-L.; Tan, W., Automated modular synthesis of aptamer–drug conjugates for targeted drug delivery. *J. Am. Chem. Soc.* **2014,** *136* (7), 2731-2734.

44. Leamon, C. P.; Low, P. S., Folate-mediated targeting: from diagnostics to drug and gene delivery. *Drug Discov. Today* **2001,** *6* (1), 44-51.

45. Yang, W.; Cheng, Y.; Xu, T.; Wang, X.; Wen, L.-p., Targeting cancer cells with biotin–dendrimer conjugates. *Eur. J. Med. Chem.* **2009,** *44* (2), 862-868.

46. Kozikowski, A. P.; Nan, F.; Conti, P.; Zhang, J.; Ramadan, E.; Bzdega, T.; Wroblewska, B.; Neale, J. H.; Pshenichkin, S.; Wroblewski, J. T., Design of remarkably simple, yet potent urea-based inhibitors of glutamate carboxypeptidase II (NAALADase). *J. Med. Chem.* **2001,** *44* (3), 298-301.

47. Supuran, C. T., Carbonic anhydrase inhibition and the management of hypoxic tumors. *Metabolites* **2017,** *7* (3), 48.

48. Vergote, I.; Leamon, C. P., Vintafolide: a novel targeted therapy for the treatment of folate receptor expressing tumors. *Ther. Adv. Med. Oncol.* **2015,** *7* (4), 206-218.

49. Krall, N.; Pretto, F.; Neri, D., A bivalent small molecule-drug conjugate directed against carbonic anhydrase IX can elicit complete tumour regression in mice. *Chem. Sci.* **2014,** *5* (9), 3640-3644.

50. Ibsen, S.; Zahavy, E.; Wrasdilo, W.; Berns, M.; Chan, M.; Esener, S., A novel doxorubicin prodrug with controllable photolysis activation for cancer chemotherapy. *Pharm. Res.* **2010,** *27* (9), 1848-1860.

51. Maiti, S.; Park, N.; Han, J. H.; Jeon, H. M.; Lee, J. H.; Bhuniya, S.; Kang, C.; Kim, J. S., Gemcitabine–coumarin–biotin conjugates: a target specific theranostic anticancer prodrug. *J. Am. Chem. Soc.* **2013,** *135* (11), 4567-4572.

52. Chen, S.; Zhao, X.; Chen, J.; Chen, J.; Kuznetsova, L.; Wong, S. S.; Ojima, I., Mechanism-based tumor-targeting drug delivery system. Validation of efficient vitamin receptor-mediated endocytosis and drug release. *Bioconjugate Chem.* **2010,** *21* (5), 979-987.

53. Cui, H.; Webber, M. J.; Stupp, S. I., Self-assembly of peptide amphiphiles: From molecules to nanostructures to biomaterials. *Peptide Science: Original Research on Biomolecules* **2010,** *94* (1), 1-18.

54. Gao, C.; Bhattarai, P.; Chen, M.; Zhang, N.; Hameed, S.; Yue, X.; Dai, Z., Amphiphilic Drug Conjugates as Nanomedicines for Combined Cancer Therapy. *Bioconjugate Chem.* **2018,** *29* (12), 3967-3981.

55. Chen, X.; Plasencia, C.; Hou, Y.; Neamati, N., Synthesis and biological evaluation of dimeric RGD peptide− paclitaxel conjugate as a model for integrin-targeted drug delivery. *J. Med. Chem.* **2005,** *48* (4), 1098-1106.

56. Bidwell III, G. L.; Fokt, I.; Priebe, W.; Raucher, D., Development of elastin-like polypeptide for thermally targeted delivery of doxorubicin. *Biochem. Pharmacol.* **2007,** *73* (5), 620-631.

57. Kale, A. A.; Torchilin, V. P., Enhanced transfection of tumor cells in vivo using "Smart" pH-sensitive TAT-modified pegylated liposomes. *J. Drug Target.* **2007,** *15* (7-8), 538-545.

58. Sethuraman, V. A.; Bae, Y. H., TAT peptide-based micelle system for potential active targeting of anti-cancer agents to acidic solid tumors. *J. Control. Release* **2007,** *118* (2), 216-224.

59. Wang, R.-H.; Bai, J.; Deng, J.; Fang, C.-J.; Chen, X., TAT-modified gold nanoparticle carrier with enhanced anticancer activity and size effect on overcoming multidrug resistance. *ACS Appl. Mater. Interfaces* **2017,** *9* (7), 5828-5837.

60. Pan, L.; He, Q.; Liu, J.; Chen, Y.; Ma, M.; Zhang, L.; Shi, J., Nuclear-targeted drug delivery of TAT peptide-conjugated monodisperse mesoporous silica nanoparticles. *J. Am. Chem. Soc.* **2012,** *134* (13), 5722-5725.

61. Shi, K.; Li, J.; Cao, Z.; Yang, P.; Qiu, Y.; Yang, B.; Wang, Y.; Long, Y.; Liu, Y.; Zhang, Q., A pH-responsive cell-penetrating peptide-modified liposomes with active recognizing of integrin αvβ3 for the treatment of melanoma. *J. Control. Release* **2015,** *217*, 138-150.

62. Yang, X.; Hong, H.; Grailer, J. J.; Rowland, I. J.; Javadi, A.; Hurley, S. A.; Xiao, Y.; Yang, Y.; Zhang, Y.; Nickles, R. J., cRGD-functionalized, DOX-conjugated, and 64Cu-labeled superparamagnetic iron oxide nanoparticles for targeted anticancer drug delivery and PET/MR imaging. *Biomaterials* **2011,** *32* (17), 4151-4160.

63. Schiffelers, R. M.; Ansari, A.; Xu, J.; Zhou, Q.; Tang, Q.; Storm, G.; Molema, G.; Lu, P. Y.; Scaria, P. V.; Woodle, M. C., Cancer siRNA therapy by tumor selective delivery with ligand-targeted sterically stabilized nanoparticle. *Nuc. Acids Res.* **2004,** *32* (19), e149-e149.

64. Zhang, N.; Tao, J.; Hua, H.; Sun, P.; Zhao, Y., Low-density lipoprotein peptide-combined DNA nanocomplex as an efficient anticancer drug delivery vehicle. *Eur. J. Pharm. Biopharm* **2015,** *94*, 20-29.

65. Costantino, L.; Gandolfi, F.; Tosi, G.; Rivasi, F.; Vandelli, M. A.; Forni, F., Peptide-derivatized biodegradable nanoparticles able to cross the blood–brain barrier. *J. Control. Release* **2005,** *108* (1), 84-96.

66. Nagy, A.; Schally, A. V.; Armatis, P.; Szepeshazi, K.; Halmos, G.; Kovacs, M.; Zarandi, M.; Groot, K.; Miyazaki, M.; Jungwirth, A., Cytotoxic analogs of luteinizing hormone-releasing hormone containing doxorubicin or 2-pyrrolinodoxorubicin, a derivative 500-1000 times more potent. *Proc. Natl. Acad. Sci. U.S.A.* **1996,** *93* (14), 7269-7273.

67. Green, M.; Loewenstein, P. M., Autonomous functional domains of chemically synthesized human immunodeficiency virus tat trans-activator protein. *Cell* **1988,** *55* (6), 1179-1188.

68. Accardo, A.; Mansi, R.; Morisco, A.; Mangiapia, G.; Paduano, L.; Tesauro, D.; Radulescu, A.; Aurilio, M.; Aloj, L.; Arra, C., Peptide modified nanocarriers for selective targeting of bombesin receptors. *Mol. BioSyst.* **2010,** *6* (5), 878-887.

69. Wender, P. A.; Mitchell, D. J.; Pattabiraman, K.; Pelkey, E. T.; Steinman, L.; Rothbard, J. B., The design, synthesis, and evaluation of molecules that enable or enhance cellular uptake: peptoid molecular transporters. *Proc. Natl. Acad. Sci. U.S.A.* **2000,** *97* (24), 13003-13008.

70. Cheetham, A. G.; Zhang, P.; Lin, Y.-a.; Lock, L. L.; Cui, H., Supramolecular nanostructures formed by anticancer drug assembly. *J. Am. Chem. Soc.* **2013,** *135* (8), 2907-2910.

71. Lin, R.; Cheetham, A. G.; Zhang, P.; Lin, Y.-a.; Cui, H., Supramolecular filaments containing a fixed 41% paclitaxel loading. *Chem. Commun.* **2013,** *49* (43), 4968-4970.

72. Jin, Q.; Mitschang, F.; Agarwal, S., Biocompatible drug delivery system for photo-triggered controlled release of 5-fluorouracil. *Biomacromolecules* **2011,** *12* (10), 3684-3691.

73. Tan, X.; Li, B. B.; Lu, X.; Jia, F.; Santori, C.; Menon, P.; Li, H.; Zhang, B.; Zhao, J. J.; Zhang, K., Light-triggered, self-immolative nucleic Acid-drug nanostructures. *J. Am. Chem. Soc.* **2015,** *137* (19), 6112-6115.

74. Huang, P.; Wang, D.; Su, Y.; Huang, W.; Zhou, Y.; Cui, D.; Zhu, X.; Yan, D., Combination of small molecule prodrug and nanodrug delivery: amphiphilic drug–drug conjugate for cancer therapy. *J. Am. Chem. Soc.* **2014,** *136* (33), 11748-11756.

75. Hu, M.; Huang, P.; Wang, Y.; Su, Y.; Zhou, L.; Zhu, X.; Yan, D., Synergistic combination chemotherapy of camptothecin and floxuridine through self-assembly of amphiphilic drug–drug conjugate. *Bioconjugate Chem.* **2015,** *26* (12), 2497-2506.

76. Wang, Y.; Huang, P.; Hu, M.; Huang, W.; Zhu, X.; Yan, D., Self-delivery nanoparticles of amphiphilic methotrexate-gemcitabine prodrug for synergistic combination chemotherapy via effect of deoxyribonucleotide pools. *Bioconjugate Chem.* **2016,** *27* (11), 2722-2733.

77. Lee, M. H.; Sessler, J. L.; Kim, J. S., Disulfide-based multifunctional conjugates for targeted theranostic drug delivery. *Acc. Chem. Res.* **2015,** *48* (11), 2935-2946.

78. Duan, X.; Bai, T.; Du, J.; Kong, J., One-pot synthesis of glutathione-responsive amphiphilic drug self-delivery micelles of doxorubicin–disulfide–methoxy polyethylene glycol for tumor therapy. *J. Mater. Chem. B* **2018,** *6* (1), 39-43.

79. Agasti, S. S.; Chompoosor, A.; You, C.-C.; Ghosh, P.; Kim, C. K.; Rotello, V. M., Photoregulated release of caged anticancer drugs from gold nanoparticles. *J. Am. Chem. Soc.* **2009,** *131* (16), 5728-5729.

80. Dubowchik, G. M.; Firestone, R. A.; Padilla, L.; Willner, D.; Hofstead, S. J.; Mosure, K.; Knipe, J. O.; Lasch, S. J.; Trail, P. A., Cathepsin B-labile dipeptide linkers for lysosomal release of doxorubicin from internalizing immunoconjugates: model studies of enzymatic drug release and antigen-specific in vitro anticancer activity. *Bioconjugate Chem.* **2002,** *13* (4), 855-869.

81. Yin, S.; Huai, J.; Chen, X.; Yang, Y.; Zhang, X.; Gan, Y.; Wang, G.; Gu, X.; Li, J., Intracellular delivery and antitumor effects of a redox-responsive polymeric paclitaxel conjugate based on hyaluronic acid. *Acta Biomater.* **2015,** *26*, 274-285.

82. Patil, R.; Portilla-Arias, J.; Ding, H.; Konda, B.; Rekechenetskiy, A.; Inoue, S.; Black, K. L.; Holler, E.; Ljubimova, J. Y., Cellular delivery of doxorubicin via pH-controlled hydrazone linkage using multifunctional nano vehicle based on poly (β-L-malic acid). *Int. J. Mol. Sci.* **2012,** *13* (9), 11681-11693.

83. Vemula, P. K.; Cruikshank, G. A.; Karp, J. M.; John, G., Self-assembled prodrugs: An enzymatically triggered drug-delivery platform. *Biomaterials* **2009,** *30* (3), 383-393.

84. Shim, M. S.; Xia, Y., A reactive oxygen species (ROS)-responsive polymer for safe, efficient, and targeted gene delivery in cancer cells. *Angew. Chem. Int. Ed.* **2013,** *52* (27), 6926-6929.

85. Saravanakumar, G.; Lee, J.; Kim, J.; Kim, W. J., Visible light-induced singlet oxygen-mediated intracellular disassembly of polymeric micelles co-loaded with a photosensitizer and an anticancer drug for enhanced photodynamic therapy. *Chem. Commun.* **2015,** *51* (49), 9995-9998.

86. Linsley, C. S.; Wu, B. M., Recent advances in light-responsive on-demand drug-delivery systems. *Ther. Delivery* **2017,** *8* (2), 89-107.

87. Klán, P.; Solomek, T.; Bochet, C. G.; Blanc, A. l.; Givens, R.; Rubina, M.; Popik, V.; Kostikov, A.; Wirz, J., Photoremovable protecting groups in chemistry and biology: reaction mechanisms and efficacy. *Chem. Rev.* **2012,** *113* (1), 119-191.

88. Wang, C.; Zhang, G.; Liu, G.; Hu, J.; Liu, S., Photo-and thermo-responsive multicompartment hydrogels for synergistic delivery of gemcitabine and doxorubicin. *J. Control. Release* **2017,** *259*, 149-159.

Chapter 2

Synthesis of a Peptide Conjugated 5-Fluorouracil Gelator for Controlled Drug Delivery

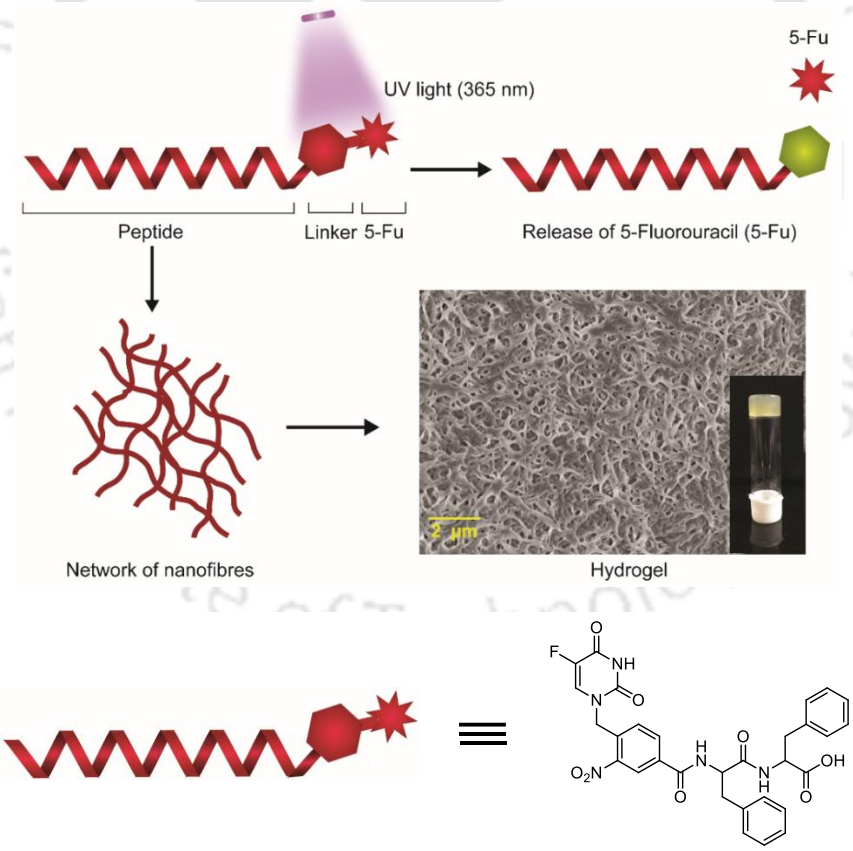

2.1 Introduction

Short peptides, oligonucleotides and other synthetic biomolecules have shown remarkable advantages as therapeutic agents[1-3] and also as cargo[4] to carry pharmaceutically active molecules. Design and synthesis of biomolecules covalently tethered to a drug can be made target specific.[5-6] Secondly, such covalent attachment could be utilized to inactivate the drug, thereby reducing the side effects. This is particularly very important for cancer treatment, as most of the antitumor agents show high cytotoxicity towards normal cells. With the rapid progression in therapeutic research, drug delivery has emerged as a pivotal area in medicinal chemistry.[7] It is now well known that the efficacy of a therapeutic agent depends on the pharmacokinetics and pharmacodynamics of the drug after administration. So controlling these two factors is urgently needed in order to achieve utmost potency of a drug. After decades of research, drug delivery systems (DDS) not only address the issue of efficiency of a drug but also improves the tolerability, target specificity, controlled release of the drugs and solubility of hydrophobic drugs. Various synthetic strategies have been adopted to achieve a better solution to such factors. For targeting the cancer cells, a number of pathways were followed. Prof. Tan and other research groups have used DNA aptamers[8-9] to target tumor cells. The DDS was made by conjugating the drug with the aptamer moiety. Not only aptamer, peptides have also been used to target cancer cells. Wu and his coworkers have used CGNSNPKSC peptide sequence to target the vasculature endothelial cells of human gastric cancer.[10] Nishimoto and his team have used CNGRC peptide for targeting the tumor cells.[11] Along with these tumor homing peptides, antibodies,[12-13] oligonucleotides,[14] were also adopted for specific targeting of tumor cells, so that antitumor drugs can be delivered in a site-specific manner. To improve solubility, a number of drug carriers have been explored.[15-16] Prof Tamanoi and his group have shown the delivery of hydrophobic drug camptothecin by incorporating it inside mesoporous silica nanoparticles.[17] In addition, macromolecules,[18] including bio-compatible and bio-degradable polymers,[19] have been employed in the past, for loading antitumor agents such as 5-Fu,[20] doxorubicin [21] and camptothecin [22] through non-covalent interactions.

Such carriers were used to improve solubility, cell-permeability as well as various material properties of the drug delivery systems, such as nanomaterials or gel properties.

In this report, we demonstrate the development of a model peptide-prodrug conjugate to deliver chemotherapeutic drug 5-Fu. It is a renowned anticancer agent, widely used to manage malignancy in colon cancer. It also has major application as an antimetabolite drug to treat respiratory, head, breast and neck cancer.[23] However, its clinical application is limited due to a number of reasons, such as low bioavailability and side effects generated by nonspecific absorption.[24] Therefore, numerous DDSs were designed to increase their efficacy. A vast array of nanoparticle formulations were proposed to encapsulate 5-Fu to gain better delivery. Apart from nanoparticles, vesicular systems, namely liposomes, niosomes, beads, lipoproteins, hydrogel and clay materials have also been extensively studied as carriers of 5-Fu.[25]

In most of the cases, drugs are encased inside the delivery vehicle by non-covalent interactions. However, this process often suffers from various disadvantages like low drug loading and uncontrolled release of the encapsulated drug. Interestingly, a new strategy had been adopted where the drug is covalently attached with the DDS, allowing a fixed and better drug loading content. In such cases, drug release is controlled by the careful selection of the cleavable linker, which connects the drug with the rest of the DDS. This prodrug strategy,[26] *i.e.* covalent attachment of a drug with the carrier is broadly utilized to conjugate a drug molecule with peptides,[27] polymers,[28] dendrimers[29] and nanoparticles.[30] Most recently peptide-based drug amphiphiles were developed which can self-assemble to form hydrogels [31-32] as well as various nanostructures for the delivery of antitumor agents. [33-34]

Herein, we have developed a dipeptide conjugated 5-Fu amphiphile as a potential delivery system of the targeted drug. Furthermore, this synthesized DDS can self-assemble to form hydrogel. The photocleavable linker is preferred for model study because of its ability to cleave and release the payload by irradiation at 365 nm, which falls under relatively harmless UV-A region.[35] The advantage of covalently conjugated 5-Fu is that, it can act as a non-toxic prodrug and the active drug (5-Fu) could only be released under external stimulation, in a dose-dependent and controlled manner.

2.2 Results and Discussion

2.2.1 Design and synthesis of 5-Fu-peptide conjugated amphiphiles 2d and 2e

In this article, a phenylalanine-phenylalanine (FF) dipeptide was covalently conjugated to antitumor agent 5-Fu through a photo-cleavable 4-bromomethyl-3-nitrobenzoic acid moiety. Such covalent attachment of drugs has several advantages over the encapsulated drugs. Being covalently linked, the drugs could be made nontoxic to the unaffected cells, unless being cleaved upon stimulation. Moreover, the concentration of the effective drug could be controlled by varying the dose of the external stimuli. Scheme 2.1 demonstrates the step-wise synthesis of the FF-5-Fu conjugate **2d** and **2e**, respectively.

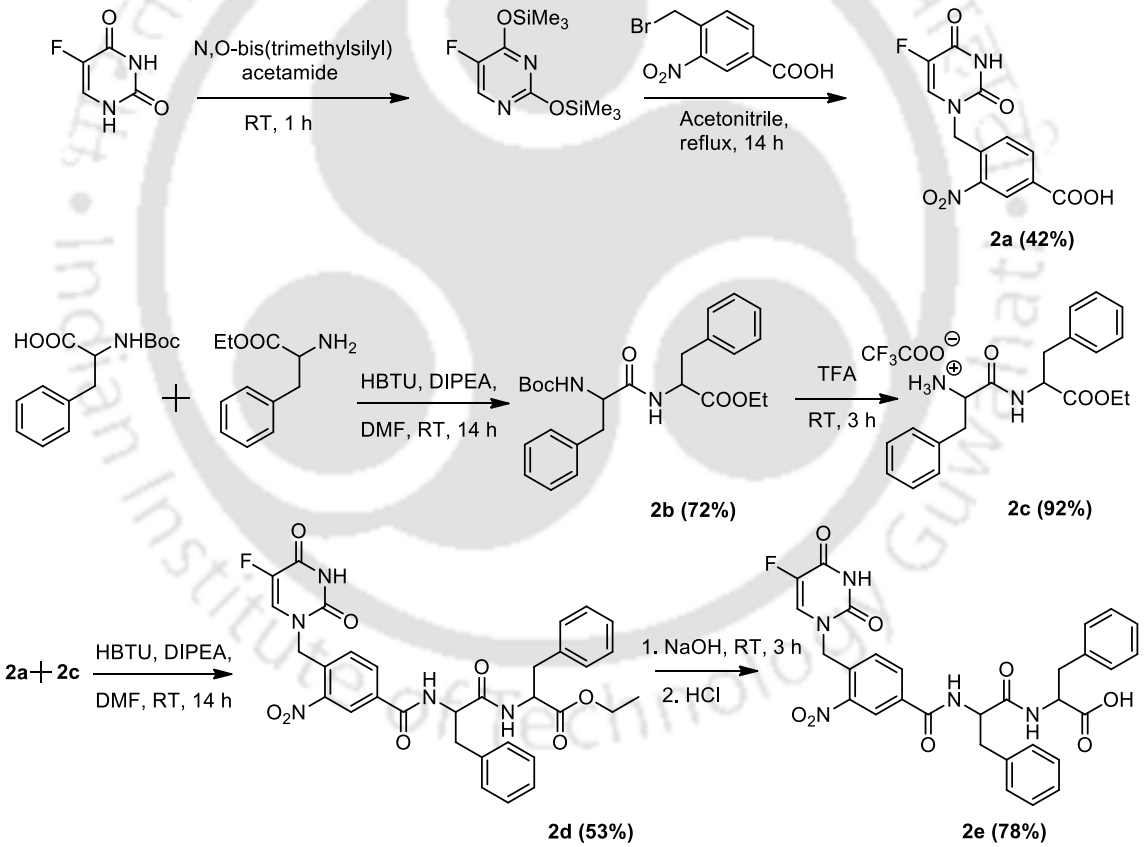

Scheme 2.1 Schematic presentation for the synthesis of 5-Fu-FF dipeptide conjugate.

The attachment of 5-Fu with 4-bromomethyl-3-nitrobenzoic acid was performed following a published protocol with minor modification for improvement of the yield.[11]

In short, 5-Fu was reacted with the linker *N*,*O*-bis(trimethylsilyl) acetamide to produce 5-fluoro-2,4-bis((trimethylsilyl)oxy)-1,2,3,4-tetrahydropyrimidine which was refluxed further with 4-bromomethyl-3-nitrobenzoic acid in dry acetonitrile under the dark condition to obtain the 5-Fu-linker (compound **2a**). The FF dipeptide having both protected *N*- and C-terminal (compound **2b**) was prepared separately by the standard solution-phase protocol using *N*,*N*,*N*′,*N*′-Tetramethyl-*O*-(1*H*-benzotriazol-1-yl)uronium hexafluorophosphate (HBTU) and *N*, *N*-Diisopropylethylamine (DIPEA) as the activator. The acid-labile *N*-terminal protecting group of the dipeptide was deprotected by using trifluoroacetic acid (TFA), producing compound **2c**. The resultant *N*-terminal free FF dipeptide was again coupled with compound **2a** that yielded **2d**. The ester group at the C-terminal of **2d** was further hydrolyzed by base-catalyzed hydrolysis reaction to produce compound **2e** (5-Fu-FF-COOH).

2.2.2 Preparation of gels from 2d and 2e

The self-assembly properties of our synthesized compounds were extensively studied by varying solvents and pH. Compound **2d** and **2e** both were highly soluble in DMSO and at a certain concentration, both of them formed nanofibers that can entrap the solvent, producing an organogel. The formation of gel was confirmed by inverse vial test (Figure 1a, 1b). The minimum concentration required to exhibit gelation property was 1 wt% for both the compounds. Compound **2d**, having a free ester group, was sparingly soluble in water whereas compound **2e** was found to be readily soluble in water above pH 8. However, it started precipitating below pH 6. Between this narrow pH window of 6 to 8, compound **2e** successfully formed the desired hydrogel (2 wt%). The sol-gel transition temperature (T_g) of the hydrogel of compound **2e** was estimated to be 62 ˚C and that of the DMSO gel of compound **2d** was 65 ˚C.

2.2.3 Morphological analysis of self-assembled structures

The morphology of the self-assembled structures of compound **2d** in DMSO and **2e** in different solvents were investigated by field emission scanning electron microscope (FESEM). Compound **2e** was dissolved in different solvents and the solution was drop casted on a glass plate covered with aluminium foil whereas all the gels were dried and the obtained xerogels were subjected to FESEM analysis. A fibrillar morphology was

observed for hydrogel and both the DMSO gels (Figure 2.1 a, b, c). The fibers were several micrometers long and the width was in the nanometer range. They also displayed aggregation tendency, as evident from their varying widths observed in the FESEM images. Due to this aggregation, the fibers became intertwined, forming a closely packed network with inter-fibrillar pores, which were clearly visible in the FESEM images. These pores might be responsible for entrapping the solvents, causing the gelation.[36] Additionally, compound **2e** displayed various types of self-assembled structures in methanol, ethanol, dimethylformamide (DMF) solvents (Figure 2.1d, e, f, g).

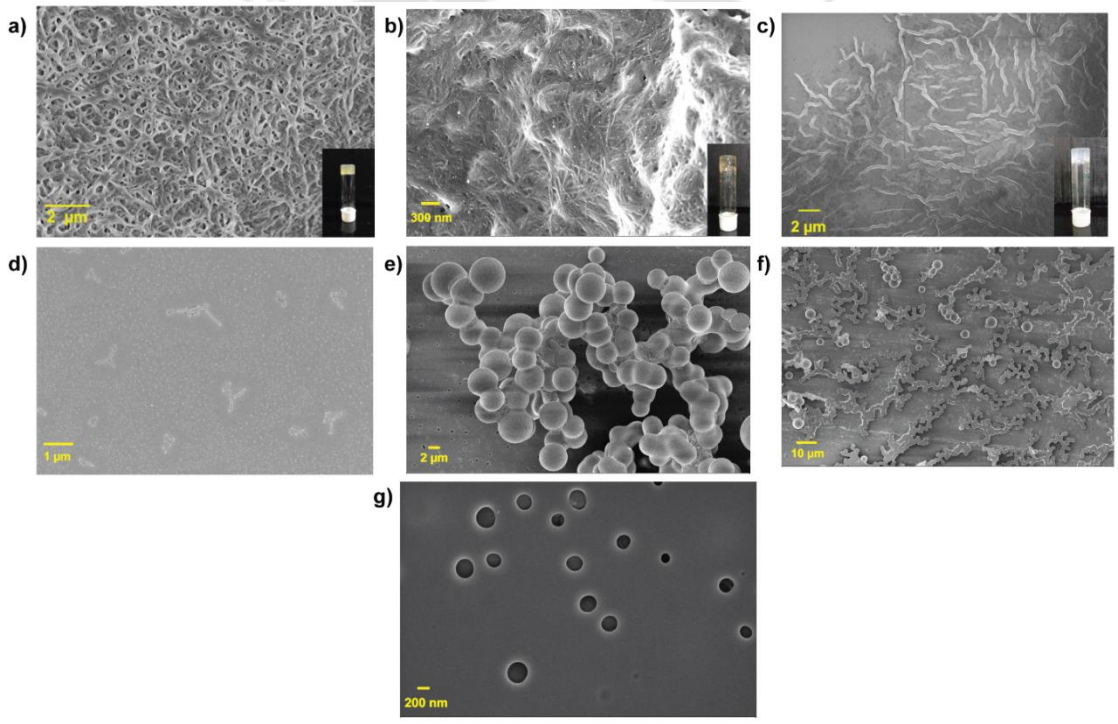

Figure 2.1 FESEM images of a) hydrogel formed by compound **2e**, b) DMSO gel formed by compound **2e**, c) DMSO gel formed by compound **2d**, self-assembly of compound **2e** in d) DMF, e), f) methanol, g) ethanol.

2.2.4 Rheological studies of peptide drug hydrogel

In order to measure the mechanical strength of the hydrogel, rheological studies were performed at 25 ºC using Anton-Paar MCR 102 rheometer having a measuring system of 20 mm parallel plate. At first, an amplitude sweep test was done to measure, the linear viscoelastic region (LVR) within which the applied strain does not have any effect on the

storage modulus *G´* and loss modulus *G´´*. In the strain sweep graph (Figure 2.2a), it is noticeable that the storage modulus *G´* is enough larger than the loss modulus *G´´* and the difference between them remained almost constant up to a strain of 10%. With the identified LVR for our hydrogel frequency sweep study was carried out at a constant strain of 0.1% and the hydrogel has shown a frequency-independent behavior within the range of 0.1-10 rad/s (Figure 2.2b). From the frequency sweep graph, it can also be noted that G´ is higher than G´´ in the lower LVE which demonstrates a gel phase formation by the material.[37] Frequency sweeps are usually performed to have an idea about the stiffness of a hydrogel.[38] The gel was found to display a comparatively high storage modulus (*G´*) around 10^3 Pa, which implicates about the formation of a quite stiff hydrogel.

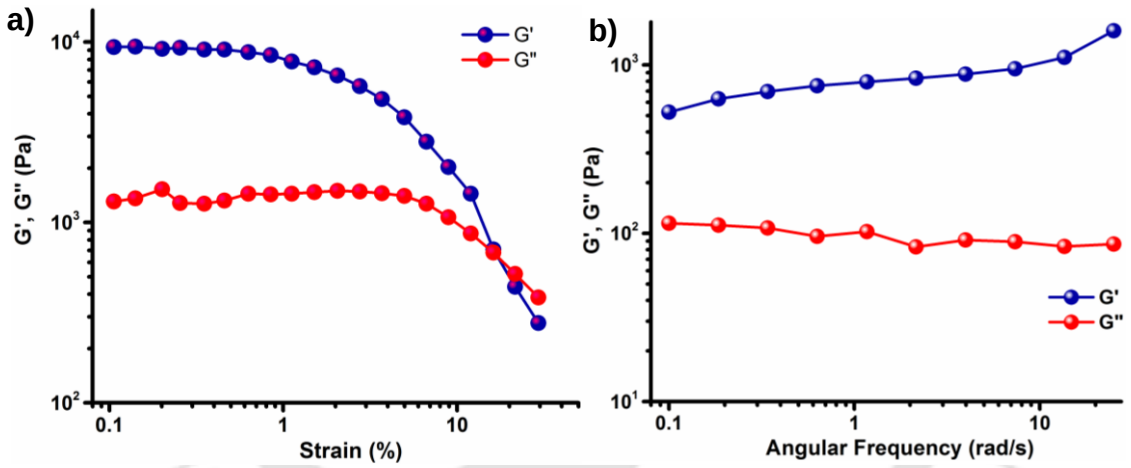

Figure 2.2 Rheological study of the hydrogel showing a) amplitude sweep b) frequency sweep.

2.2.5 Orientation of compound 2e during hydrogelation:

The conformation of the 5-Fu-FF drug-peptide conjugate, during gelation, is further investigated by circular dichroism (CD) and Fourier-transform infrared spectroscopy (FTIR). Figure 2.3b demonstrates CD spectra of the aqueous solution of compound **2e** in various concentration. A negative peak around 227 nm in the CD spectrum of compound **2e** indicates a *β*-sheet-like conformation.[39] The disappearance of the *β*-sheet structure was observed upon dilution below 18 µM concentration, apparently, due to loss of self-assembly structure.

The above observation was further supported by the FTIR analysis of the dried hydrogel. Useful information about the amide I stretching band and amide II bending peak can be acquired from the range of 1500-1800 cm^{-1} in FTIR spectra.[40] The obtained spectra of the dried hydrogel displayed (Figure 2.3a) a strong band at 1637 cm^{-1} and weak bands at 1695 cm^{-1} and 1733 cm^{-1} which suggests about an antiparallel *β*-sheet conformation[41-44] adopted by the peptide drug conjugate by extensive hydrogen bonding interaction. Another strong band at 1532 cm^{-1} is also known to be associated with antiparallel *β*-sheet conformation. However, this band may also arise from the C-N stretching frequency of the $–NO_2$ group present in our molecule.

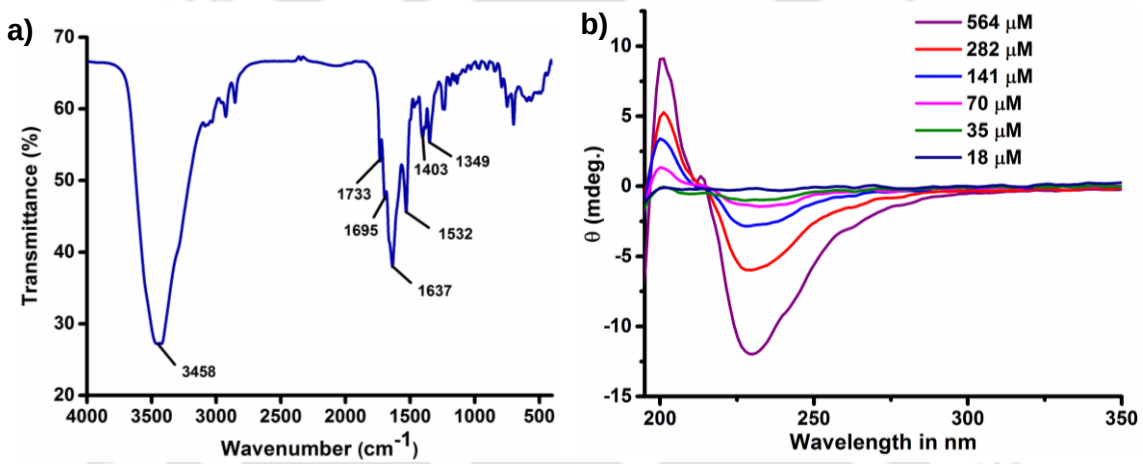

Figure 2.3 a) FTIR spectra of the dried hydrogel of compound **2e**, b) concentration-dependent CD spectra of compound **2e** in water.

2.2.6 Controlled, dose-dependent in vitro release of 5-Fu upon UV irradiation

Irradiation experiment was carried out to estimate the time-dependent release of 5-Fu under UV light (365 nm). An 85 µM solution of compound **2e** in acetonitrile/water (6:1 v/v), taken in a quartz cell, was irradiated and the course of photocleavage was monitored by reverse-phase (RP) HPLC. At a regular time interval, a fixed quantity of photolysate was collected and analyzed by RP-HPLC. The HPLC profile, depicted in Figure 2.4b, shows the appearance of a new peak upon irradiation. A control experiment with pure 5-Fu clearly proves that the new peak with a retention time of 3.5 min is that of 5-Fu. Moreover, this peak was isolated and a subsequent HRMS analysis confirms the compound to be 5-Fu. It is, therefore, evident that a clear photocleavage reaction had

occurred producing free 5-Fu as the photoproduct. The percentage release of 5-Fu was quantified using RP-HPLC. As evident from Figure 2.4b, with increasing irradiation, the peak area of 5-Fu was gradually increasing, whereas the peak area of compound **2e** was decreasing. As calculated from the HPLC, about 16% drug was released after 20 minutes of irradiation and the amount increased up to 26% when irradiated for 40 minutes. Another set of solution having the same concentration as previous was kept in dark and the release of 5-Fu was also monitored from this solution. It was observed that the photocleavage phenomenon did not occur in absence of UV light (365 nm). This implies the release of 5-Fu from the synthesized prodrug peptide conjugate (compound **2e**) in a photo-responsive manner.

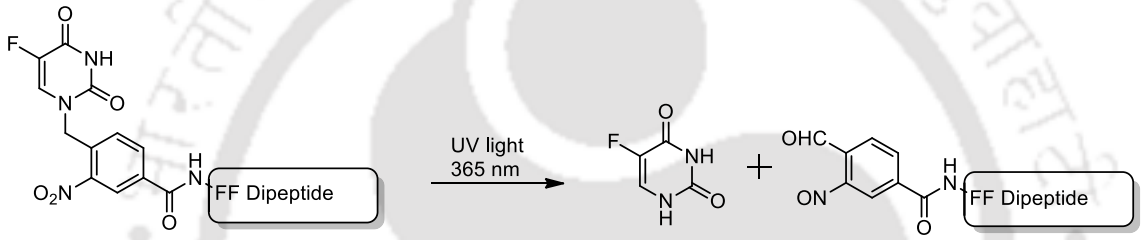

Scheme 2.2 The mechanism of photo cleavage reaction for the release of 5-Fu and *o*-nitrosobenzaldehyde.

The progress of the photocleavage reaction was also followed by UV-Vis spectroscopy. The appearance of a weak absorption band at 325 nm, which corresponds to the generation of photoproduct (Scheme 2.2) *o*-nitroso benzaldehyde[45-46] was clearly noticeable in the UV-Vis spectra of the irradiated solution of compound **2e** (Figure 2.4a). A gradual increase in the absorbance at 325 nm indicates the advancement of the photo-induced reaction.

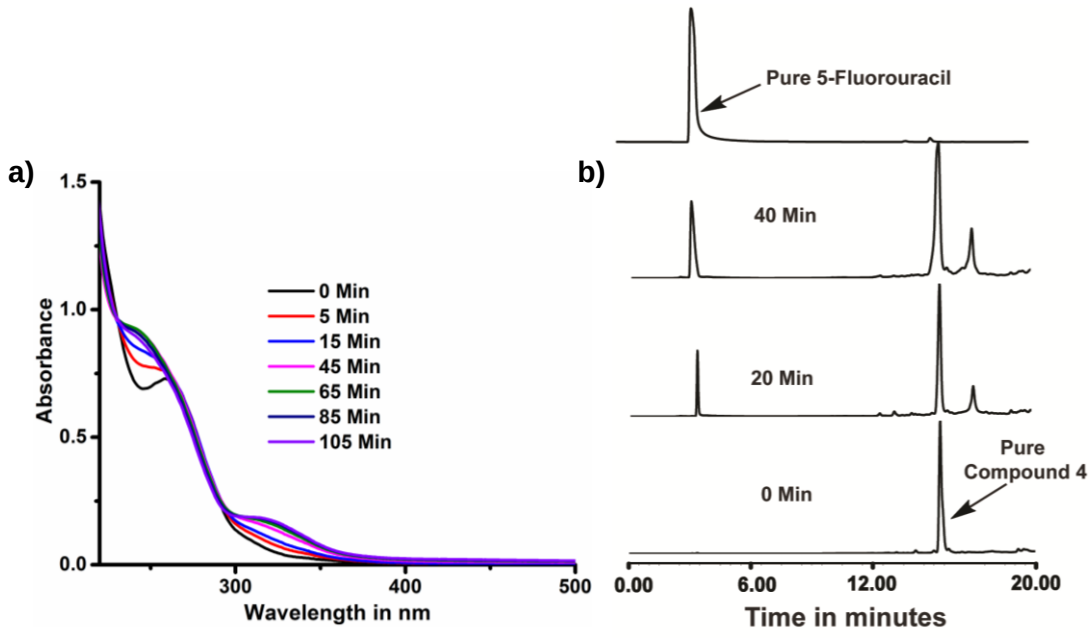

Figure 2.4 a) UV-Vis spectrum of drug release experiment for compound **2e**, b) HPLC profile of drug release study in 6:1 acetonitrile: water at 85 µM concentration of compound **2e.**

2.2.7 Photo-controlled release of 5-Fu from hydrogel

The release of 5-Fu from the hydrogel upon irradiation with UV light was observed by ^{1}H NMR. The gel was irradiated in 500 µL D_2O and the ^{1}H NMR were recorded. As can be observed from Figure 2.5 after prolonged irradiation, the peak corresponding to C6 proton of free 5-Fu appeared. Also, a slight amount of deformation of the gel was visible after irradiation.

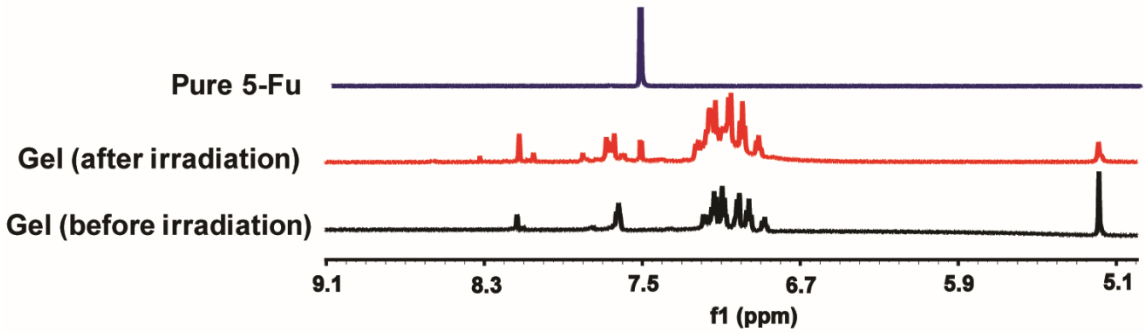

Figure 2.5 ^{1}H NMR analysis of photocleavage reaction in gel phase in D_2O.

2.2.8 Cytotoxicity measurement of the peptide drug conjugate in HeLa cells

An essential quality of a drug delivery system is that the molecule should be biologically compatible and non-toxic to the unaffected cells. To inspect the biological compatibility and irradiation-induced cytotoxic effect of our synthesized peptide-drug conjugate (compound **2e)**, cell viability was measured by MTT assay. Different concentration of compound **2e** was added to human cervical HeLa cell lines in presence and absence of irradiation. It is already well documented in the literature that pure 5-Fu shows high cytotoxicity towards HeLa cells at a concentration as low as 20-30 µg/mL.[47-48] As it can be evident from Figure 2.6, that our synthesized compound **2e** showed negligible toxicity towards HeLa cells in absence of irradiation. Almost no cell death was observed up to a concentration of 165 µM as compared to the control experiment where no peptide-drug conjugate was added. However, as soon as compound **2e** solution was subjected to irradiation, it showed substantial amount of toxicity towards HeLa cells (Figure 2.6). Thus the 5-Fu-FF conjugate (**2e**) only shows toxicity in presence of irradiation due to the liberation of active drug 5-Fu.

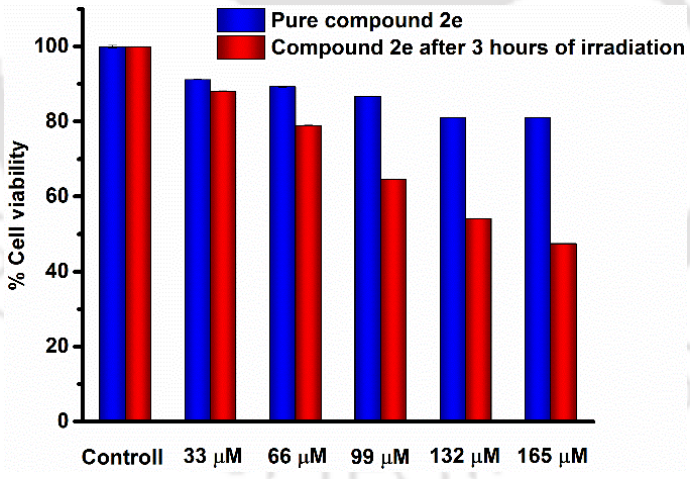

Figure 2.6 Effect of compound **2e** on the viability of HeLa cells after 48 hours of treatment. It was measured by MTT assay. The result indicates negligible cytotoxicity of the hydrogelator. Control: without compound **2e**.

2.3 Conclusions

In conclusion, this chapter provides formulation and synthesis of a gel-forming, peptide-based drug conjugate comprised of a covalently tethered 5-Fu prodrug. A dipeptide was

conjugated to an antitumor agent 5-fluorouracil through a photo-cleavable linker. The results demonstrated that the compound has the ability to control the release of the effective drug 5-Fu, by an external stimulus (light) instead of uncontrolled burst release of a drug when encapsulated by non-covalent interactions. Cell viability study in human cervical HeLa cell lines confirmed the non-toxic nature of the synthesized compound in absence of stimulus. This system can further be improved by inclusion of a cancer cell targeting peptide, which will provide a target-specific delivery of the drug in addition to the controlled and dose-dependent release.

2.4 Experimental Section

2.4.1 Synthetic procedures for compound 2a-2e.

A. Synthesis of prodrug (4-((5-fluoro-2,4-dioxo-3,4-dihydropyrimidin-1(2*H*)-yl) methyl)-3-nitrobenzoic acid) (2a): The prodrug was synthesized according to the literature.[11] Initially 5-Fu was silylated by using *N*,*O*-bis(trimethylsilyl) acetamide to form the intermediate 5-fluoro-2,4-bis((trimethylsilyl)oxy)-1,2,3,4-tetrahydropyrimidine. This intermediate (1.07 g, 3.8 mmole) was reacted in reflux condition for 14 hours with 4-bromomethyl-3-nitrobenzoic acid (1.17 g, 4.5 mmole) in the dark under nitrogen atmosphere using dry acetonitrile (5 mL) as solvent. After completion of the reaction, the mixture was cooled down to room temperature and treated with 7 mL methanol. The solvent was evaporated under vacuum and the obtained crude residue was purified by using (1:3:0.004 v/v methanol:ethyl acetate:acetic acid) solvent system to obtain a pale yellow powder (508 mg, 42%). Characterization of (4-((5-fluoro-2,4-dioxo-3,4-dihydropyrimidin-1(2*H*)-yl) methyl)-3-nitrobenzoic acid) **2a**: ^{1}H NMR (600MHz, DMSO-d_6) δ_{ppm} 8.53 (s, 1H), 8.18 (m, 2H), 7.46 (d, 1H, J = 6Hz), 5.23(s, 2H); ^{13}C NMR (150 MHz, DMSO-d_6) δ_{ppm} 166.3, 158.2 (d, C-4, $J_{C\text{-}F}$ = 25 Hz), 150.3, 147.8, 141.3 (s, C-5, $J_{C\text{-}F}$ = 228 Hz), 135.9, 134.8, 130.5 (d, C-6, $J_{C\text{-}F}$ = 34 Hz), 128.9, 125.9, 49.0: IR (KBR): $\tilde{\nu}$=3436, 3134, 1703, 1647, 1543, 1400, 1233 cm^{-1}; HRMS (ESI) *m/z* [M + H]$^{+}$calcd. for $C_{12}H_8FN_3O_6$: 310.0470, found: 310.0488.

B. Synthesis of ethyl *L*-phenylalanyl-*L*-phenylalaninate (2b and 2c): The peptide was synthesized according to the solution phase protocol. Boc protected *L*-phenylalanine (1

g, 3.8 mmole) was coupled with C-terminal ester protected *L*-phenylalanine (867 mg. 3.8 mmole) utilizing *N*,*N*,*N*′,*N*′-Tetramethyl-*O*-(1*H*-benzotriazol-1-yl)uronium hexafluorophosphate (HBTU, 1.57 g, 4.1 mmole) and *N*, *N*-Diisopropylethylamine (DIPEA, 637 mg, 4.9 mmole) in room temperature for 12 h. After the completion of the reaction, the product was extracted with brine solution using ethyl acetate as the organic solvent. The organic layer was dried over sodium sulphate and further purified by column chromatography using 1:4 ethyl acetate: hexane as the mobile phase. The dipeptide (compound **2b**) was obtained as white powder (1.19 g, 72%). Characterization of ethyl L-phenylalanyl-L-phenylalaninate: ^{1}H NMR (600 MHz, $CDCl_3$) δ 7.30 (dd, *J* = 12.9, 5.4 Hz, 3H), 7.25 (dt, *J* = 10.0, 5.0 Hz, 4H), 7.21 (d, *J* = 7.8 Hz, 2H), 7.04 – 7.00 (m, 2H), 6.39 (s, 1H), 5.01 (s, 1H), 4.77 (d, *J* = 5.2 Hz, 1H), 4.15 (ddd, *J* = 17.2, 10.6, 7.3 Hz, 2H), 3.06 (dd, *J* = 10.9, 5.5 Hz, 4H), 1.42 (s, 9H), 1.21 (t, *J* = 7.1 Hz,3H).^{13}C NMR (150 MHz, $CDCl_3$) δ_{ppm} 170.9, 170.8, 155.3, 136.5, 135.7, 129.5, 129.3, 128.7, 128.5, 128.3, 127.1, 126.9, 80.2, 77.3, 77.1, 76.9, 61.4, 55.6, 53.3, 38.0, 28.3, 27.9, 14.1; IR (KBR): $\tilde{\nu}$=3412, 3277, 2982, 1742, 1694, 1527, 1170, 1010, 704 cm^{-1}; HRMS (ESI) *m/z* $[M + H]^+$ calcd. for $C_{25}H_{32}N_2O_5$: 441.2384, found: 441.2397. Thus synthesized peptide was deprotected at the *N*- terminal by using trifluoroacetic acid (TFA) giving the desirable compound **2c** (92%).

C. Synthesis of ethyl (4-((5-fluoro-2,4-dioxo-3,4-dihydropyrimidin-1(2*H*)-yl) methyl)-3-nitrobenzoyl)-*L*-phenylalanyl-*L*-phenylalaninate (2d): The prodrug **2a** (500 mg, 1.6 mmole) was reacted with trifluoroacetate salt of diphenylalanine ethyl ester **2c** (734.62 mg, 1.6 mmole) in presence of HBTU (674.59 mg, 1.8 mmole) and DIPEA (0.7 mL, 4.0 mmole) with DMF as solvent. The solution was stirred overnight under nitrogen atmosphere before being washed with cold water (50 mL). After washing, the organic layer was dried over sodium sulphate and the crude residue was purified with silica gel column chromatography to give a pale yellow solid (541 mg, 53%) yield (Mp.: 206 ºC). Characterization of ethyl (4-((5-fluoro-2,4-dioxo-3,4-dihydropyrimidin-1(2*H*)-yl)methyl)-3-nitrobenzoyl)-*L*-phenylalanyl-*L*-phenylalaninate (**2d**): ^{1}H NMR (600MHz, DMSO-d_6) δppm 11.94 (br s, 1H), 8.99 (d, *J* = 6Hz, 1H), 8.61 (d, *J* = 6Hz 1H), 8.50 (s, 1H), 8.11 (d, *J* = 6Hz, 1H), 8.06-8.04 (m, 1H), 7.49 (d, *J* = 8.2 Hz, 1H), 7.33-7.32 (m, 1H), 7.26-7.22 (m, 5H), 7.20-7.17 (m, 1H), 7.16-7.14 (m, 1H), 5.20 (s, 2H), 4.81-4.77

(m, 1H), 4.51-4.47 (m, 1H), 4.04 (q, *J* = 7.1 Hz, 2H), 3.12-2.89 (m, 4H), 1.10 (t, *J* = 7.1 Hz, 3H). ; ^{13}C NMR (150 MHz, DMSO-d_6) δppm 171.3, 171.2, 163.7, 149.8, 147.2, 140.9, 139.4, 138.1, 137.0, 134.9, 134.2, 132.7, 129.7, 129.1, 128.4, 128.2, 128.0, 126.5, 126.3, 123.8, 60.5, 54.5, 53.8, 48.4, 37.0, 36.5, 13.9; IR (KBR): $\tilde{\nu}$=3436, 3293, 3070, 2927, 2855, 1694, 1639, 1527, 1336, 1241, 704cm^{-1}; HRMS (ESI) *m/z* [M + H]$^+$calcd. for $C_{32}H_{30}FN_5O_8$: 632.2151, found: 632.2166.

D. Synthesis of (4-((5-fluoro-2,4-dioxo-3,4-dihydropyrimidin-1(2*H*)-yl) methyl)-3-nitrobenzoyl)-*L*-phenylalanyl-*L*-phenylalanine (2e): The above product (**2d**) (200 mg) was dissolved in THF (1 mL). After dissolution, 1 mL of 2(N) sodium hydroxide was added to it and the solution was stirred for 3 hours. The completion of the reaction was monitored by thin-layer chromatography (TLC). After the reaction, THF was evaporated and 4(N) HCl was added dropwise (around 1.5 mL) in cold condition to give a pale yellow precipitate. The precipitate was obtained by filtration followed by washing with cold water to get the pure compound **2e** (149 mg) in 78% yield (Mp.: 216 ºC). Characterization of (4-((5-fluoro-2,4-dioxo-3,4-dihydropyrimidin-1(2*H*)-yl) methyl)-3-nitrobenzoyl)-L-phenylalanyl-L-phenylalanine (**2e**): ^{1}H NMR (600MHz, DMSO-d_6): δ_{ppm} 12.79 (br s, 1H), 11.94 (br s, 1H), 8.98-8.97 (m, 1H), 8.48-8.47 (m, 1H), 8.42-8.41 (m, 1H), 8.10 (d, *J* = 6.6 Hz, 1H), 8.04-8.03 (m, 1H), 7.48 (d, *J* = 8.2 Hz, 1H), 7.32-7.30 (m, 1H), 7.23-7.19 (m, 6H), 7.16-7.13 (m, 2H), 5.20 (s, 2H), 4.77-4.74 (m, 1H), 4.48-4.44 (m, 1H), 3.10-3.07 (m, 2H), 2.97-2.89 (m, 2H); ^{13}C NMR (150 MHz, DMSO-d_6): δ_{ppm} 172.8, 171.3, 163.9, 157.9 (d, C-4, $J_{C\text{-}F}$ = 25), 150, 147.4, 141 (s, C-5, $J_{C\text{-}F}$ = 237), 138.2, 137.6, 135, 134.4, 132.8, 130.2 (d, C-6, $J_{C\text{-}F}$ = 34), 129.3, 128.6, 128.3, 128.2, 126.6, 126.4, 124, 54.9, 53.8, 48.6, 39.9, 39.8, 39.7, 39.5, 39.4, 39.3, 39.1, 37, 36.6; IR (KBR): $\tilde{\nu}$=3436, 3070, 2927, 1694, 1655, 1527, 1345, 1241, 701 cm^{-1}; HRMS (ESI) *m/z* [M + H]$^+$calcd. for $C_{30}H_{26}FN_5O_8$: 604.1838, found: 604.1848.

2.4.2 Preparation and characterization of gels

10 mg (1 wt%) of compound **2d** was dissolved in 1 mL of DMSO in a 5 mL glass vial and kept in room temperature. After 5 days, a white-colored gel was obtained. Formation of gel was confirmed by vial inversion test. For preparing hydrogel, 10 mg (2 wt%) of compound **2e** was taken in a 5 mL glass vial. 150 µL of millipore water was added to the

vial. Then 50 µL of 1(N) NaOH was added and the pH of the solution was adjusted to nine by adding 1(N) HCl. The solution was vortexed until the compound dissolved completely. Finally, the pH of the solution was made seven by adding a total of 46 µL of 1(N) HCl gradually. The final volume of the solution was made 500 µL and kept in 37ºC for one hour to form a gel, which was assured by vial inversion test.

2.4.3 Identification of sol-gel transition temperature (T_g)

Sol-gel transition temperature was determined by dropping ball method. Briefly, a small ball was placed on the top of the hydrogel kept in a glass vial and it was heated slowly in a water bath at a rate of 1ºC/minutes. The temperature at which the ball touched the bottom of the glass vial was noted as T_g. The experiment was carried out in triplicate.

2.4.4. FESEM analysis

FESEM measurement was performed by placing a small portion of the lyophilized hydrogel sample on carbon tape. The DMSO gel was dried in a vacuum oven at 40ºC and the dried gel was used in a similar fashion like the hydrogel for FESEM analysis. All the samples were coated with gold prior to analysis.

2.4.5 Circular Dichroism

The CD spectra were recorded by using a JASCO J-600C spectropolarimeter at room temperature. The samples were measured at different concentrations of 564, 282, 141, 70, 35, 18 µM in water. A cuvette having 0.1cm path length was used. All CD profiles were an average of three scans at a scan speed of 100 nm/minutes.

2.4.6 FTIR Spectra

FTIR spectra of the dried hydrogel were recorded on Nicolet iS10 spectrometer at room temperature using KBr disk technique.

2.4.7 Rheological measurement

Rheological studies were carried out with 2 wt% hydrogel using Anton-Paar MCR 102 rheometer consisting of a measuring system of 20 mm parallel plate at 25ºC. The strain sweep study was performed at a constant oscillatory frequency of 1 rad/s within the

range of 0.1- 100% strain. The frequency sweep was done over a range of 0.1-100 rad/s against the constant strain of 0.1% as determined from the LVR.

2.4.8 Irradiation of 5-Fu-FF-COOH (compound 2e)

Irradiation was carried out using 365 nm LED light of 24W. 3 mL solution of compound **2e** (Scheme 1) having a concentration of 85 µM was placed in a quartz cuvette and irradiated under 365 nm UV light at 25 ˚C. The experiment was monitored by UV-Vis spectrophotometer as well as by RP-HPLC. After each irradiation, the change in UV absorption was monitored at a time interval of 5, 10, 40, 60, 80 and 100 minutes by a Perkin Elmer UV-Vis spectrometer. A new broad peak gradually appeared at around 325 nm which clearly indicated the photo-cleavage of the ortho-nitro benzyl group. The release of 5-Fu was clearly observed in HPLC measurement. It was observed that the percentage of the release of 5-Fu was increased with respect to irradiation time.

The photo-induced release of 5-Fu from compound **2e** was also monitored by ^{1}H NMR. For NMR study, 5 mg of compound **2e** was dissolved in DMSO-d_6. The sample was irradiated under 365 nm UV light and ^{1}H NMR spectra were recorded after 6 hours of irradiation.

2.4.9 Cytotoxicity of compound 2e

To determine the cytotoxic effect of our peptide-drug conjugate, colorimetric assay was carried out. The cell viability assay was carried out in human cervical HeLa cell lines, obtained from National Centre for Cell Sciences (NCCS), Pune, India, by following previously demonstrated procedure.[49] For this purpose, $5x10^3$ cells were seeded into 96-well microplate in 90 µL Dulbecco's modified Eagle's medium (DMEM) and were incubated for 24 hours in presence of 5% CO_2 at 37˚C. Cells were then treated with varying concentrations of compound **2e** (33, 66, 99, 132, 165 µM) both in presence and absence of irradiation for 48 hours under similar condition. After the incubation, the cell viability assay was carried out by using 3-(4, 5-dimethylthiazol-2-yl)-2, 5-diphenyltetrazolium bromide (MTT). MTT is reduced by living cells to produce blue-colored formazan and this reaction is used as a measurement of living cells. MTT was added to each plate and was incubated for 2 hours at 37˚C. The medium then was

removed and 60 µL of DMSO was added which produces formazan having absorption (A) at 550 nm. The optical density (OD) of each well-plate was measured with the background reference at 690 nm. All the tests were performed in triplicates. The control experiment was also carried out in similar way but without the addition of compound **2e**. The percentage cell viability with respect to the control was calculated by using the standard formula as given below. The cell viability percentage of the control was taken as 100%.

$$\%\ of\ cell\ viability = \frac{(A_{550} - A_{690})\ of\ treated\ cells}{(A_{550} - A_{690})\ of\ control\ cells} \times 100\ \%$$

2.5 References

1. Strøm, M. B.; Haug, B. E.; Skar, M. L.; Stensen, W.; Stiberg, T.; Svendsen, J. S., The pharmacophore of short cationic antibacterial peptides. *J. Med. Chem.* **2003,** *46* (9), 1567-1570.

2. Ramesh, S.; Govender, T.; Kruger, H. G.; de la Torre, B. G.; Albericio, F., Short AntiMicrobial Peptides (SAMPs) as a class of extraordinary promising therapeutic agents. *J. Pept. Sci.* **2016,** *22* (7), 438-451.

3. Seth, P. P.; Siwkowski, A.; Allerson, C. R.; Vasquez, G.; Lee, S.; Prakash, T. P.; Wancewicz, E. V.; Witchell, D.; Swayze, E. E., Short antisense oligonucleotides with novel 2′− 4′ conformationaly restricted nucleoside analogues show improved potency without increased toxicity in animals. *J. Med. Chem.* **2008,** *52* (1), 10-13.

4. Wang, H.; Yang, Z., Short-peptide-based molecular hydrogels: novel gelation strategies and applications for tissue engineering and drug delivery. *Nanoscale* **2012,** *4* (17), 5259-5267.

5. Chen, X.; Plasencia, C.; Hou, Y.; Neamati, N., Synthesis and biological evaluation of dimeric RGD peptide− paclitaxel conjugate as a model for integrin-targeted drug delivery. *J. Med. Chem.* **2005,** *48* (4), 1098-1106.

6. Chen, Z.; Zhang, P.; Cheetham, A. G.; Moon, J. H.; Moxley Jr, J. W.; Lin, Y.-a.; Cui, H., Controlled release of free doxorubicin from peptide–drug conjugates by drug loading. *J. Control. Release* **2014,** *191*, 123-130.

7. Rosen, H.; Abribat, T., The rise and rise of drug delivery. *Nat. Rev. Drug Discovery* **2005,** *4* (5), 381-385.

8. Wang, R.; Zhu, G.; Mei, L.; Xie, Y.; Ma, H.; Ye, M.; Qing, F.-L.; Tan, W., Automated modular synthesis of aptamer–drug conjugates for targeted drug delivery. *J. Am. Chem. Soc.* **2014,** *136* (7), 2731-2734.

9. Tan, W.; Wang, H.; Chen, Y.; Zhang, X.; Zhu, H.; Yang, C.; Yang, R.; Liu, C., Molecular aptamers for drug delivery. *Trends Biotechnol.* **2011,** *29* (12), 634-640.

10. Hui, X.; Han, Y.; Liang, S.; Liu, Z.; Liu, J.; Hong, L.; Zhao, L.; He, L.; Cao, S.; Chen, B., Specific targeting of the vasculature of gastric cancer by a new tumor-homing peptide CGNSNPKSC. *J. Control. Release* **2008,** *131* (2), 86-93.

11. Zhang, Z.; Hatta, H.; Ito, T.; Nishimoto, S.-i., Synthesis and photochemical properties of photoactivated antitumor prodrugs releasing 5-fluorouracil. *Org. Biomol. Chem.* **2005,** *3* (4), 592-596.

12. Alley, S. C.; Okeley, N. M.; Senter, P. D., Antibody–drug conjugates: targeted drug delivery for cancer. *Curr. Opin. Chem. Biol.* **2010,** *14* (4), 529-537.

13. Firer, M. A.; Gellerman, G., Targeted drug delivery for cancer therapy: the other side of antibodies. *J. Hematol. Oncol.* **2012,** *5* (1), 70.

14. Sun, H.; Zhu, X.; Lu, P. Y.; Rosato, R. R.; Tan, W.; Zu, Y., Oligonucleotide aptamers: new tools for targeted cancer therapy. *Mol. Ther. Nucleic Acids.* **2014,** *3* (8), e182.

15. Leuner, C.; Dressman, J., Improving drug solubility for oral delivery using solid dispersions. *Eur. J. Pharm. Biopharm.* **2000,** *50* (1), 47-60.

16. Khadka, P.; Ro, J.; Kim, H.; Kim, I.; Kim, J. T.; Kim, H.; Cho, J. M.; Yun, G.; Lee, J., Pharmaceutical particle technologies: An approach to improve drug solubility, dissolution and bioavailability. *Asian J. Pharm.* **2014,** *9* (6), 304-316.

17. Lu, J.; Liong, M.; Zink, J. I.; Tamanoi, F., Mesoporous silica nanoparticles as a delivery system for hydrophobic anticancer drugs. *Small* **2007,** *3* (8), 1341-1346.

18. Szekerke, M.; Driscoll, J. S., The use of macromolecules as carriers of antitumor drugs. *Eu.r J. Cancer* **1977,** *13* (6), 529-537.

19. Anwunobi, A.; Emeje, M., Recent applications of natural polymers in nanodrug delivery. *J. Nanomedic Nanotechnol.* **2011,** *S4*:002.

20. Rejinold, N. S.; Chennazhi, K.; Nair, S.; Tamura, H.; Jayakumar, R., Biodegradable and thermo-sensitive chitosan-g-poly (N-vinylcaprolactam) nanoparticles as a 5-fluorouracil carrier. *Carbohydr. Polym.* **2011,** *83* (2), 776-786.

21. Sun, H.; Guo, B.; Cheng, R.; Meng, F.; Liu, H.; Zhong, Z., Biodegradable micelles with sheddable poly (ethylene glycol) shells for triggered intracellular release of doxorubicin. *Biomaterials* **2009,** *30* (31), 6358-6366.

22. Berrada, M.; Serreqi, A.; Dabbarh, F.; Owusu, A.; Gupta, A.; Lehnert, S., A novel non-toxic camptothecin formulation for cancer chemotherapy. *Biomaterials* **2005,** *26* (14), 2115-2120.

23. Longley, D. B.; Harkin, D. P.; Johnston, P. G., 5-fluorouracil: mechanisms of action and clinical strategies. *Nat. Rev. Cancer* **2003,** *3* (5), 330-338.

24. Diasio, R. B.; Harris, B. E., Clinical pharmacology of 5-fluorouracil. *Clin Pharmacokinet.* **1989,** *16* (4), 215-237.

25. Arias, J. L., Novel strategies to improve the anticancer action of 5-fluorouracil by using drug delivery systems. *Molecules* **2008,** *13* (10), 2340-2369.

26. Kratz, F.; Müller, I. A.; Ryppa, C.; Warnecke, A., Prodrug strategies in anticancer chemotherapy. *ChemMedChem* **2008,** *3* (1), 20-53.

27. Wang, Y.; Cheetham, A. G.; Angacian, G.; Su, H.; Xie, L.; Cui, H., Peptide–drug conjugates as effective prodrug strategies for targeted delivery. *Adv. Drug Delivery Rev.* **2017,** *110*, 112-126.

28. Larson, N.; Ghandehari, H., Polymeric conjugates for drug delivery. *Chem. Mater.* **2012,** *24* (5), 840-853.

29. Navath, R. S.; Kurtoglu, Y. E.; Wang, B.; Kannan, S.; Romero, R.; Kannan, R. M., Dendrimer− drug conjugates for tailored intracellular drug release based on glutathione levels. *Bioconjugate Chem.* **2008,** *19* (12), 2446-2455.

30. Agasti, S. S.; Chompoosor, A.; You, C.-C.; Ghosh, P.; Kim, C. K.; Rotello, V. M., Photoregulated release of caged anticancer drugs from gold nanoparticles. *J. Am. Chem. Soc.* **2009,** *131* (16), 5728-5729.

31. Lin, C.; Gitsov, I., Preparation and characterization of novel amphiphilic hydrogels with covalently attached drugs and fluorescent markers. *Macromolecules* **2010,** *43* (23), 10017-10030.

32. Sun, Y.; Kaplan, J. A.; Shieh, A.; Sun, H.-L.; Croce, C. M.; Grinstaff, M. W.; Parquette, J. R., Self-assembly of a 5-fluorouracil-dipeptide hydrogel. *Chem. Commun.* **2016,** *52* (30), 5254-5257.

33. Cheetham, A. G.; Zhang, P.; Lin, Y.-a.; Lock, L. L.; Cui, H., Supramolecular nanostructures formed by anticancer drug assembly. *J. Am. Chem. Soc.* **2013,** *135* (8), 2907-2910.

34. Hu, M.; Huang, P.; Wang, Y.; Su, Y.; Zhou, L.; Zhu, X.; Yan, D., Synergistic combination chemotherapy of camptothecin and floxuridine through self-assembly of amphiphilic drug–drug conjugate. *Bioconjugate Chem.* **2015,** *26* (12), 2497-2506.

35. Klán, P.; Šolomek, T. s.; Bochet, C. G.; Blanc, A. l.; Givens, R.; Rubina, M.; Popik, V.; Kostikov, A.; Wirz, J., Photoremovable protecting groups in chemistry and biology: reaction mechanisms and efficacy. *Chem. Rev.* **2013,** *113* (1), 119-191.

36. Bhattacharya, S.; Acharya, S. G., Pronounced hydrogel formation by the self-assembled aggregates of N-alkyl disaccharide amphiphiles. *Chem. Mater.* **1999,** *11* (12), 3504-3511.

37. Tiwari, P.; Rajagopalan, R.; Moin, M.; Soni, R.; Trivedi, P.; DuttKonar, A., Can self-assembled hydrogels composed of aromatic amino acid derivatives function as drug delivery carriers? *New J. Chem.* **2017,** *41* (1), 308-315.

38. Martin, A. D.; Wojciechowski, J. P.; Warren, H.; Thordarson, P., Effect of heterocyclic capping groups on the self-assembly of a dipeptide hydrogel. *Soft Matter* **2016,** *12* (10), 2700-2707.

39. Muraoka, T.; Cui, H.; Stupp, S. I., Quadruple helix formation of a photoresponsive peptide amphiphile and its light-triggered dissociation into single fibers. *J. Am. Chem. Soc.* **2008,** *130* (10), 2946-2947.

40. Dado, G. P.; Gellman, S. H., Intramolecular Hydrogen Bonding in Derivatives of. beta.-Alanine and. gamma.-Amino Butyric Acid; Model Studies for the Folding of Unnatural Polypeptide Backbones. *J. Am. Chem. Soc.* **1994,** *116* (3), 1054-1062.

41. Niu, L.; Liu, L.; Xi, W.; Han, Q.; Li, Q.; Yu, Y.; Huang, Q.; Qu, F.; Xu, M.; Li, Y., Synergistic inhibitory effect of peptide–organic coassemblies on amyloid aggregation. *ACS nano* **2016,** *10* (4), 4143-4153.

42. Bera, S.; Jana, P.; Maity, S. K.; Haldar, D., Inhibition of fibril formation by tyrosine modification of diphenylalanine: crystallographic insights. *Cryst. Growth Des.* **2014,** *14* (3), 1032-1038.

43. Miyazawa, T.; Blout, E., The infrared spectra of polypeptides in various conformations: amide I and II bands1. *J. Am. Chem. Soc.* **1961,** *83* (3), 712-719.

44. Das, A. K.; Collins, R.; Ulijn, R. V., Exploiting enzymatic (reversed) hydrolysis in directed self-assembly of peptide nanostructures. *Small* **2008,** *4* (2), 279-287.

45. Marriott, G.; Miyata, H.; Kinosita Jr, K., Photomodulation of the nucleating activity of a photocleavable crosslinked actin dimer. *Biochem. Int.* **1992,** *26* (5), 943-951.

46. Il'ichev, Y. V.; Schwörer, M. A.; Wirz, J., Photochemical reaction mechanisms of 2-nitrobenzyl compounds: methyl ethers and caged ATP. *J. Am. Chem. Soc.* **2004,** *126* (14), 4581-4595.

47. Hemaiswarya, S.; Doble, M., Combination of phenylpropanoids with 5-fluorouracil as anti-cancer agents against human cervical cancer (HeLa) cell line. *Phytomedicine* **2013,** *20* (2), 151-158.

48. Byfield, J. E.; Calabro-Jones, P.; Klisak, I.; Kulhanian, F., Pharmacologic requirements for obtaining sensitization of human tumor cells in vitro to combined 5-

fluorouracil or ftorafur and X rays. *Int. J. Radiat. Oncol. Biol. Phys.* **1982,** *8* (11), 1923-1933.

49. Ghosh, R.; Goswami, U.; Ghosh, S. S.; Paul, A.; Chattopadhyay, A., Synergistic anticancer activity of fluorescent copper nanoclusters and cisplatin delivered through a hydrogel nanocarrier. *ACS Appl. Mater. Interfaces* **2014,** *7* (1), 209-222.

2.6 NMR and HRMS spectra of synthesized compounds

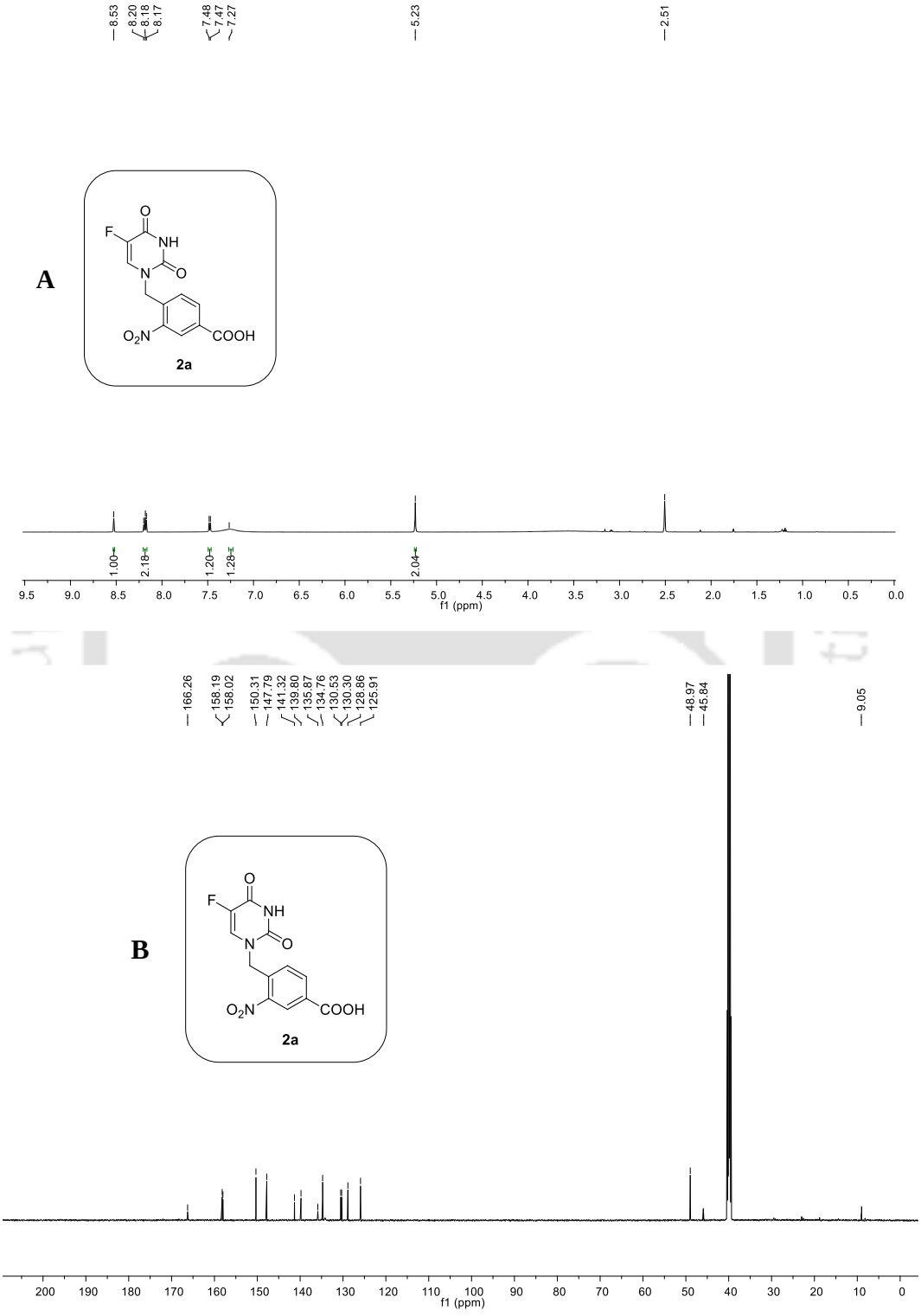

^{1}H (A) and ^{13}C (B) spectra of compound **2a**

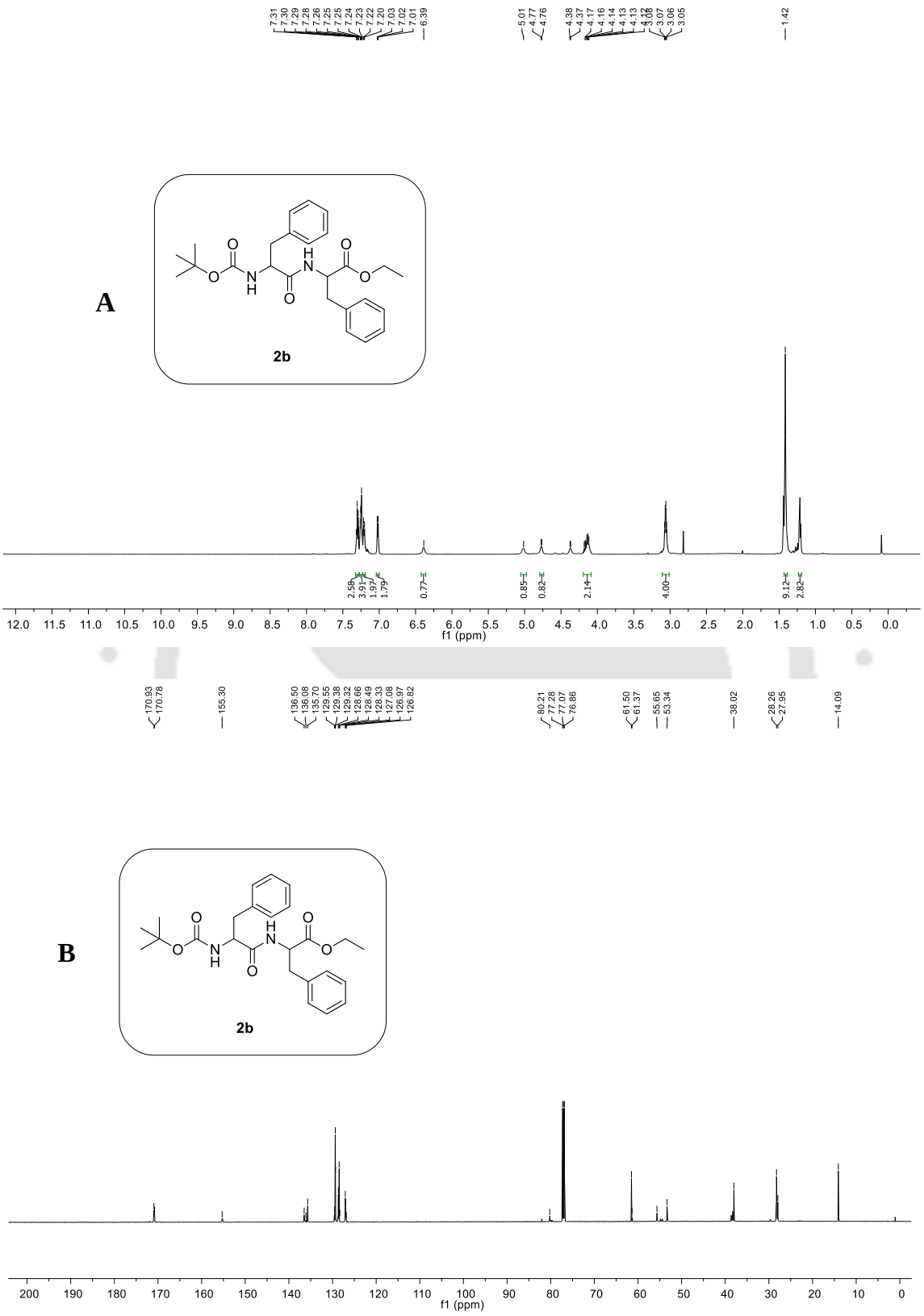

^{1}H (A) and ^{13}C (B) spectra of compound **2b**

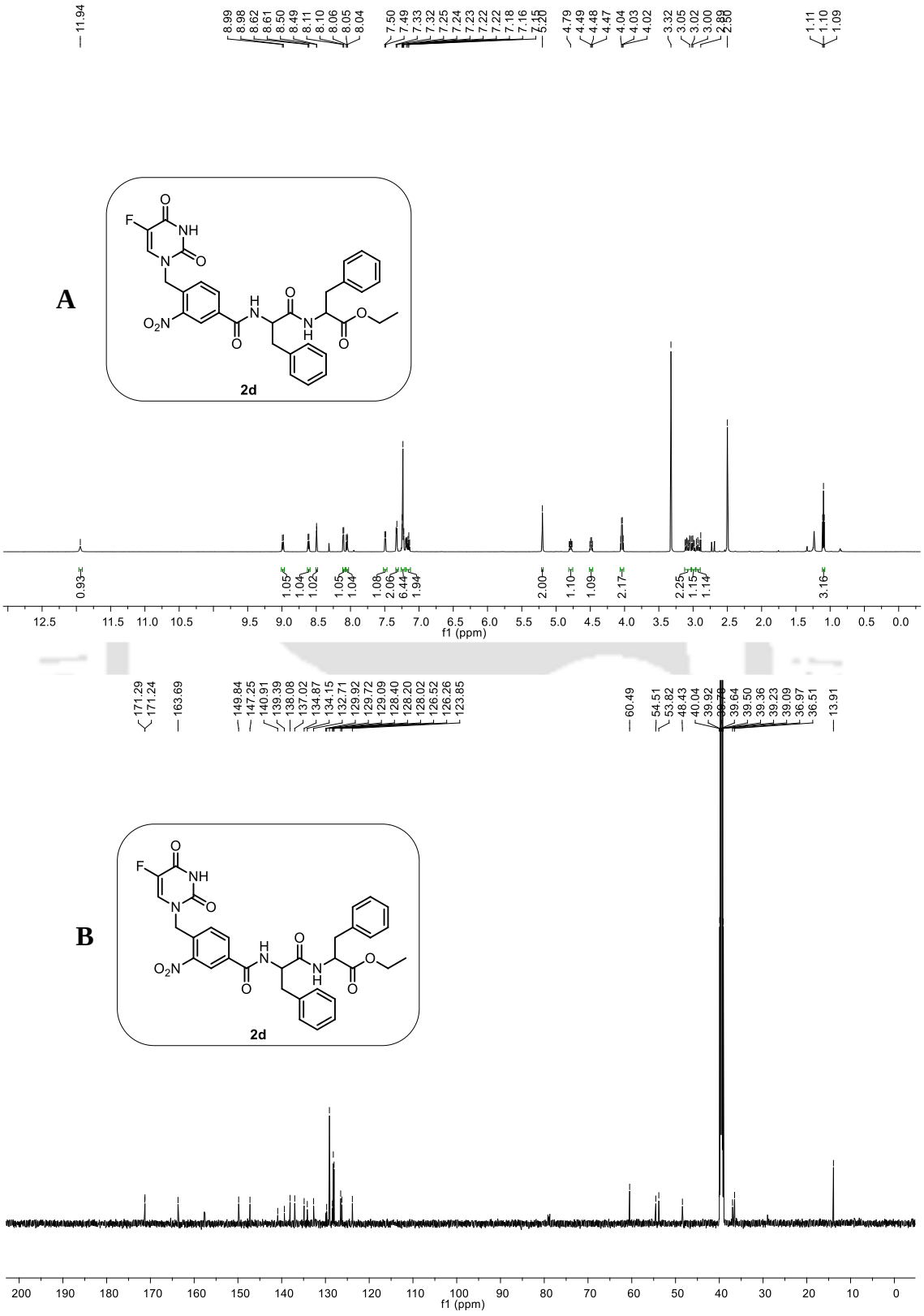

^{1}H (A) and ^{13}C (B) spectra of compound **2d**

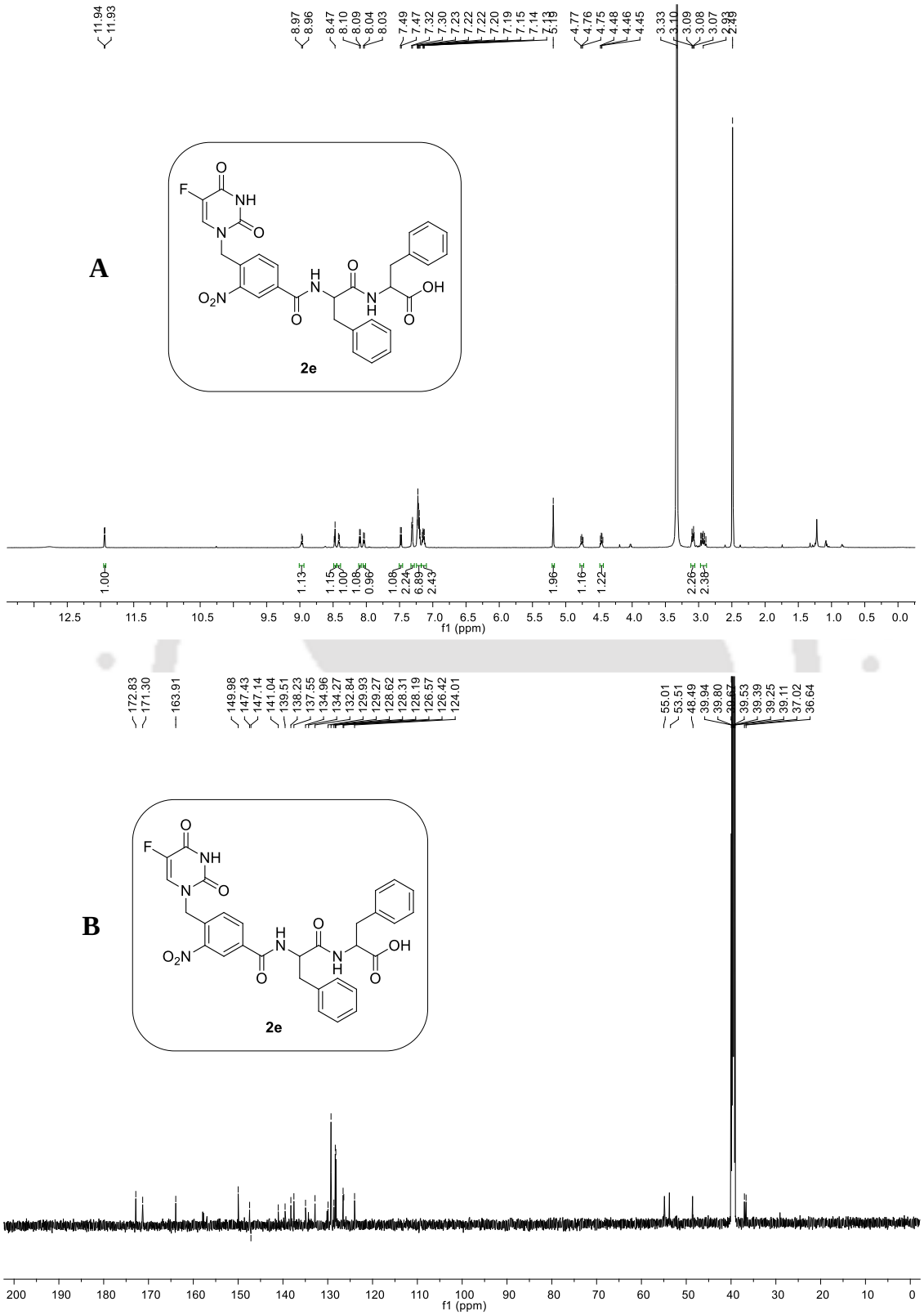

^{1}H (A) and ^{13}C (B) spectra of compound **2e**

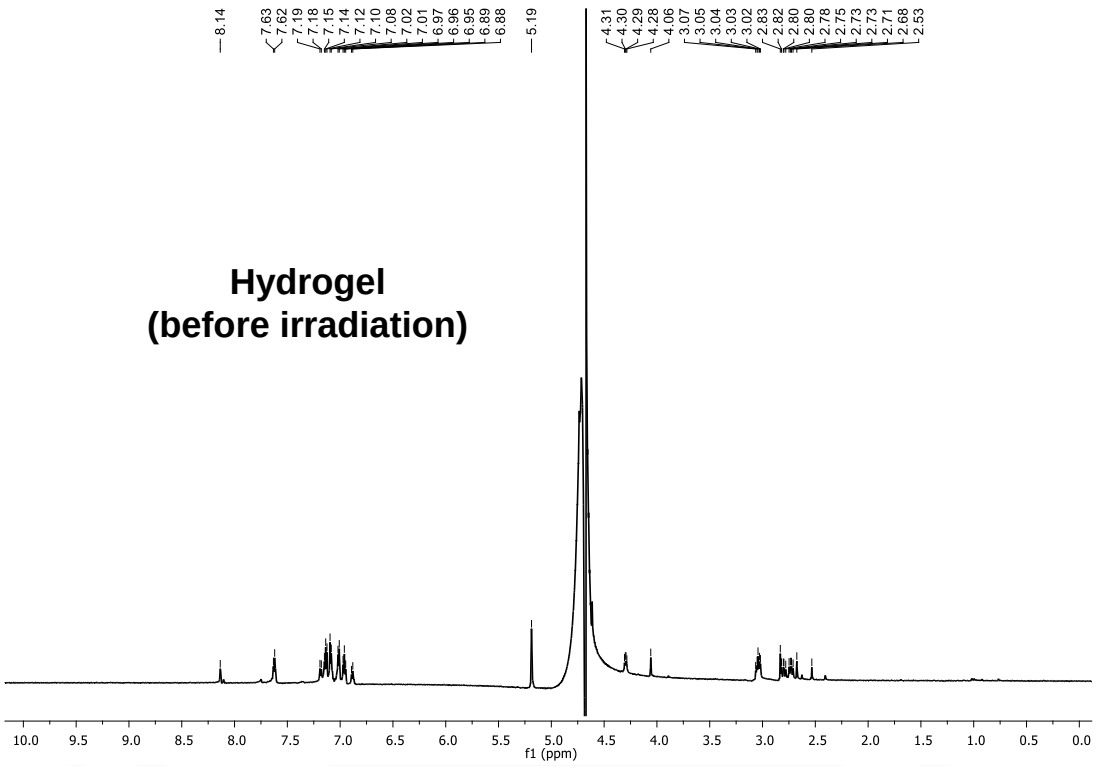

^{1}H spectra of hydrogel (before irradiation) in D_2O.

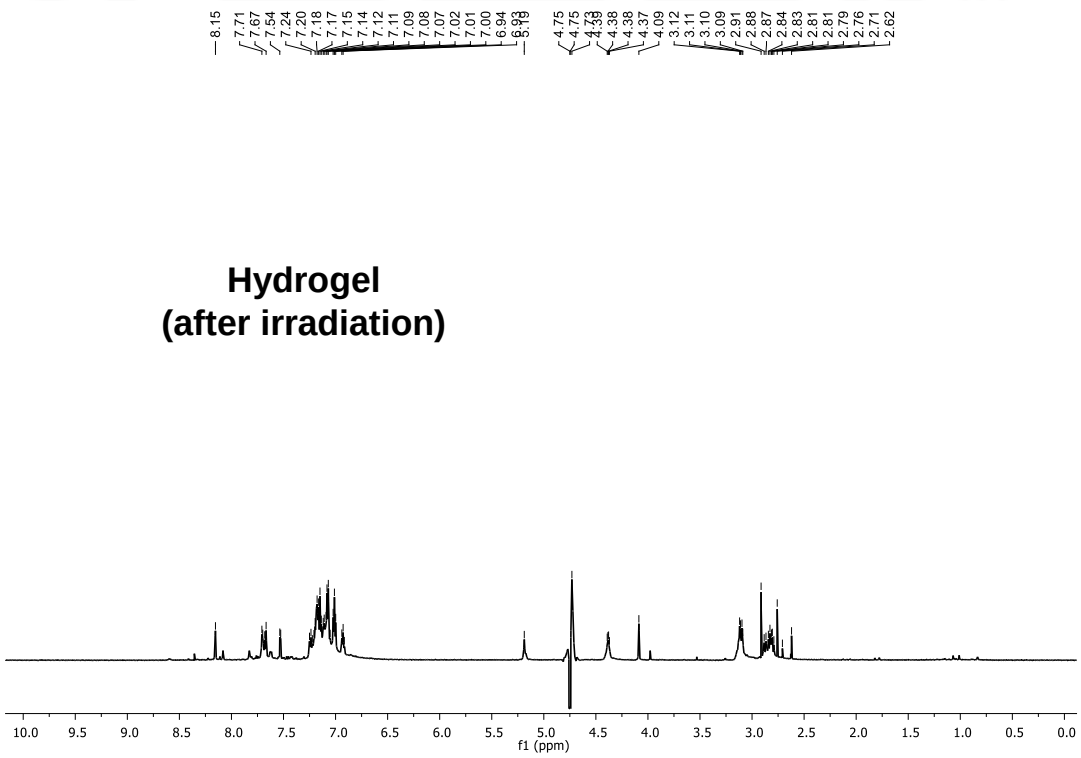

^{1}H spectra of hydrogel (before irradiation) in D_2O.

Pure 5-Fu

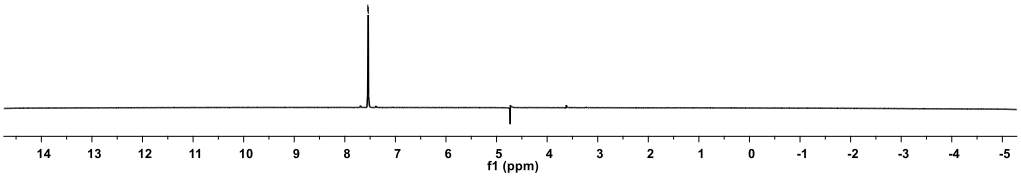

^{1}H spectra pure 5-Fu in D_2O.

Sample Name	SD-18-FL	**Position**	Vial 1	**Instrument Name**	QTOF	**User Name**	
Inj Vol	-1	**InjPosition**		**SampleType**	Sample	**IRM Calibration Status**	Success
Data Filename	SD-18-FL.d	**ACQ Method**		**Comment**		**Acquired Time**	6/18/2018 12:40:57 PM

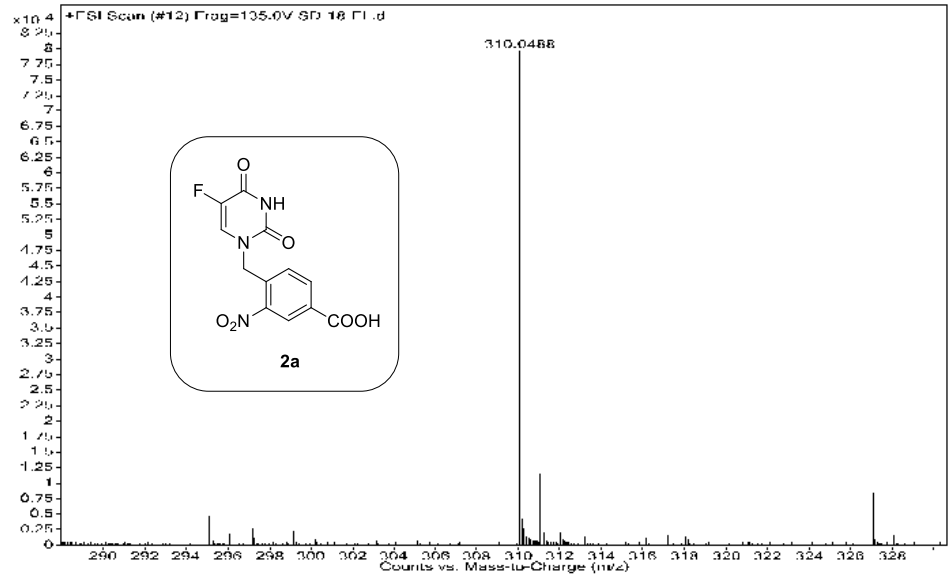

HRMS spectra of compound **2a**

Sample Name	SD-18-DIPFP	**Position**	Vial 1	**Instrument Name**	QTOF	**User Name**	
Inj Vol	-1	**InjPosition**		**SampleType**	Sample	**IRM Calibration Status**	Success
Data Filename	SD-18-DIPFP.d	**ACQ Method**		**Comment**		**Acquired Time**	6/18/2018 12:39:02 PM

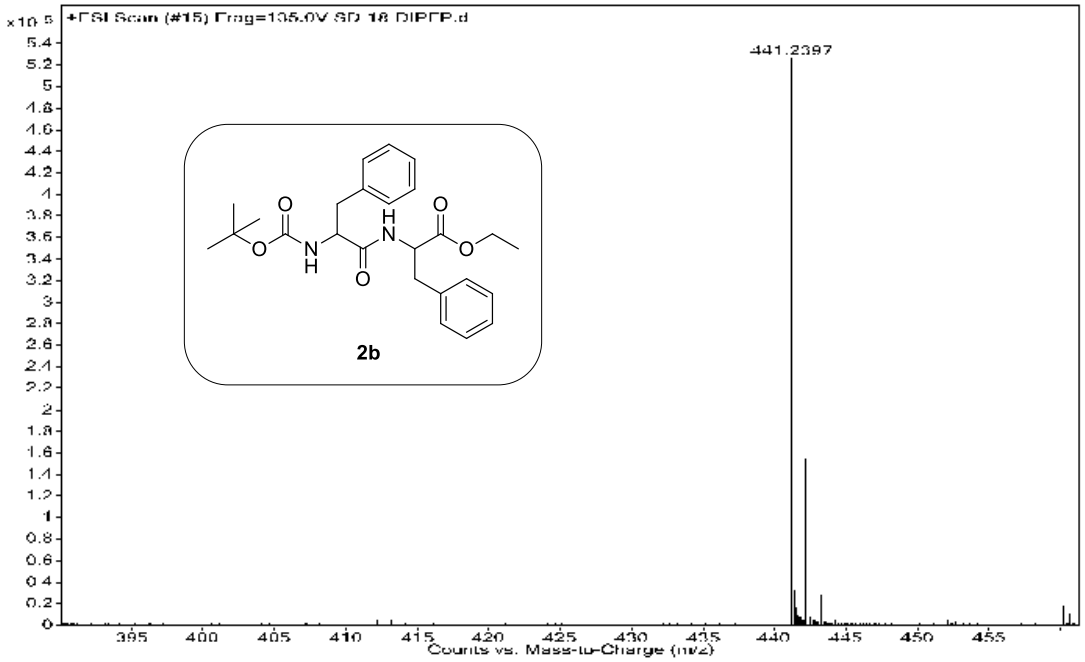

HRMS spectra of compound **2b**

Sample Name	SD-18-OET	**Position**	Vial 1	**Instrument Name**	QTOF	**User Name**	
Inj Vol	-1	**InjPosition**		**SampleType**	Sample	**IRM Calibration Status**	Success
Data Filename	SD-18-OET.d	**ACQ Method**		**Comment**		**Acquired Time**	6/18/2018 12:44:40 PM

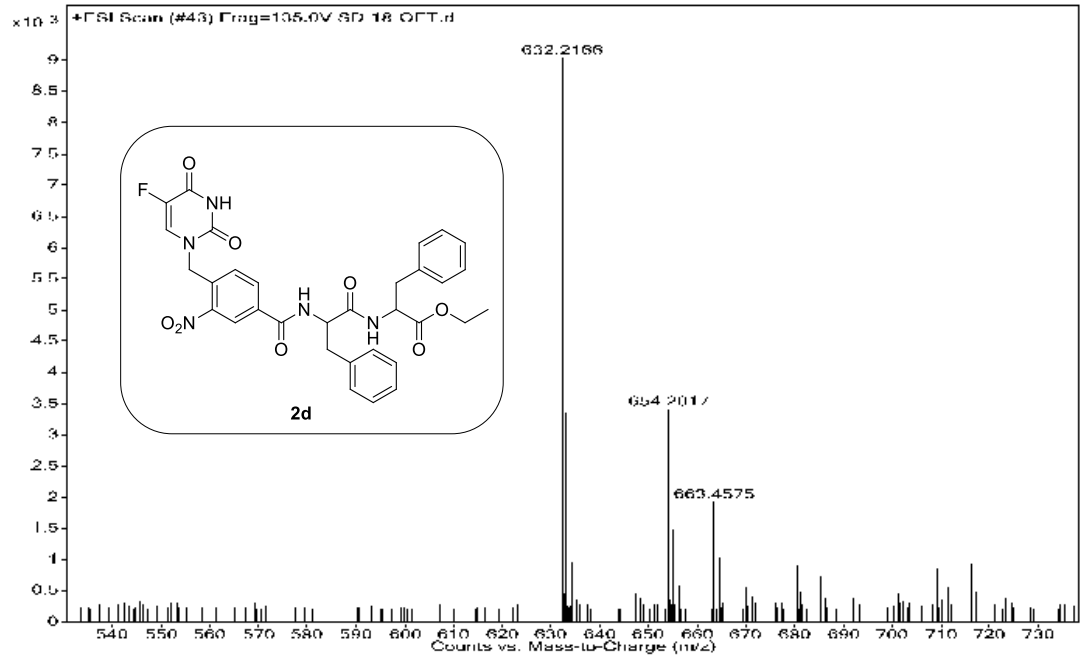

HRMS spectra of compound **2d**

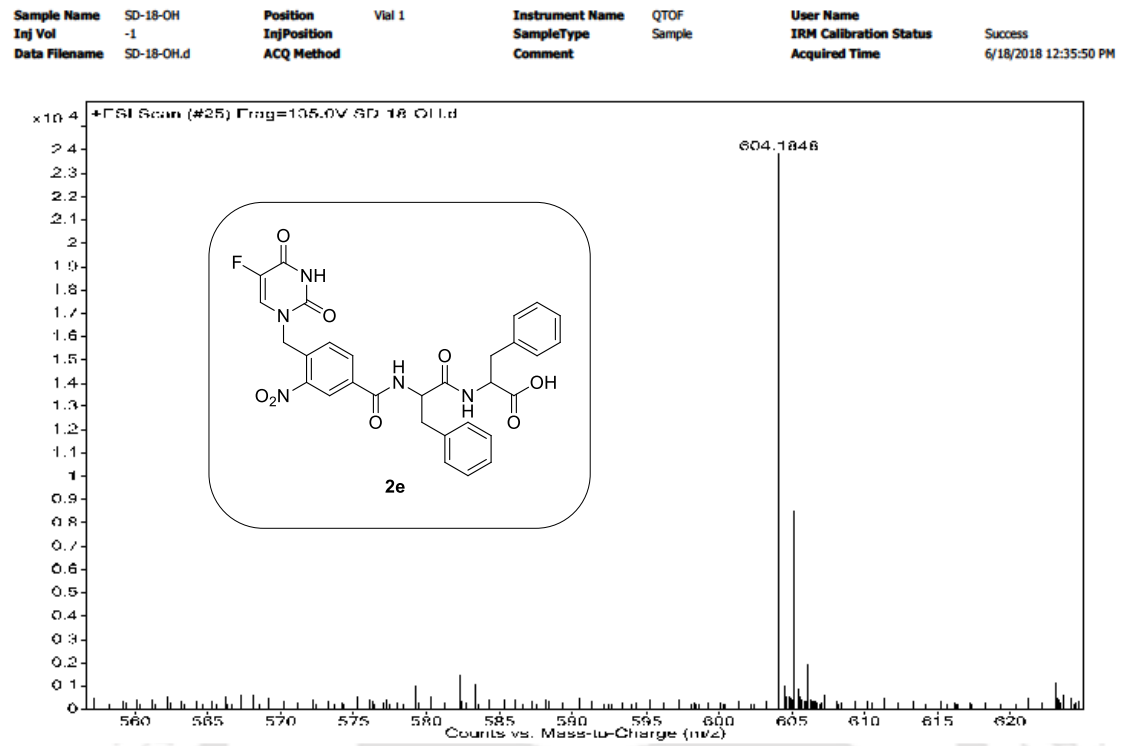

HRMS spectra of compound **2e**

Chapter 3

Synthesis of 5-Fu Conjugated Peptide Nanoparticles as Stimuli Responsive Therapeutic Cargo

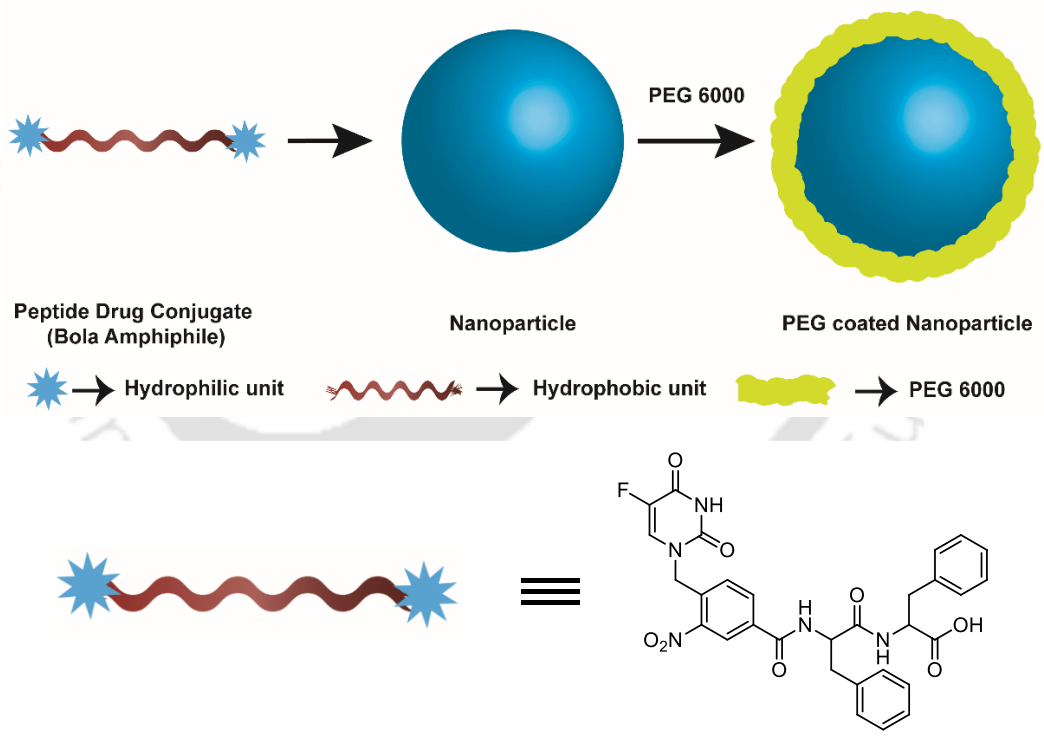

3.1 Introduction

Short, synthesized peptides and peptide-based nanomaterials are rapidly emerging as powerful biomolecules that escalated its application widely, including in therapeutic research, due to their excellent biocompatibility and biodegradability. Self-assembly of peptides has been explored to a great extent to prepare various nanostructures such as nanofibers,[1-3] nanotubes,[4-5] nanobelts,[6-7] and nanospheres,[8]. Peptide-based nanoparticles are remarkably popular in theranostics: bioimaging[9-10] and drug delivery.[11-12] Zhang and his research group developed a tryptophan-phenylalanine dipeptide based nanoparticles for bioimaging as well as the delivery of doxorubicin.[9] Peptides are not only used to formulate nanostructures for successful entrapment of drugs but also are covalently conjugated with pharmaceutically active molecules.

Peptide drug conjugates (PDCs) are often employed as a useful strategy to develop prodrugs.[13] A prodrug increases the therapeutic efficacy of a drug by improving its bioavailability and other beneficial pharmacokinetic properties. Upon specific stimulation, the prodrug liberates the active therapeutic agent that increases target specificity,[14] cell permeability,[15] and material property.[16-17] Cui and his co-workers have developed a supramolecular filament from amphiphilic PDC, comprised of CPT. [18] The hydrophobic chemotherapeutic molecule was covalently attached to a hydrophilic peptide derived from Tau protein, through a cleavable disulfylbutyrate (buSS) linker. Our group has recently reported the design of a hydrogelator by attaching hydrophilic chemotherapeutic 5-Fu with diphenylalanine peptide,[19] polymer.[20]

Herein, we report the design and synthesis of dual-drug cargo peptide nanoparticles with conjugated 5-Fu and encapsulated CPT. The prevalent antitumor agent was covalently attached to the *N*-terminal of the dipeptide by a photoresponsive *o*-nitrobenzyl unit to accomplish controlled release of the drug.[21] Previously we have developed hydrogels from this 5-Fu-FF conjugate in a pH-responsive manner.[19] In this report, we have studied that an N-terminal 5-Fu-modified diphenylalanine (FF) peptide can also be fabricated into nanoparticles having a size within 200 nm. Moreover, the hydrophobic core of the self-assembled dipeptide nanoparticle, constituted by the phenyl rings, was found to entrap another hydrophobic molecule CPT.

3.2 Results and Discussion

3.2.1 Design and synthesis of the 5-Fu-FF conjugate (2e)

In this study, we have modified the *N*-terminal of FF dipeptide with a photo-sensitive prodrug of 5-Fu. The short FF dipeptide was chosen for its known self-assemble nature. Various reports have studied the effect of *N*-terminal and C-terminal modifications on the self-assembly of FF dipeptide. For example, an introduction of naphthyl,[24] benzyl[25] or fmoc[26] group at the *N*-terminal of FF dipeptide were reported to enhance the self-assembly and produces hydrogel by trapping water inside a network of nanofibers. Attachment of a cysteine residue at the *N*-terminal of the dipeptide was found to change its self-assembly property and initiate nanosphere formation.[27] Herein, we have substituted the *N*-terminal of the dipeptide with a hydrophilic , not only to change the self-assembly pattern of the dipeptide but also to use it as a biocompatible vector for the controlled delivery of the drug. Addition of the hydrophilic moiety at the N-terminal and presence of the free carboxylic group at the C-terminal makes the dipeptide a bola amphiphile, with two hydrophilic heads, which increases its water solubility and reduces the aggregation of the nanoparticles. The synthesis of the 5-Fu-FF conjugate has been described in section 2.4.1 (Chapter 2).[19] Herein, a slightly alternative procedure has been adopted (Scheme 3.1). At first, 5-Fu was attached with a photo-cleavable 4-bromomethyl-3- nitrobenzoic acid (compound **2a**).[22]. The free carboxylic end of the linker was then conjugated with the ethyl ester of phenylalanine by standard solution-phase coupling using *N*,*N*,*N′*,*N′*-Tetramethyl-*O*-(1*H*-benzotriazol-1-yl)uronium hexafluorophosphate (HBTU) and *N*, *N*-Diisopropylethylamine (DIPEA) as the activator. The acid-labile *N*-terminal protecting group of the amino-phenylalanine drug conjugate (**3a**) was deprotected using trifluoroacetic acid (TFA), producing compound **3b**. The resultant *N*-terminal free unit was further coupled with compound **2a** that yielded **2d**. Lastly, compound **2d** was hydrolyzed by base-catalyzed hydrolysis reaction to produce the final compound **2e** (5-Fu-FF-COOH).

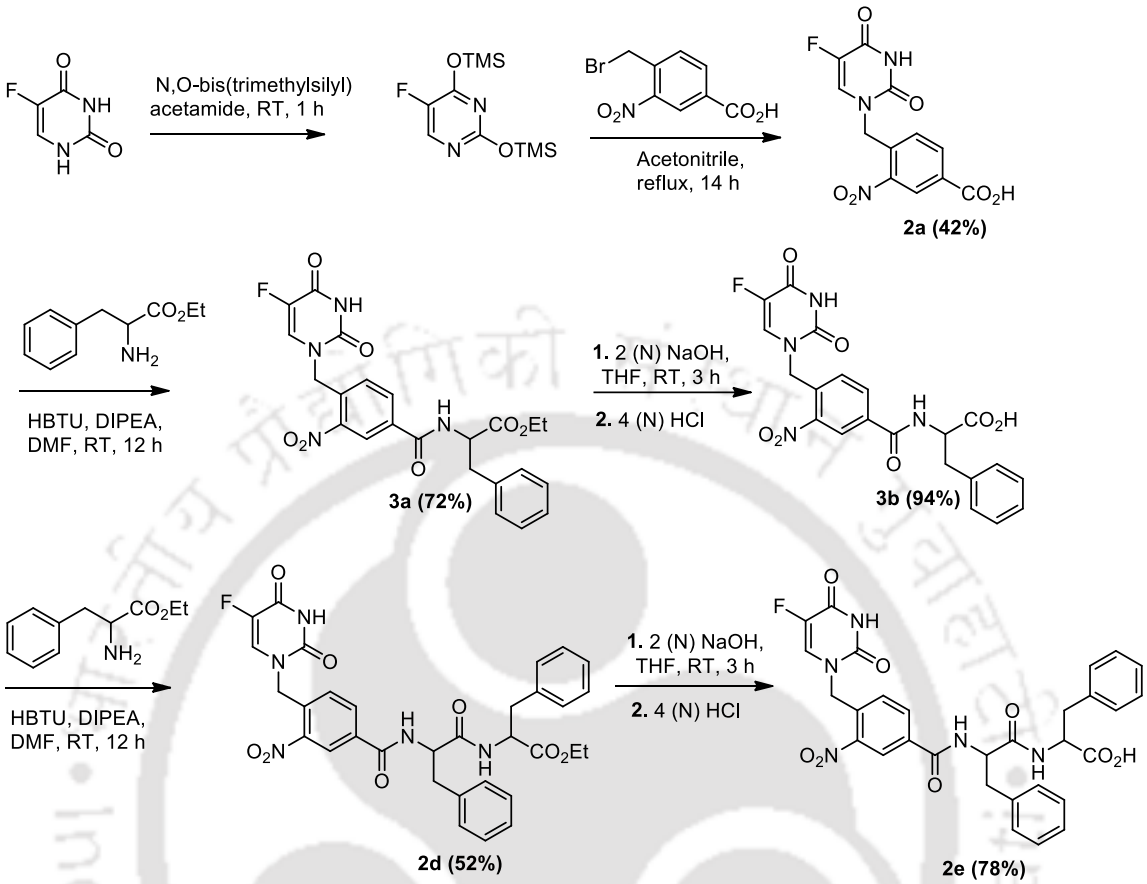

Scheme 3.1 Schematic presentation for the synthesis of 5-Fu-FF conjugate.

3.2.2 Fabrication and characterization of nanoparticles 5-Fu-FF NPs (optimization of size and stability of nanoparticles)

In order to develop a stimuli-responsive, dual-drug nanocarrier, compound **2e** was fabricated into nanoparticles. 5-Fu-FF nanoparticles were synthesized by nanoprecipitation or solvent displacement method, a well-known procedure for preparing various polymeric nanoparticles.[28] Briefly, compound **2e** was dissolved in acetone and added dropwise to an aqueous solution of polyethylene glycol (PEG) 6000. PEG 6000 was introduced to stabilize the nanoparticles. PEG is one of the extensively used polymers in drug delivery due to its remarkable biocompatibility, biodegradability and as a stabilizing agent for nanoparticles.[29-30] The PEG-coated nanoparticles have been shown to have prolonged circulation in bloodstream. The heterogeneous mixture was then kept incubated at room temperature. The energy generated from extensive stirring allows compound **2e** to self-assemble into the nanoparticles.

The physicochemical characteristics of the nanoparticles are of great importance in order to ensure its applications in therapeutic research. The size of the particles, polydispersity index, and zeta potential was recorded by dynamic light scattering (DLS). The synthesized nanoparticles showed a uniform size distribution within the range of 159.3±2.3 nm, with zeta potential being -26.2±1.5 mV.

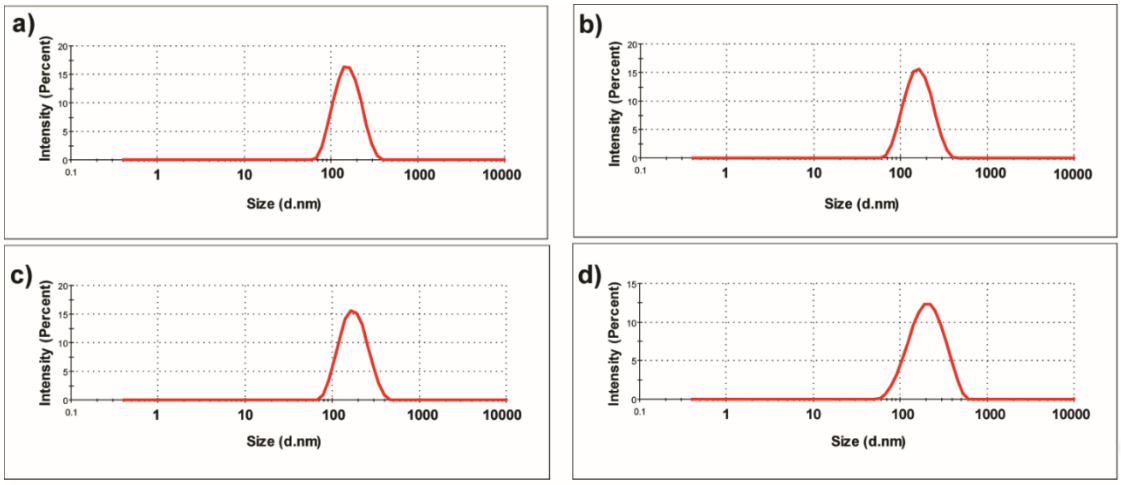

Figure 3.1 Size distribution of blank nanoparticles made using PEG 6000 concentration (w/v %) a) 0.025, b) 0.075, c) 0.1, d) 0.2.

The nanoparticles were found to be negatively charged which may be due to the presence of free carboxyl group or 5-Fu.[31] Before the addition of PEG 6000, the zeta potential of the particles was found to be -14.7±0.9 mV. Whereas, after using an optimized concentration of PEG 6000, the zeta potential was changed to -26.2 mV, indicating better stability of the nanoparticles.

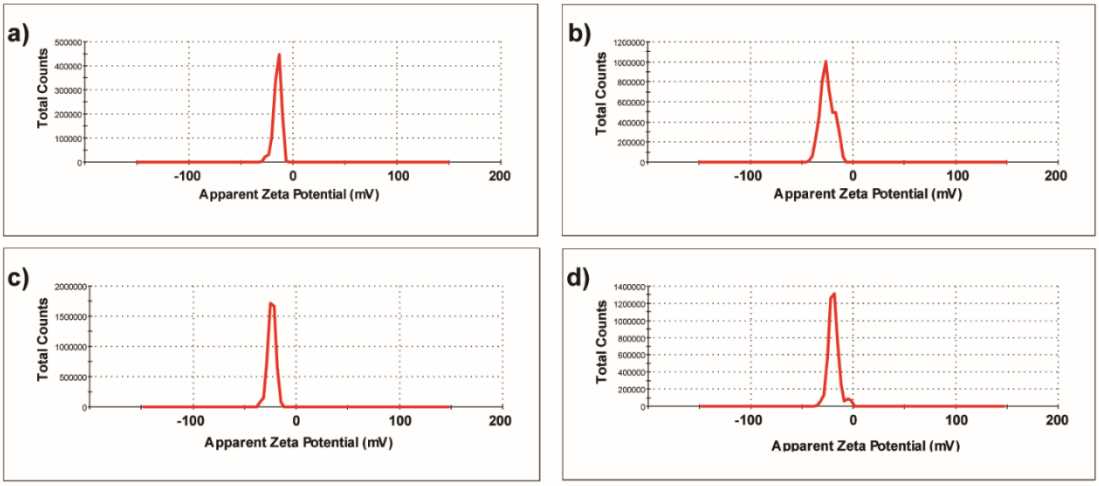

Figure 3.2 Zeta potentials of blank nanoparticles made using PEG 6000 concentration (w/v %) a) 0.025, b) 0.075, c) 0.1, d) 0.2.

The negative surface charge is also expected to make the nanoparticles less cytotoxic compared to positively charged nanoparticles.[32] Table 3.1 shows the variation of size and zeta potential of the nanoparticles with varying concentration of PEG 6000.

Table 3.1 Measurement of particle size and zeta potential of the nanoparticles from compound **2e** using different PEG 6000 concentration

Set no.	Compound 2e concentration mg/ml	PEG 6000 Concentration (w/v)	Size of nanoparticles (nm)	Zeta potential (mV)
1	1	0.025	148.2±1.4	-16.5±3.76
2	1	0.05	159.3±2.35	-26.2±1.5
3	1	0.075	155.9±5.41	-24.47±2.64
4	1	0.1	163.37±4.54	-24.57±2.65
5	1	0.2	193.5±2.37	-19.3±0.71

3.2.3 Synthesis of CPT loaded 5-Fu-FFNPs (under optimized condition)

The presence of the hydrophobic region in compound **2e** confers it the ability to entrap a hydrophobic compound inside the self-assembled nanoparticles. Another notable anticancer agent CPT was chosen as the model hydrophobic compound, to develop a dual-drug nano-carrier. The topoisomerase inhibitor is a natural product that shows poor solubility in an aqueous medium. Therefore, CPT encapsulation into the nanoparticles is expected to have better cell internalization.

CPT loaded nanoparticles were also prepared by the nanoprecipitation method as adopted for preparing 5-Fu-FFNPs. A mixture of CPT and 5-Fu-FF (compound **2e**) in various ratios, was added to water containing PEG 6000, followed by stirring at room temperature for five hours. A detailed DLS analysis (supporting information) showed the optimum size of the nanoparticles as 248.5±66.0 nm, with a zeta potential value -21.6±2.6 mV. An increase in particle size compared to CPT free 5-Fu-FFNPs indicates the formation of CPT loaded nanoparticles.

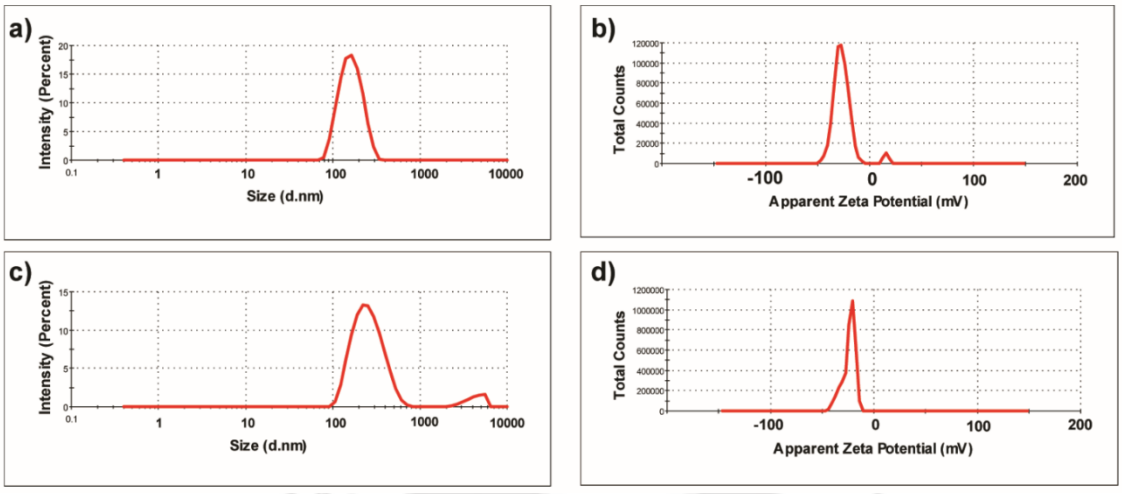

Figure 3.3 a) Size distribution of blank nanoparticles, b) size distribution of CPT loaded nanoparticle (compound **2e**/CPT w/w in 8:1 ratio), c) zeta potential of blank nanoparticles, d) zeta potential of CPT loaded nanoparticles.

The UV-visible spectrum of the nanoparticles showed both the characteristic peaks of compound **2e** as well as CPT (Figure **1a**), confirming the presence of CPT in the nanoparticles.[33]

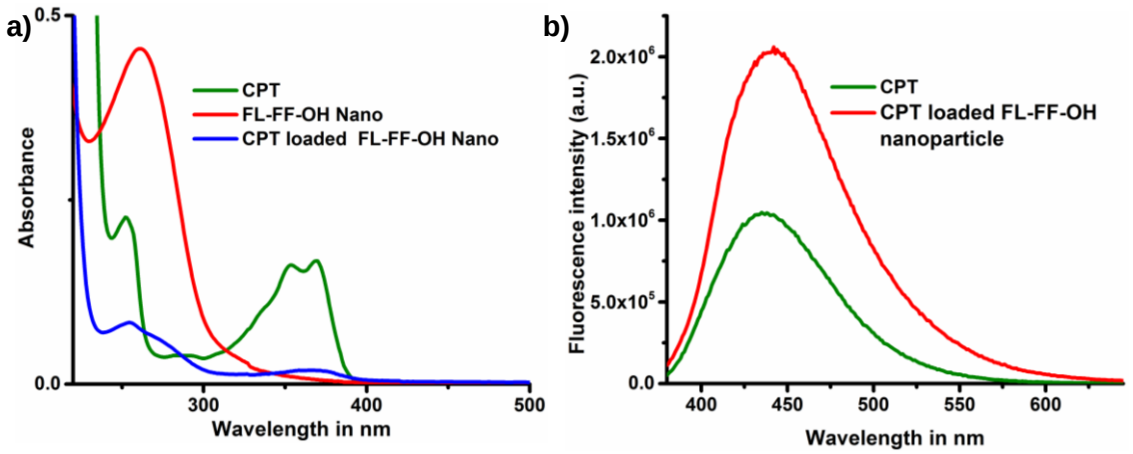

Figure 3.4 Loading of CPT inside 5-Fu-FF nanoparticles a) UV-Visible spectra showing the presence of CPT in the nanoparticles, b) Fluorescence profile confirming CPT was encapsulated into the nanoparticles

In Figure **3.4**, the fluorescence spectrum of CPT in PBS buffer is compared with the spectrum of CPT-loaded nanoparticles. About 7 nm red shift of emission maxima was

observed after the loading of CPT, indicating the incorporation of CPT inside the hydrophobic region of nanoparticles.[34]

As evident from Table 3.2, the highest CPT entrapment efficiency (EE) of the nanoparticles reached about 15% with the compound **2e**/CPT ratio 8:1.

Table 3.2. CPT encapsulation at different compound **2e**/CPT w/w ratio

Set no.	Compound 2e/ CPT w/w ratio	PEG 6000 Concentration (w/v)	EE (%)
1	10:1	0.05%	7.5
2	8:1	0.05%	15.05
3	6:1	0.05%	9.38
4	1:1	0.05%	4.45

3.2.4 Field emission scanning electron microscope (FESEM) images

The collected nanoparticles (both blank 5-Fu-FF NPs and CPT loaded) were resuspended in distilled water and drop cast on a glass plate covered with aluminum foil. The samples were air-dried and coated with gold for imaging. The images for the nanoparticles showed the spherical shape and smooth surface. The distribution of the nanoparticles was also uniform (Figure 2).

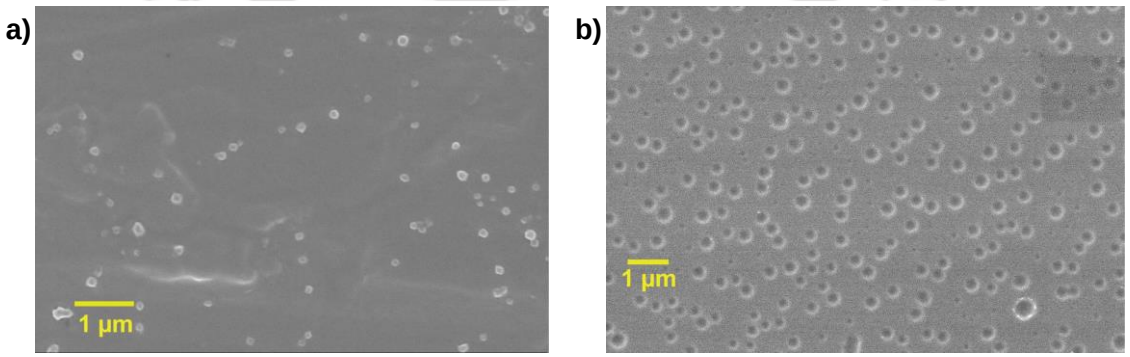

Figure 3.5 FESEM images of a) 5-Fu-FF NPs (size 159.3±2.3), b) CPT loaded 5-Fu-FF NPs (size 248.5±66.0). The images indicate an increase in the size of the nanoparticles after loading of CPT.

3.2.5 Controlled release of 5-Fu from compound 2e

The release of 5-Fu from the synthesized compound **2e** was monitored by UV-Vis and ^{1}H NMR spectroscopy. For photodegradation, 5-Fu-FF nanoparticles (666 µg) were dispersed in 3 mL phosphate saline (PBS) buffer (pH 7.4) and irradiated under 365 nm UV lamp. Figure 3.7b shows a gradual increase in absorbance at 325 nm. This peak is attributed to the generation of *o*-nitrosobenzaldehyde, a photoproduct of the photolysis of *o*-nitrobenzyl group (Figure 3.6a).[22] *o*-nitrosobenzaldehyde usually shows a weak solvent dependent absorption at 325-360 nm.[35] Upon irradiation, 5-Fu is liberated from 5-Fu-FF nanoparticles with the production of peptide tethered *o*-nitrosobenzaldehyde.

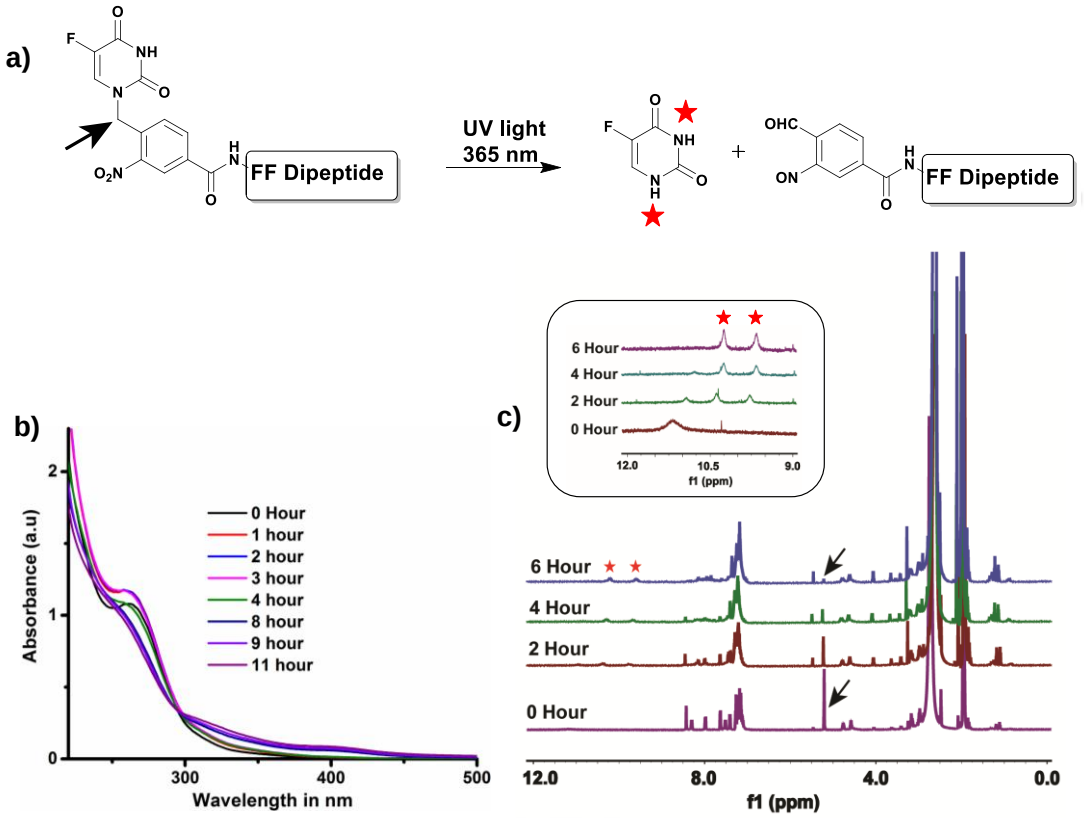

Figure 3.6 Photo-controlled release of 5-Fu under UV irradiation. (a) UV-Vis spectra of cleavage of 5-Fu from 5-Fu-FF nanoparticles, (b) ^{1}H NMR spectra of the release of 5-Fu in acetonitrile-d_3 from compound **2e** (zoomed in version showing the characteristic N1 and N3 proton signals is given in inset).

Furthermore, ^{1}H NMR study (Figure 3.6c) was also performed to monitor the photochemistry. Compound **2e** was dissolved in acetonitrile-d_3 and subjected to

irradiation under 365 nm. As shown in the time-dependent ^{1}HNMR spectra, the singlet at 5.2 ppm corresponding to the methylene proton of the *o*-nitrobenzaldehyde group tethering with the peptide backbone, decreases with time and finally disappeared after 6-hours of irradiation. Three new peaks also appeared at 7.4, 9.6 and 10.3 ppm which corresponds to the C6, N1 and N3 protons of free 5-Fu, respectively. The disappearance of the signal at 5.2 ppm and the appearance of the peaks of free 5-Fu demonstrates the liberation of 5-Fu from the 5-Fu-FF conjugate, upon irradiation.

We also have analyzed the effect of irradiation on the morphology of the nanoparticles. Before irradiation, the 5-Fu-FF nanoparticles were found to have a spherical shape with size 159.3±2.3 nm. However, after 5-hour irradiation the shape of the nanoparticles was slightly changed, and they did not appear to be perfectly spherical (Figure 3.7). Slight distortion from the spherical shape was observed for most of the nanoparticles, and the size was also found to be larger. This observation may be attributed to the change in amphiphilicity of the conjugate peptide, upon cleavage of 5-Fu, and thus may induce a higher tendency of aggregation.

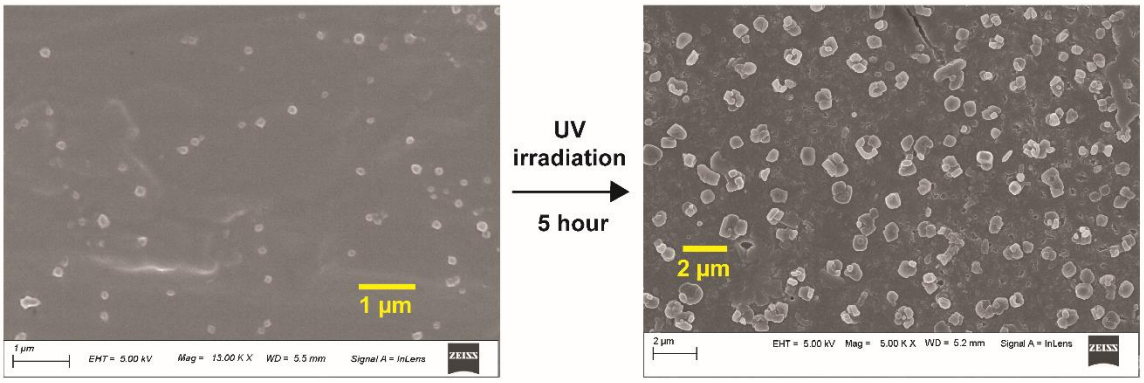

Figure 3.7 Change in shape and size of the nanoparticles after irradiation.

3.2.6 Release of CPT from 5-Fu-FF nanoparticles

The *in vitro* release of CPT from the nanoparticles was achieved by dialysis of the CPT loaded 5-Fu-FF nanoparticles. The sink condition was maintained carefully throughout the experiment. The release of CPT was measured by fluorescence with an excitation wavelength of 370 nm and emission at 435 nm. The concentration of released CPT at different time intervals were obtained from the standard curve of CPT prepared in PBS

buffer (pH 7.4). An increase in fluorescence intensity indicates the release of CPT in the media. The drug release profile (Figure 3.8) suggests sustained release of CPT from the nanoparticles. Within 24 hours, an estimated 18% of CPT was deloaded. However, after 24 hours, the release occurred in a sustained manner producing 67% of CPT after three days.

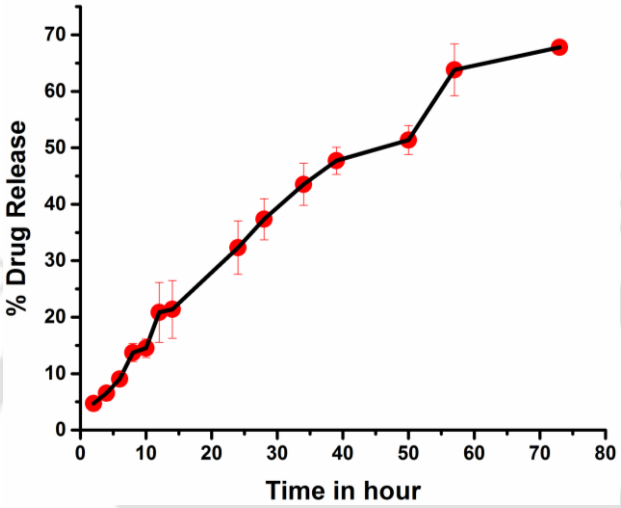

Figure 3.8 CPT release profile measured by taking fluorescence of the collected solutions in dialysis method. It showed 67% release of CPT after 3 days in a sustained manner.

3.2.7 MTT assay in HeLa cell lines

In order to establish the validity of the synthesized nanoparticles, MTT assay was carried out in human cervical HeLa cell lines. Cells were incubated in combination with various concentrations of blank 5-Fu-FF-NPs, CPT loaded NPs both in absence and presence of external stimulation. Figure 6 demonstrates the cell viability after 24-hours incubation with NPs in four different conditions. As evident from the cell viability assay (Figure 3.9), the blank nanoparticles containing covalently attached 5-Fu showed almost no toxicity even at a very high concentration of 500 µg/mL, justifying the prodrug nature of the synthesized peptide nanoparticles. However, it showed substantial amount of toxicity when irradiated with UV-light (365nm). This, as anticipated, may be attributed to the photo-induced release of the antitumor agent from the nanoparticles, thereby killing the cancer cells. The visible reduction of cell viability of CPT loaded nanoparticles, in absence of irradiation, clearly suggests cell death due to sustained release of CPT in a

diffusion-controlled manner. It is worthy to mention that the highest amount of cytotoxicity was observed when the CPT loaded nanoparticles were irradiated with UV-light. The high percentage of cell death could be attributed to the combined release of both and CPT. Hence, the synthesized dual-drug carrier peptide nanoparticles were able to retain the inherent cytotoxicity of the therapeutic agents after the release from the nanoparticles.

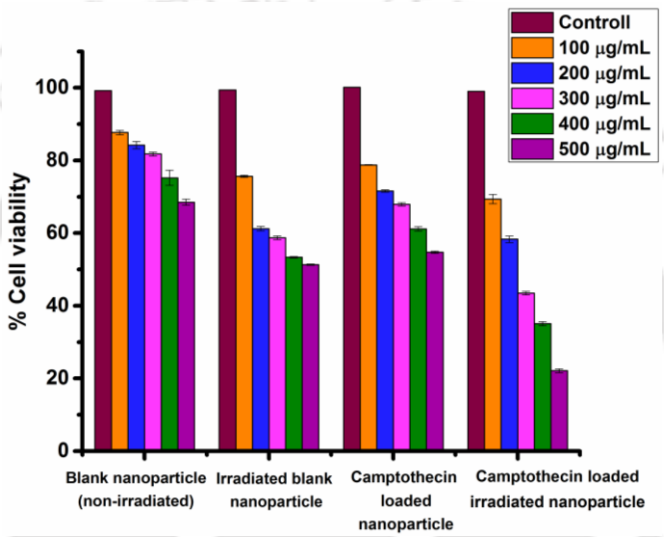

Figure 3.9 Cytotoxicity assay of the synthesized nanoparticles in HeLa cells after 48 hours of incubation. Inset: concentration of nanoparticles.

3.3 Experimental Section

3.3.1 Instrumentation and Characterization

All reagents were bought commercially from reputed sources and used directly. For compound purification, column chromatography technique was followed using Silica gel (60-120 mesh). For reactions monitoring, thin-layer chromatography (TLC) was utilized on glass-backed TLC plates, precoated with silica gel 60 F254 (0.25 mm). All the ^{1}H NMR and ^{13}C NMR spectra were recorded by 600 and 150 MHz, respectively, with Brucker spectrometer. For recording NMR spectra DMSO-d_6 and acetonitrile-d_3 were used as solvents with tetramethysilane (TMS) as an internal standard. The chemical shifts (δ_{ppm}) and coupling constants (J) were presented in parts per million (ppm) and Hertz (Hz), respectively. Peak multiplicities were designated by abbreviations such as: s

(singlet), d (doublet), t (triplet), m (multiplet) and br (broadened). Agilent Q-TOF mass spectrometer with Z-spray source was employed for the acquisition of high-resolution mass spectra (HRMS). All HRMS data were analyzed by built-in software. To prepare all the nanoparticles, Millipore water was used. Field emission scanning electron microscope (FESEM) was carried out in a SIGMA 300 instrument. UV-Vis experiments and fluorescence studies were performed by using Perkin Elmer UV-Vis spectrophotometer and Horiba scientific Fluoromax-4 spectrofluorometer, respectively.

3.3.2 Synthetic procedures of compounds 2e

A. Synthesis of prodrug (4-((5-fluoro-2,4-dioxo-3,4-dihydropyrimidin-1(2*H*)-yl) methyl)-3-nitrobenzoic acid) (2a): The prodrug was synthesized according to the literature[19, 26] and also described in 2.4.1A.

B. Synthesis of 2-(4-((5-fluoro-2,4-dioxo-3,4-dihydropyrimidin-1(2*H*)-yl)methyl)-3-nitrobenzamido)-3-phenylpropanoic acid (3b): The phenylalanine prodrug conjugate was synthesized following a coupling reaction. The prodrug **2a** (500 mg, 1.6 mmole) was made to react with L-Phenylalanine ethyl ester hydrochloride (372 mg, 1.6 mmole) in dry dimethylformamide (DMF) using *N*,*N*,*N*′,*N*′-Tetramethyl-*O*-(1*H*-benzotriazol-1-yl)uronium hexafluorophosphate (HBTU, 675 mg, 1.8 mmole) as the coupling agent and *N*, *N*-Diisopropylethylamine (DIPEA, 271 mg, 2.1 mmole) as the basic source at room temperature for overnight. After the completion of the reaction, the mixture was extracted with cold water followed by brine solution using ethyl acetate as the organic solvent. The organic layer was dried over sodium sulfate and purified further by column chromatography using 1:10 methanol/chloroform as the mobile phase to obtain a light yellow powdered product **3a** (564 mg, 72%). ^{1}H NMR (400 MHz, DMSO-d_6) δ 11.99 (s, 1H), 9.29 (d, J = 7.8 Hz, 1H), 8.59 (d, J = 1.7 Hz, 1H), 8.18 – 8.14 (m, 2H), 7.58 (d, J = 8.2 Hz, 1H), 7.36 – 7.30 (m, 4H), 7.26 (dd, J = 6.2, 2.4 Hz, 1H), 5.27 (s, 2H), 4.73 (ddd, J = 9.7, 7.7, 5.8 Hz, 1H), 4.16 (q, J = 7.1 Hz, 2H), 3.20 (ddd, J = 23.6, 13.7, 7.8 Hz, 2H), 1.19 (t, J = 7.1 Hz, 3H). ^{13}C NMR (100 MHz, DMSO-d_6) δppm 171.8, 164.5, 158.2, 158, 150.3, 147.9, 139.5, 137.9, 135.6, 134.3, 133.2, 130, 129.5, 129.1, 128.7, 127, 124.3, 61.2, 54.9, 48.9, 40.6, 40.4, 40.2, 40, 39.9, 39.6, 39.4, 36.7, 14.4; HRMS (ESI) calcd. for $C_{23}H_{21}FN_4O_7$ $[M + H]^+$: 485.1467, found: 485.1487. The obtained product (564 mg) was

dissolved in THF and stirred for three hours by adding 2(N) sodium hydroxide at room temperature. The total loss of the starting material was monitored by thin-layer chromatography (TLC), and then 4(N) hydrochloric acid (HCl) was added dropwise to acidify the reaction mixture. The product was precipitated as a light yellow powder. It was filtered and dried to obtain 499 mg (94%) compound **3b.**

C. Synthesis of 2-(2-(4-((5-fluoro-2,4-dioxo-3,4-dihydropyrimidin-1(2*H*)-yl)methyl)-3-nitrobenzamido)-3-phenylpropanamido)-3-phenylpropanoic acid (2e): Compound **2e** was prepared from compound **2d** by base-catalyzed hydrolysis reaction as described previously in 2.4.1D following literature procedure.[19]

3.3.3 ^{1}H NMR experiment

5 mg of compound **2e** was dissolved in Acetonitrile-d_3. The sample was irradiated under 365 nm UV light and ^{1}H NMR spectra were recorded after 0, 2, 4, 6 hours respectively.

3.3.4 Preparation of 5-Fu-FF nanoparticles

The nanoparticles were prepared by nanoprecipitation method using PEG 6000 as the stabilizing agent. Briefly, 1 mg of compound **2e** was dissolved in 3:1 acetone / DMSO and added dropwise to 2 mL water containing PEG 6000 in different concentrations. The solution was stirred for four hours at room temperature until acetone is completely evaporated. After 5 hours the nanoparticles were collected by centrifugation at 15000 rpm at 10˚C and washed several times to remove the excess stabilizing agent. Finally, nanoparticles were dispersed in fresh PBS buffer and used for further analysis.

3.3.5 Preparation of CPT-loaded 5-Fu-FF nanoparticles

For the preparation of CPT-loaded nanoparticles, similar nanoprecipitation method was employed as used for 5-Fu-FF nanoparticles, with minor changes. To prepare CPT-loaded nanoparticles CPT was dissolved in DMSO and mixed with the acetone solution of compound **2e** in such a way that the final acetone/ DMSO proportion will be in 3:1 ratio. The compound **2e** and CPT amount were also varied from 10:1, 8:1, 6:1, 2:1 and 1:1. This mixture of organic solvents containing CPT and compound **2e** was stirred for 30 minutes to dissolve the drug completely. The solution was then added to water

containing PEG 6000 and left for stirring to evaporate acetone completely. After 5 hours, the unloaded drug was removed by centrifugation at a speed of 2000 rpm for 5 minutes, and the CPT loaded nanoparticles were collected by centrifugation at a speed of 15000 rpm for 35 minutes. The collected nanoparticles were washed with distilled water three times for removing excess stabilizer (PEG 6000) and unloaded CPT and DMSO. The recovered nanoparticles were resuspended in water and used for further analysis.

3.3.6 Entrapment efficiency

The loading of CPT and encapsulation efficiency (EE) was measured by lyophilizing the obtained nanoparticles and dissolving them in DMSO. To this DMSO solution of the nanoparticles, acetonitrile was added in such an amount that the final volume ratio would be 1:1. The CPT concentration was measured by UV spectrophotometry at 365 nm. The measured absorbance was compared with a standard curve prepared in the same solvent. The following formula calculates the encapsulation efficiency.

$$\textbf{Encapsulation Efficiency (\%)} = \frac{\text{Weight of the drug entrapped}}{\text{Weight of total drug added}}$$

3.3.7 Characterization of nanoparticles

The particle size and zeta potential were measured by dynamic light scattering (DLS) at 25˚C with Malvern Zetasizer Nano ZS90 using appropriate viscosity and refractive index.

3.3.8 Field emission scanning electron microscope (FESEM)

1 mg of synthesized nanoparticle was suspended in PBS (pH 7.4) buffer. The nanoparticle suspension was placed on a glass plate covered with aluminum foil and coated with gold before analysis with SIGMA 300 FESEM instrument.

3.3.9 *In vitro* release of CPT from the nanoparticles

The *in vitro* release of CPT from the nanoparticles was monitored by dialysis. The lyophilized nanoparticles equivalent to 7.5 µg of CPT was resuspended in 1 mL PBS buffer (pH 7.4) and poured into a dialysis bag (MWCO 1kDa). The dialysis bag was then

immersed into 30 ml release media (PBS buffer, pH 7.4) with a stirring speed of 100 rpm. At specific time intervals, 1 mL aliquot was withdrawn from the release media and was replaced by 1 mL fresh PBS buffer, pH 7.4 to maintain sink condition. The release of CPT was measured by fluorescence with an excitation wavelength of 370 nm and emission at 435 nm. The concentration of released CPT at different time interval was compared with a standard curve of CPT prepared in the same PBS buffer.

3.3.10 Cytotoxicity of nanoparticles

To determine the cytotoxic effect of our nanoparticles, MTT assay was carried out. The cell viability assay was conducted in human cervical HeLa cell lines, obtained from National Centre for Cell Sciences (NCCS), Pune, India, following the previously demonstrated procedure.[35] For this study, $5x10^3$ cells were seeded into 96-well microplate in 90 µL Dulbecco's modified Eagle's medium (DMEM) and were incubated for 24 hours in presence of 5% CO_2 at 37˚C. Cells were then treated with varying concentrations of the blank (5-Fu-FF NPs) and CPT loaded nanoparticles (100, 200, 300, 400, 500 µg/mL) both in presence and absence of radiation for 24 hours. After the incubation, the cell viability assay was carried out by using 3-(4, 5-dimethylthiazol-2-yl)-2, 5-diphenyltetrazolium bromide (MTT). After the addition of MTT, each plate was incubated for 2 hours at 37˚C. The medium was then removed and 60 µL of DMSO was added to produce formazan that showed absorption (A) at 570 nm. The optical density (OD) of each well-plate was measured with the background reference at 690 nm. All the tests were performed in triplicates. The control experiment was also carried out in similar way but without the addition of nanoparticles. The percentage cell viability with respect to the control was calculated by using the standard formula as given below

$$\%\ of\ cell\ viability = \frac{(A_{570} - A_{690})\ of\ treated\ cells}{(A_{570} - A_{690})\ of\ control\ cells} \times 100\ \%$$

3.4 Conclusion

In this report, we have developed a polyethyleneglycol stabilized 5-Fu tethered peptide nanoparticles with remarkably reduced cytotoxicity but releases 5-Fu in a dose-dependent photo-responsive manner. The size of the nanoparticles was found to be in between 130-170 nm, which enhances its probability for improved cell penetration. Furthermore, the synthesized nanoparticles found greater importance with its ability to entrap another hydrophobic therapeutic molecule inside its hydrophobic core, making it a dual-responsive, dual-drug scaffold. CPT was shown as a model hydrophobic drug to be encased into the nanoparticles. In summary, this report provided a strategy to fabricate nanoparticles from a biocompatible peptide drug conjugate and further delivery of a second drug by physically encapsulating it inside nanoparticles. This conformity can further be improved by the introduction of a tumor-targeting moiety or a fluorescence molecule for bioimaging.

3.5 References

1. Hartgerink, J. D.; Beniash, E.; Stupp, S. I., Peptide-amphiphile nanofibers: a versatile scaffold for the preparation of self-assembling materials. *Proc. Natl. Acad. Sci. U.S.A.* **2002,** *99* (8), 5133-5138.

2. Hartgerink, J. D.; Beniash, E.; Stupp, S. I., Self-assembly and mineralization of peptide-amphiphile nanofibers. *Science* **2001,** *294* (5547), 1684-1688.

3. Debnath, S.; Roy, S.; Ulijn, R. V., Peptide nanofibers with dynamic instability through nonequilibrium biocatalytic assembly. *J. Am. Chem. Soc.* **2013,** *135* (45), 16789-16792.

4. Kol, N.; Adler-Abramovich, L.; Barlam, D.; Shneck, R. Z.; Gazit, E.; Rousso, I., Self-assembled peptide nanotubes are uniquely rigid bioinspired supramolecular structures. *Nano Lett.* **2005,** *5* (7), 1343-1346.

5. Reches, M.; Gazit, E., Controlled patterning of aligned self-assembled peptide nanotubes. *Nat. Nanotechnol.* **2006,** *1* (3), 195-200.

6. Cui, H.; Muraoka, T.; Cheetham, A. G.; Stupp, S. I., Self-assembly of giant peptide nanobelts. *Nano Lett.* **2009,** *9* (3), 945-951.

7. Li, Y.; Yan, L.; Liu, K.; Wang, J.; Wang, A.; Bai, S.; Yan, X., Solvothermally Mediated Self-Assembly of Ultralong Peptide Nanobelts Capable of Optical Waveguiding. *Small* **2016,** *12* (19), 2575-2579.

8. Matsuura, K.; Murasato, K.; Kimizuka, N., Artificial peptide-nanospheres self-assembled from three-way junctions of β-sheet-forming peptides. *J. Am. Chem. Soc.* **2005,** *127* (29), 10148-10149.

9. Fan, Z.; Sun, L.; Huang, Y.; Wang, Y.; Zhang, M., Bioinspired fluorescent dipeptide nanoparticles for targeted cancer cell imaging and real-time monitoring of drug release. *Nat. Nanotechnol.* **2016,** *11* (4), 388-394.

10. Li, S.; Liu, Y.; Xing, R.; Yan, X., Covalently Assembled Dipeptide Nanoparticles with Adjustable Fluorescence Emission for Multicolor Bioimaging. *ChemBioChem* **2019**, *20*, 555-560.

11. Zhang, H.; Fei, J.; Yan, X.; Wang, A.; Li, J., Enzyme-responsive release of doxorubicin from monodisperse dipeptide-based nanocarriers for highly efficient cancer treatment in vitro. *Adv. Funct. Mater.* **2015,** *25* (8), 1193-1204.

12. Sun, B.; Wang, L.; Li, Q.; He, P.; Liu, H.; Wang, H.; Yang, Y.; Li, J., Bis (pyrene)-doped cationic dipeptide nanoparticles for two-photon-activated photodynamic therapy. *Biomacromolecules* **2017,** *18* (11), 3506-3513.

13. Wang, Y.; Cheetham, A. G.; Angacian, G.; Su, H.; Xie, L.; Cui, H., Peptide–drug conjugates as effective prodrug strategies for targeted delivery. *Adv. Drug Delivery Rev.* **2017,** *110*, 112-126.

14. Chen, X.; Plasencia, C.; Hou, Y.; Neamati, N., Synthesis and biological evaluation of dimeric RGD peptide− paclitaxel conjugate as a model for integrin-targeted drug delivery. *J. Med. Chem.* **2005,** *48* (4), 1098-1106.

15. Zhu, L.; Wang, T.; Perche, F.; Taigind, A.; Torchilin, V. P., Enhanced anticancer activity of nanopreparation containing an MMP2-sensitive PEG-drug conjugate and cell-penetrating moiety. *Proc. Natl. Acad. Sci. U.S.A.* **2013**, *110* (42), 17047-17052.

16. Lin, Y.-A.; Cheetham, A. G.; Zhang, P.; Ou, Y.-C.; Li, Y.; Liu, G.; Hermida-Merino, D.; Hamley, I. W.; Cui, H., Multiwalled nanotubes formed by catanionic mixtures of drug amphiphiles. *ACS Nano* **2014,** *8* (12), 12690-12700.

17. Sun, Y.; Kaplan, J. A.; Shieh, A.; Sun, H.-L.; Croce, C. M.; Grinstaff, M. W.; Parquette, J. R., Self-assembly of a 5-fluorouracil-dipeptide hydrogel. *Chem. Commun.* **2016,** *52* (30), 5254-5257.

18. Lin, R.; Cheetham, A. G.; Zhang, P.; Lin, Y.-a.; Cui, H., Supramolecular filaments containing a fixed 41% paclitaxel loading. *Chem. Commun.* **2013,** *49* (43), 4968-4970.

19. Das, S.; Horo, H.; Goswami, U.; Kundu, L. M., Synthesis of a Peptide Conjugated 5-Fluorouracil Gelator Prodrug for Photo-Controlled Release of the Antitumor Agent. *ChemistrySelect* **2019,** *4* (22), 6778-6783.

20. Horo, H.; Das, S.; Mandal, B.; Kundu, L. M., Development of a photoresponsive chitosan conjugated prodrug nano-carrier for controlled delivery of antitumor drug 5-fluorouracil. *Int. J. Biol. Macromol.* **2019,** *121*, 1070-1076.

21. Klán, P.; Solomek, T.; Bochet, C. G.; Blanc, A. l.; Givens, R.; Rubina, M.; Popik, V.; Kostikov, A.; Wirz, J., Photoremovable protecting groups in chemistry and biology: reaction mechanisms and efficacy. *Chem. Rev.* **2012,** *113* (1), 119-191.

22. Zhang, Z.; Hatta, H.; Ito, T.; Nishimoto, S.-i., Synthesis and photochemical properties of photoactivated antitumor prodrugs releasing 5-fluorouracil. *Org. Bimol. Chem.* **2005,** *3* (4), 592-596.

23. Ghosh, R.; Goswami, U.; Ghosh, S. S.; Paul, A.; Chattopadhyay, A., Synergistic anticancer activity of fluorescent copper nanoclusters and cisplatin delivered through a hydrogel nanocarrier. *ACS Appl. Mater. Interfaces* **2014,** *7* (1), 209-222.

24. Chen, L.; Morris, K.; Laybourn, A.; Elias, D.; Hicks, M. R.; Rodger, A.; Serpell, L.; Adams, D. J., Self-assembly mechanism for a naphthalene− dipeptide leading to hydrogelation. *Langmuir* **2009,** *26* (7), 5232-5242.

25. Wu, F.-Y.; Hsu, S.-M.; Cheng, H.; Hsu, L.-H.; Lin, H.-C., The effect of fluorine on supramolecular hydrogelation of 4-fluorobenzyl-capped diphenylalanine. *New J. Chem.* **2015,** *39* (6), 4240-4243.

26. Raeburn, J.; Pont, G.; Chen, L.; Cesbron, Y.; Lévy, R.; Adams, D. J., Fmoc-diphenylalanine hydrogels: understanding the variability in reported mechanical properties. *Soft Matter* **2012,** *8* (4), 1168-1174.

27. Reches, M.; Gazit, E., Formation of closed-cage nanostructures by self-assembly of aromatic dipeptides. *Nano Lett.* **2004,** *4* (4), 581-585.

28. Govender, T.; Stolnik, S.; Garnett, M. C.; Illum, L.; Davis, S. S., PLGA nanoparticles prepared by nanoprecipitation: drug loading and release studies of a water soluble drug. *J. Controlled Release* **1999,** *57* (2), 171-185.

29. Semete, B.; Booysen, L.; Kalombo, L.; Venter, J. D.; Katata, L.; Ramalapa, B.; Verschoor, J. A.; Swai, H., In vivo uptake and acute immune response to orally administered chitosan and PEG coated PLGA nanoparticles. *Toxicol. Appl. Pharmacol.* **2010,** *249* (2), 158-165.

30. Christian, P.; Bromfield, M., Preparation of small silver, gold and copper nanoparticles which disperse in both polar and non-polar solvents. *J. Mater. Chem.* **2010,** *20* (6), 1135-1139.

31. Bildstein, L.; Dubernet, C.; Couvreur, P., Prodrug-based intracellular delivery of anticancer agents. *Adv. Drug Delivery Rev.* **2011,** *63* (1-2), 3-23.

32. Crucho, C. I.; Barros, M. T., Formulation of functionalized PLGA polymeric nanoparticles for targeted drug delivery. *Polymer* **2015,** *68*, 41-46.

33. Concellón, A.; Clavería-Gimeno, R.; Velázquez-Campoy, A.; Abian, O.; Piñol, M.; Oriol, L., Polymeric micelles from block copolymers containing 2, 6-diacylaminopyridine units for encapsulation of hydrophobic drugs. *RSC Adv.* **2016,** *6* (29), 24066-24075.

34. Burke, T. G.; Mishra, A. K.; Wani, M. C.; Wall, M. E., Lipid bilayer partitioning and stability of camptothecin drugs. *Biochemistry* **1993,** *32* (20), 5352-5364.

35. Nazemi, A.; Schon, T. B.; Gillies, E. R., Synthesis and degradation of backbone photodegradable polyester dendrimers. *Org. Lett.* **2013,** *15* (8), 1830-1833.

3.6 NMR and HRMS spectra of synthesized compounds.

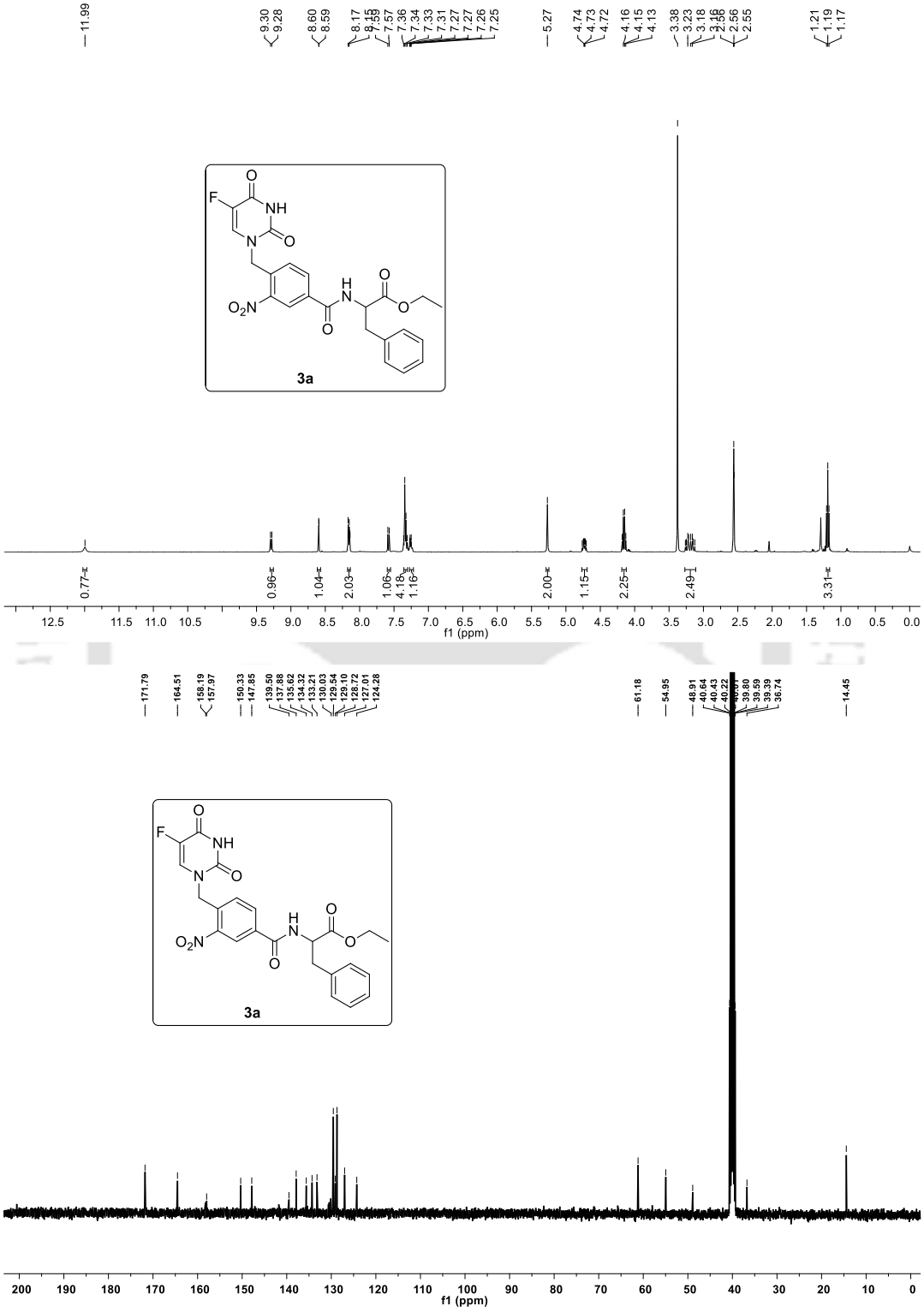

^{1}H (A) and ^{13}C (B) spectra of compound **3a**

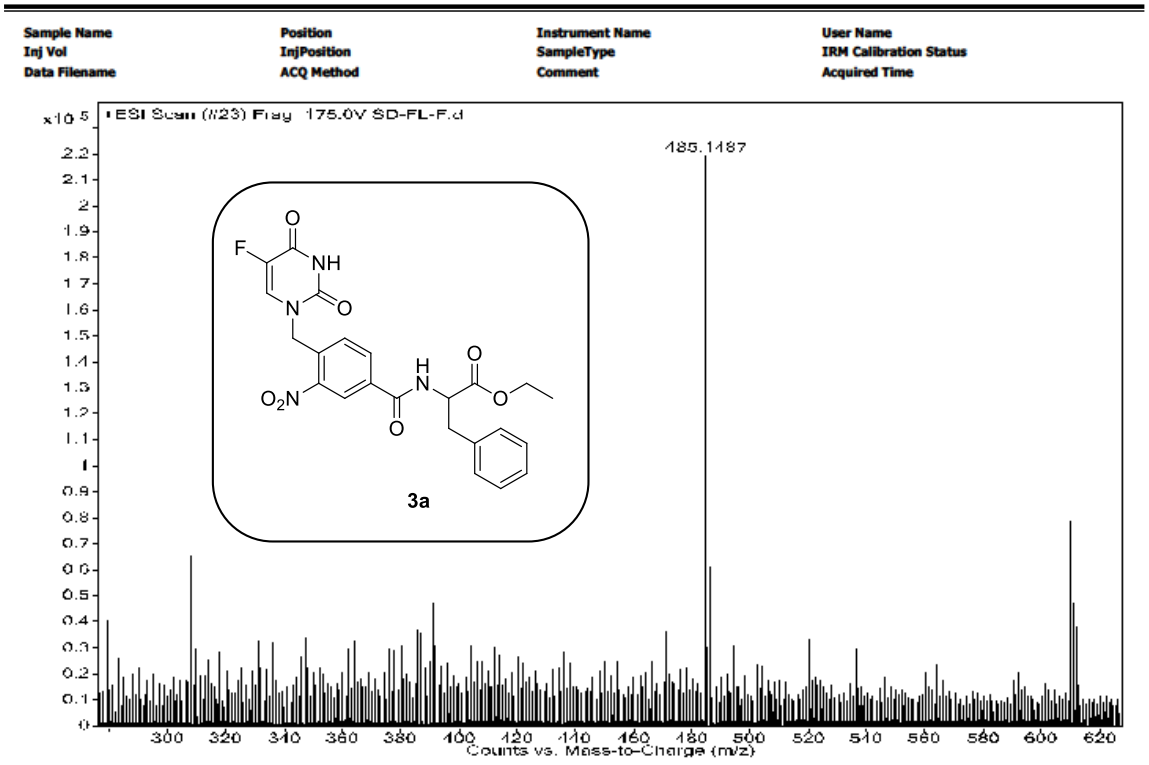

HRMS spectra of compound **3a.**

Chapter 4

Synthesis and Fabrication of Nanoparticles for Dual Responsive Dual Drug Delivery

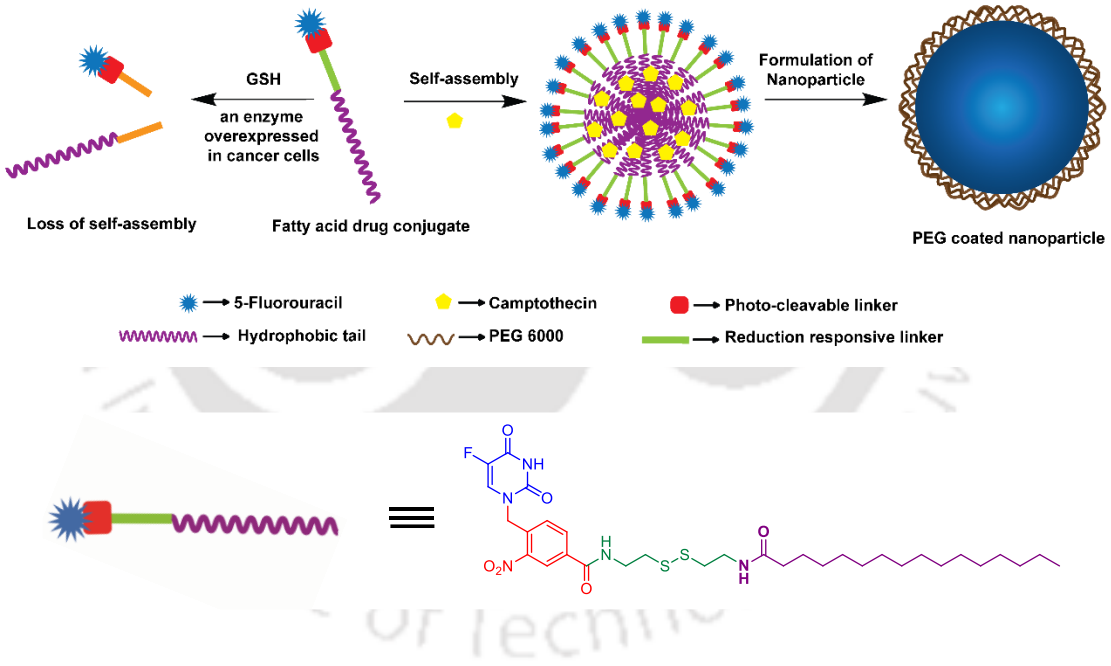

4.1 Introduction

For the last few decades, multiple efforts have been made to improve the efficacy of contemporary anticancer drugs by means of various drug delivery systems (DDS).[1] The fundamental purpose to design a DDS is to assimilate an existing drug into an advanced delivery vehicle and distribute it into the affected cells by minimizing the side effects associated with its journey.[2] Diverse technologies such as controlled release system,[3] target-specific release[4] etc. have been originated to achieve utmost potency of a drug. Amid all, the emergence of nanotechnology garnered significant recognition in the field of therapeutic research.[5-6] Various nanocarriers like liposomes,[7] niosomes,[8] solid lipid nanoparticles,[9] micelles,[10] dendrimers,[11] mesoporous silica nanoparticles,[12] nanoshells[13] etc. have been used for drug delivery. Nevertheless, most of these formulations usually lack target specificity, dose-dependent controlled-release capacity. Moreover, they also suffer from other issues, related to poor encapsulation efficiency of the carrier, sudden or burst release of the drug, leaching of the drug from the carrier along with systematic toxicity of the carriers.[14]

Covalent conjugation of a drug with the carrier was introduced as a potential technique[15] to overcome some of these drawbacks of DDS and successfully applied to design the nanocarriers. Generally, the drug molecule is attached with the carrier by a cleavable linker, making it a prodrug molecule. Prodrug is an inactive drug molecule, which can generate the active drug upon specific stimulation.[16] Prodrugs of different popular anticancer agents were widely used in nanocarrier based drug delivery, either by physical entrapment of the prodrug inside the nanoparticles or by covalent conjugation with the nanoparticles.[17] Several research groups have designed many amphiphiles incorporating prodrug molecules to fabricate umpteen nanostructures like nanofibers, nanospheres, nanobelts, nanoparticles etc. using their self-assembly property.

Self-assembly has found a vast application in drug delivery. Initially, self-assembled nanostructures were made from peptides, polymers, carbohydrates etc. where the drug molecules were physically entrapped inside the nanostructures. Later on, a new strategy was adopted, where the drug is covalently conjugated with a carrier and the whole system can form a nano assembly *i.e.* the drug itself will be a part of the molecular

structure. Such a strategy was followed by Cui and co-workers at the time of developing a supramolecular filament comprised of CPT, a widely used anticancer drug.[18] They have conjugated CPT, a hydrophobic drug to a hydrophilic and β sheet forming peptide sequence derived from tau protein through a reduction cleavable disulfylbutyrate (buSS) linker. This type of covalent conjugation of the drug not only increases its bioavailability but also provides a fixed predetermined drug concentration. Moreover, as the release of the drug is stimuli dependent, the dose can also be controlled as required.

Herein we propose synthesis of a drug amphiphile and fabrication of nanoparticles from it. The amphiphile was consisting of 5-Fu as the hydrophilic unit and palmitic acid as the hydrophobic one. In this strategy, instead of using 5-Fu directly in the active form, we have opted for a photoresponsive prodrug of 5-Fu where the active 5-Fu will be produced upon irradiation with UV light (365 nm). A very well-known ortho nitro benzyl moiety was employed as the photocleavable unit to construct the 5-Fu prodrug.[19] Furthermore, the prodrug component was linked with palmitic acid through a reduction cleavable cystamine, designed to be cleaved by the enzyme glutathione (GSH).[20] GSH is known to be overexpressed in tumor cells as compared to, cells,[21] thereby making the synthesized amphiphile specific to the affected cells. The formulation of nanoparticles was attained by nanoprecipitation method. The size of the nanoparticles was also modulated within 150-200 nm range by optimizing various conditions. Importantly, the hydrophobic region comprised of palmitic acid was also able to load another anticancer agent, a hydrophobic CPT and thus making our system as a dual carrier of hydrophilic as well as hydrophobic anticancer agents simultaneously. The release of CPT was found to be expedited upon treatment with GSH, that disrupts the self-assembly.

4.2 Results and Discussion

4.2.1 Design and synthesis of palmitic acid 5-Fu conjugate (4c)

The design of an amphiphilic molecule consisting of a 5-Fu prodrug is demonstrated here (Figure 4.1).

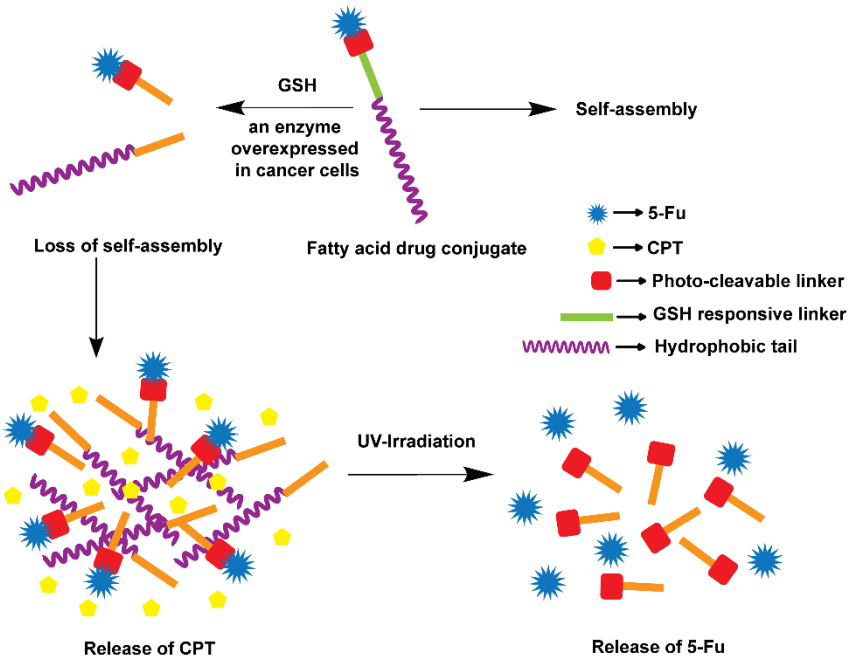

Figure 4.1. Design of dual responsive dual-drug delivery system.

Additionally, a disulfide cystamine linker was used to tether the hydrophilic and hydrophobic domain of the amphiphile. This imparts the ability to control the self-assembly behavior of the amphiphile in a reduction sensitive manner. Thus this molecule was embellished with the capability of carrying and releasing a hydrophobic drug, encapsulated in the hydrophobic region of its self-assembled nanostructure alongside 5-Fu. The hydrophilic unit of the amphiphile, a photo-responsive prodrug of 5-Fu was synthesized by a protocol previously described in section.2.4.1 A (Chapter 2) The hydrophobic part, constituted with palmitic acid, was attached with cystamine dihydrochloride following a closely related method reported by Kim and his co-workers.[22-23] The entire procedure of synthesizing the 5-Fu amphiphile (compound **4c**) is described in Scheme 4.1.

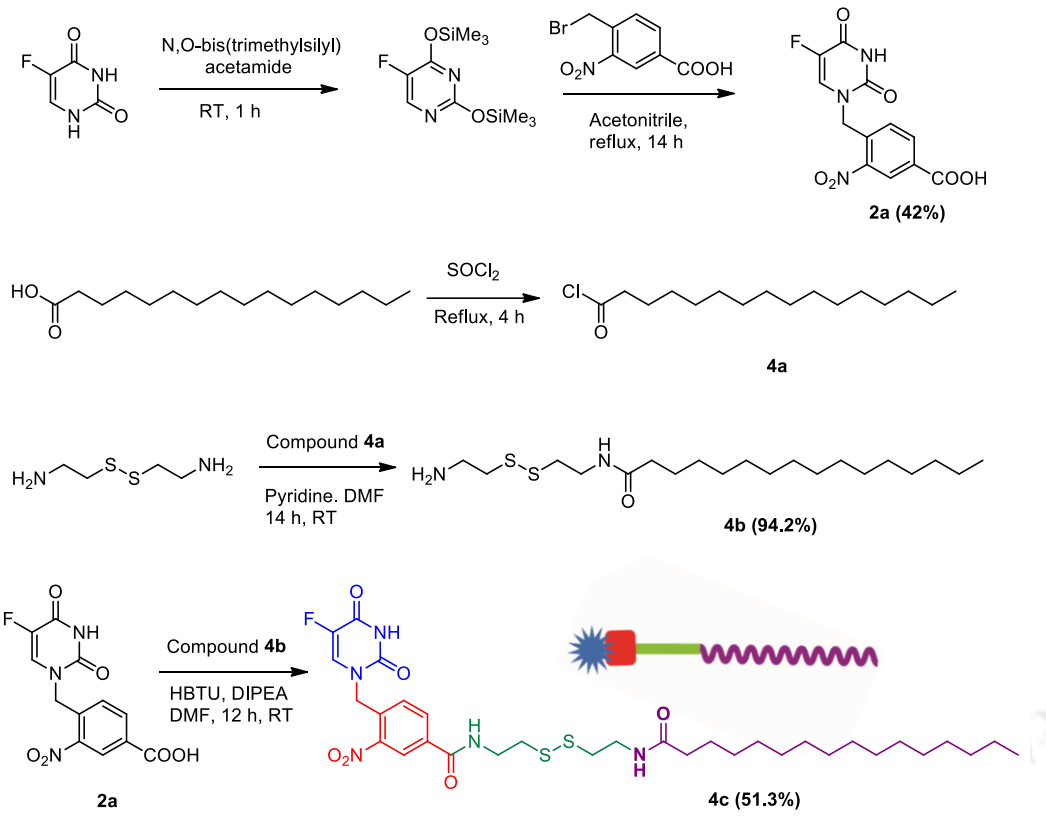

Scheme 4.1 Schematic presentation of the synthesis of 5-Fu-palmitic acid conjugate (**4c**).

The *N*-(2-((2-aminoethyl)disulfanyl)ethyl)palmitamide (compound **4b**) was prepared first by mixing cystamine dihydrochloride with pyridine in dimethylformamide (DMF) and after 10-minutes stirring, palmitoyl chloride was poured dropwise to the solution in ice cold condition. Finally compound **4b** was reacted with 5-Fu prodrug (compound **2a**) in a peptide coupling procedure utilizing *N*,*N*,*N*′,*N*′-Tetramethyl-*O*-(1*H*-benzotriazol-1-yl)uranium hexafluorophosphate (HBTU) and *N*, *N*-Diisopropylethylamine (DIPEA) as the coupling agent and base, respectively, in DMF solvent.

4.2.2 Release behavior of 5-Fu from the synthesized compound (4c).

4.2.2.1 UV-Vis experiment

5-Fu is covalently conjugated with the fatty acid through a photolabile linker which releases the effective drug 5-Fu on irradiation with UV light of 365 nm. The photo-

controlled release of 5-Fu was evaluated preliminarily by UV-Vis spectrophotometry and ^{1}H NMR analysis. 3 ml solution of compound **4c** in acetonitrile was taken in a quartz cuvette and irradiated under 365 nm LED light (24 W) at 25˚C. The UV-Vis spectra were recorded at a time interval of 15, 45, 65, 85, 105 minutes. With the progression of time, a new broad peak appeared around 320-350 nm (Figure 4.1a). This peak characterizes the generation of *o*-nitrosobenzaldehyde produced in the photocleavage reaction of compound **4c**.[24] The increasing intensity of this peak confirms the photocleavage of compound **4c** which indirectly suggests the release of 5-Fu.

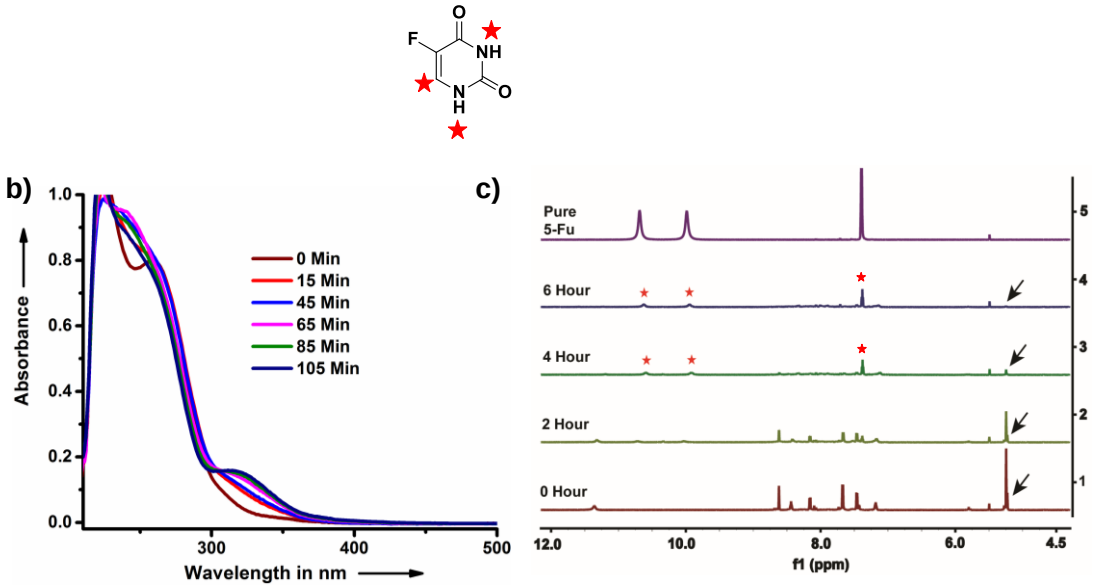

Figure 4.2 a) UV-Vis spectra, b) ^{1}H NMR study for the irradiation of **4c**, showing the release 5-Fu.

4.2.2.2 NMR experiment

The release of 5-Fu by the course of the photocleavage of the orthonitrobenzyl linker was further investigated by ^{1}H NMR studies. Compound **4c,** taken in acetonitrile-d_3, was irradiated with UV light (365 nm) and ^{1}H NMR spectra were recorded in two hours interval. Three new peaks at δ = 10.0, 10.75 and 7.47 ppm which corresponds to the N1, N3 and C6 protons of pure 5-Fu respectively, appeared and increased successively with increasing irradiation time (Figure 4.1b). Along with this, the intensity of another signal

at δ = 5.19 which represents -CH_2 protons connecting 5-Fu with the photolinker, decreased gradually and finally disappeared with increasing irradiation time. All these observations suggest the photo-regulated release of 5-Fu from compound **4c**.

4.2.3 Critical aggregation concentration (CAC) and self-assembly behavior of compound 4c

As the compound **4c** is amphiphilic in nature *i.e.* it has both hydrophilic and hydrophobic moiety in its structure; it is capable of forming self-assembled architecture. Different solvents were screened to investigate the self-assembly behavior of compound **4c**. It was found to form organogel in DMSO (Figure 3b). The self-assembly of compound **4c** in water was investigated by calculating critical aggregation constant (CAC) using pyrene as a fluorescence probe.

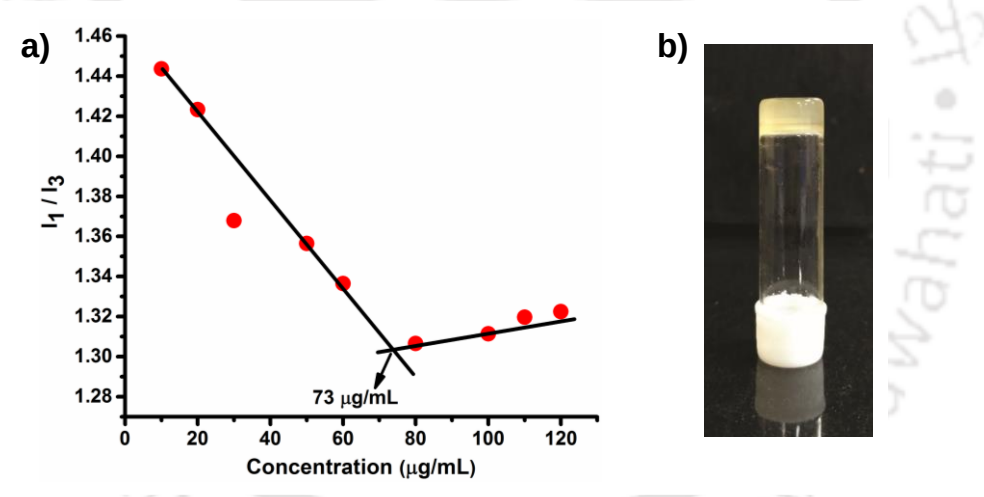

Figure 4.3 a) Plot of fluorescence intensity ratio (I_1 / I_3) against the concentration of compound **4c** nanoparticles in water. The CAC value was 73 µg/mL, b) optical image of organogel in DMSO formed by 5-Fu-palmitic acid conjugate.

At first, nanoparticles were prepared from compound **4c** in nanoprecipitation method, as mentioned earlier in section 3.2.2 (Chapter 3). Briefly, The I_3/I_1 values were recorded for all solutions and plotted against the concentration. The CAC of the nanoparticles was obtained as 73 µg/mL from the plot (Figure 4.3).

4.2.4 Morphological analysis

The morphology of the self-assembled structure was investigated by FESEM. In DMSO, compound **4c** was found to form nanofibers (Figure 4.4a,b) thus entrapping the solvent, producing organogel. These nanofibers are 80-90 nm in width whereas the length is several µm. However, in DMSO/water (1:1) mixture, the compound was able to form nanofibers of 20-30 nm width and several µm long (Figure 4.4c).

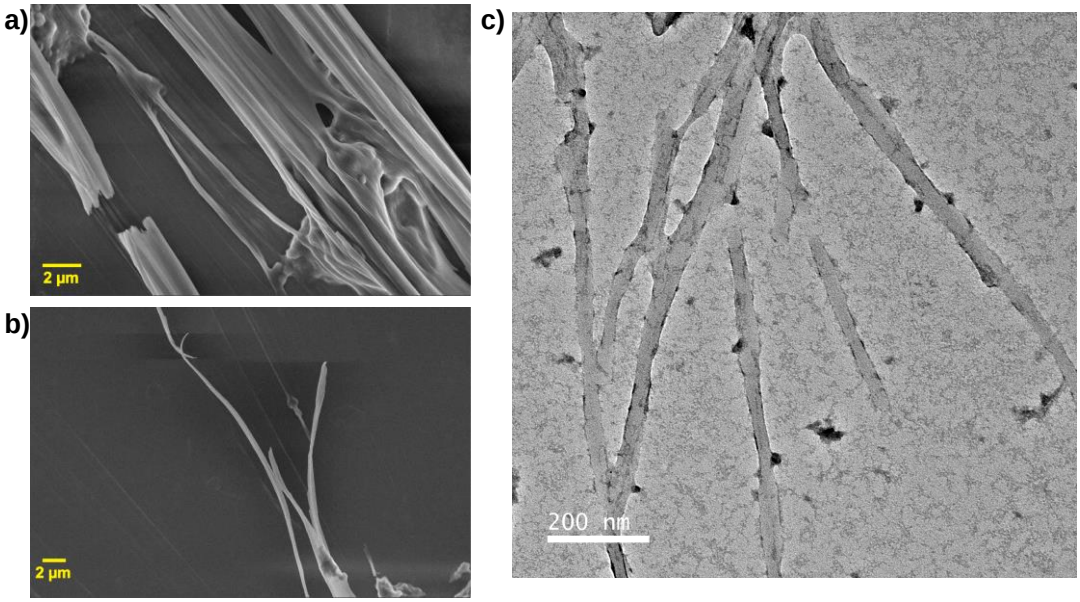

Figure 4.4 a), b) FESEM images of compound **4c** in DMSO showing fibrillary morphology, c) TEM image of compound **4c** in DMSO/water (1:1)

4.2.5. Synthesis of blank nanoparticles

For the fabrication of nanoparticles from the synthesized compound **4c**, nanoprecipitation method was adopted. Nanoprecipitation is a well-recognized method for nanoparticle synthesis from amphiphilic polymers.[25-26] Briefly, a solution of compound **4c** in organic solvent was added dropwise to water containing polyethylene glycol (PEG) 6000. A mixture of acetone/ dimethylsulphoxide (DMSO) in a ratio of 4:1 was used as the organic solvent. In order to stabilize the nanoparticles, various stabilizers were investigated but PEG 6000 was found to be the best choice. The utilization of PEG in drug delivery had been studied extensively due to its remarkable biocompatibility and

biodegradability. The heterogeneous mixture was then kept under stirring for several hours to promote the nanoparticle formation by self-assembly of compound **4c**.

4.2.6 Formulation of drug-loaded nanoparticles

As compound **4c** has hydrophobic tail, in water it assembles into nanoparticle. So these nanoparticles have a hydrophobic core and the surface of the nanoparticles are formed by the hydrophilic drug 5-Fu. Hence, due to the hydrophobicity of the core, it should encapsulate a hydrophobic compound.[27] This makes the nanoparticles capable of carrying a hydrophilic and a hydrophobic drug together. We have chosen CPT as the hydrophobic agent to be loaded inside the nanoparticles. CPT is another renowned anticancer agent, used to treat cancer.[28]

4.2.7. Characterization of the nanoparticles

4.2.7.1 Particle size and zeta potential

Dynamic light scattering (DLS) was used to measure the particle size and zeta potential of the nanoparticles, both blank and drug-loaded. As observed from the measurement of size and polydispersity index, the nanoparticles were well dispersed and uniform in nature (Figure 4.5).

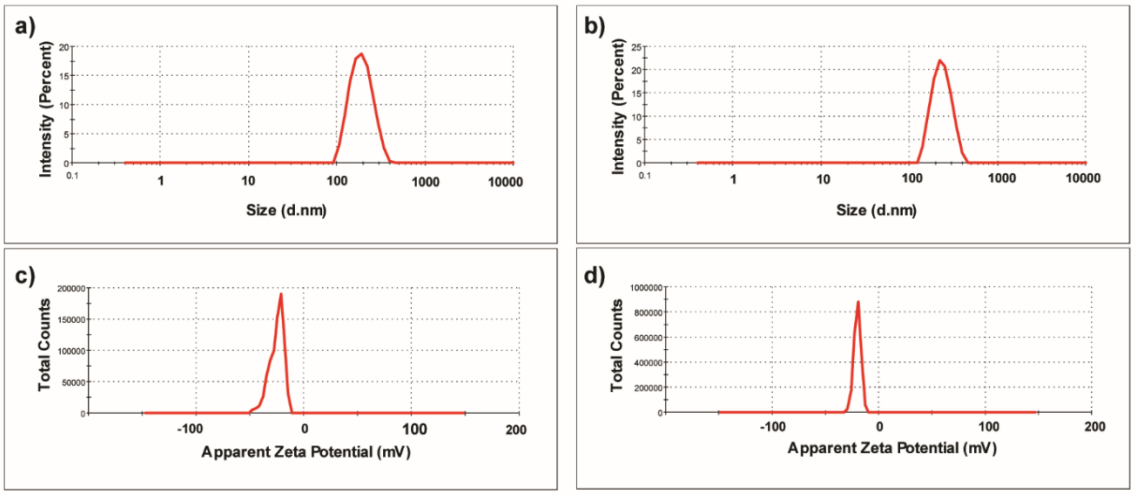

Figure 4.5 DLS graph of nanoparticles. The size distribution of a) blank, b) CPT loaded Fl-palmitic acid nanoparticles. Zeta potential of c) blank, d) CPT loaded nanoparticles.

As 5-Fu is a nucleobase derived drug, it imparts an overall negative charge to the surface of the nanoparticles. The coating of PEG 6000 may also be responsible for this negatively charged surface as confirmed from the zeta potential value (Table 4.1).

Table 4.1 Measurement of particle size and zeta potential of the nanoparticles from compound **4c.**

Set no.	Compound 4c concentration mg/ml	CPT concentration (mg/ml)	PEG 6000 Concentration (w/v %)	Size of nanoparticles (nm)	Zeta potential (mV)
1	1	0	0.05	180.5±3.01	-25.1±0.55
2	1	0.05	0.05	245.1±19.2	-20.0±1.1

4.2.7.2 FESEM analysis

The nanoparticles were further characterized by FESEM. From the images, it is evident that the nanoparticles are spherical in shape having a smooth surface (Figure 4.6). The size of the nanoparticles was also calculated from the FESEM images considering the mean of 100 values as measured by image J software. The mean size of the blank nanoparticles were found to be 87.8±15.29 nm and that of CPT loaded nanoparticle 154.263±23.04. The obtained smaller size of the nanoparticles compared to DLS study may be due to the shrinkage of them during the drying process.

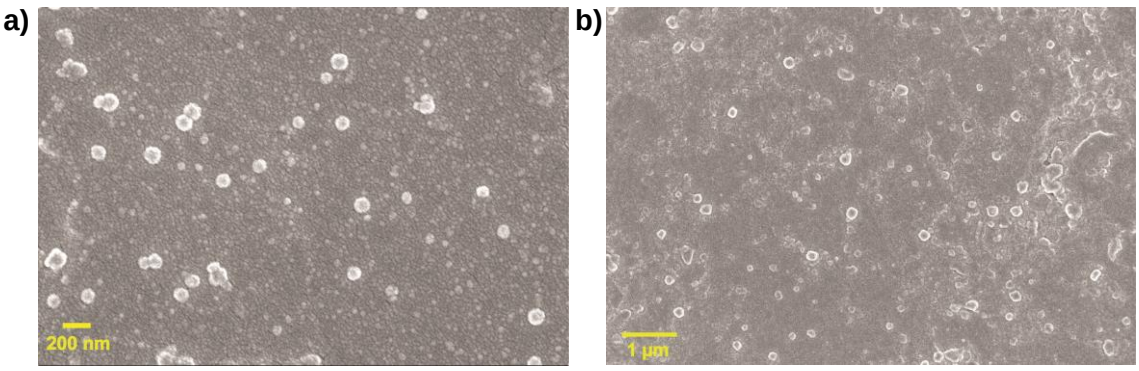

Figure 4.6 FESEM images of a) blank nanoparticles, b) CPT loaded nanoparticles.

4.2.7.3 Loading of CPT inside nanoparticles

The loading of CPT inside the nanoparticles were investigated by UV spectrophotometry as well as fluorescence spectroscopy. As evident in Figure 4.7a, CPT loaded nanoparticles contain both the characteristic absorption of CPT at 370 nm and of the compound **4c** at 260 nm, confirming the presence of CPT in the nanoparticles.[29] From fluorescence spectra a redshift of CPT emission maxima can be observed (Figure 4.7b) after loading of it inside nanoparticles. This may be attributed to the encapsulation of CPT inside the hydrophobic region of the nanoparticles.[29]

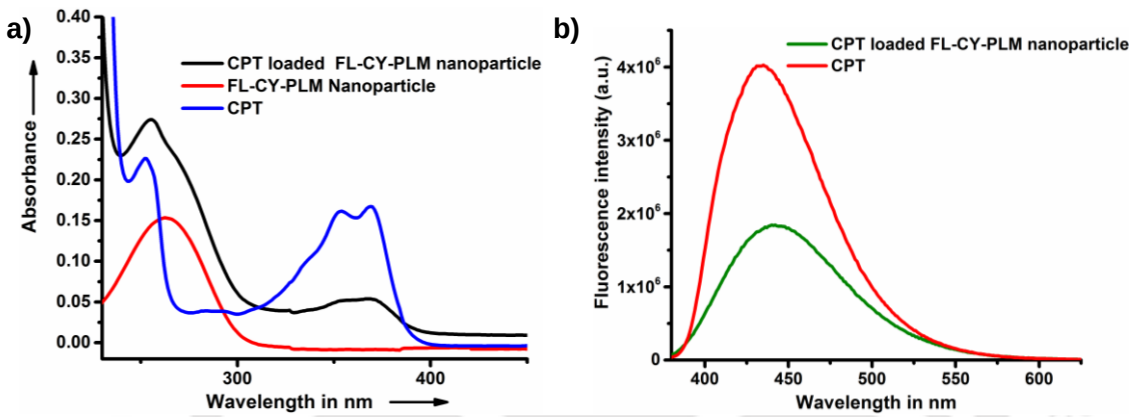

Figure 4.7 Loading of CPT in nanoparticles (a) Uv-Vis spectra of nanoparticles, (b) fluorescence spectra of nanoparticles.

4.2.8 Encapsulation efficiency (EE) and drug loading

The %EE and drug loading was calculated using the following established formula.[30-31]

$$\textbf{Encapsulation Efficiency (\%)} = \frac{\text{Weight of the drug entrapped}}{\text{Weight of total drug added}}$$

The maximum EE (%) of this system was found to be 32.7% for 20:1 ratio of compound **4c** / CPT and as the concentration of CPT increases the EE (%) decreases. At 1:1 ratio of compound **4c** / CPT the EE(%) was calculated to be 13.8%.

4.2.9 *In vitro* release of CPT from the nanoparticles

As the hydrophobic unit in compound **4c** is tethered to the hydrophilic unit by the disulfide linker which can be cleaved upon reduction, we have performed the *in vitro* release of CPT both in presence and absence of GSH. For verifying the CPT release from the nanoparticles similar method as described in the previous chapter in section 3.2.6 (Chapter 3). But to examine GSH sensitive release of CPT, the release media of PBS buffer, pH 7.4 was changed with a 10 mM solution GSH in PBS buffer, pH 7.4. After collecting 1 mL of aliquots at different time intervals, the same is replaced by the same 10 mM solution GSH in PBS buffer, pH 7.4. The amount of released CPT was measured by UV and fluorescence spectroscopy. By comparing the two curves in Figure 4.8 it can be concluded that in presence of GSH, CPT release was faster and controlled too.

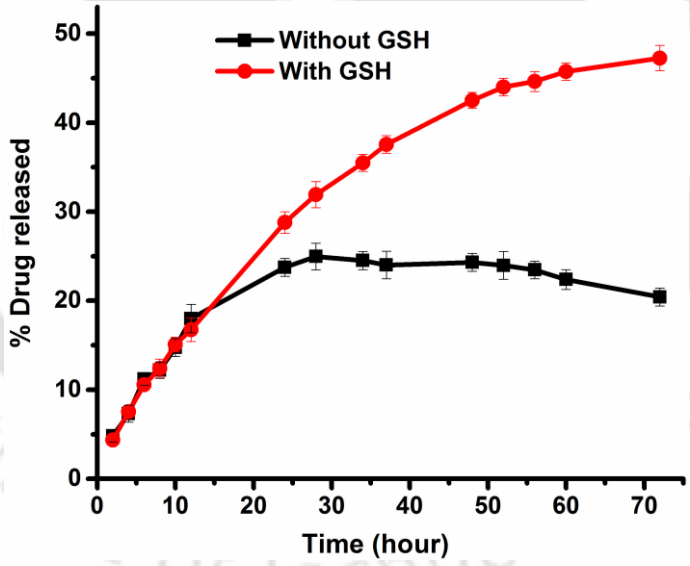

Figure 4.8 a) Fluorescence spectra of drug release behavior without GSH, b) with GSH, c) comparative profile of drug release in presence and absence of GSH.

4.2.10 5-Fu release from the nanoparticles

The release of 5-Fu from the nanoparticles was observed by UV-Vis spectrophotometry. The nanoparticles were dispersed in phosphate buffer saline (PBS) pH 7.4 and irradiated with 365 nm light. After a certain period, the nanoparticles were centrifuged and the

supernatant was analyzed for the evidence of released 5-Fu by measuring the absorption at 265 nm in UV-Vis spectrophotometer. The amount of released 5-Fu was quantified by comparing it with a standard curve of 5-Fu in the same solvent. It was found that as the time of irradiation progressed the amount of 5-Fu also increased in the supernatant (Figure 4.9)

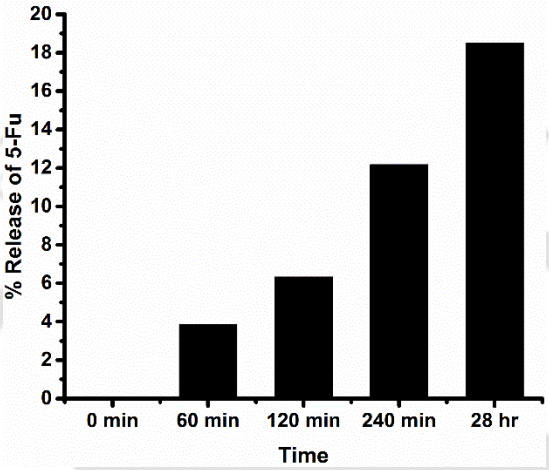

Figure 4.9 5-Fu release profile from nanoparticle.

4.2.11 Cytotoxicity of the nanoparticles

The toxicity of 5-Fu and CPT towards the cells were already proved in the previous chapters in section 3.2.7 (Chapter 3). Thus in order to be an effective DDS, our synthesized nanoparticles should not possess any inherent toxicity. The cytotoxicity of the synthesized nanoparticles was investigated by MTT assay in human cervical HeLa cell lines. Cells were incubated with blank nanoparticles. Figure 6 shows the cell viability after 48-hour incubation with different concentrations of blank NPs. It is already well-known that 5-Fu is highly toxic for the cells even at a very low concentration of 20-30 µg/mL. Our synthesized blank nanoparticles showed almost negligible toxicity at even a very high concentration such as 800 µg/mL (Figure 4.10).

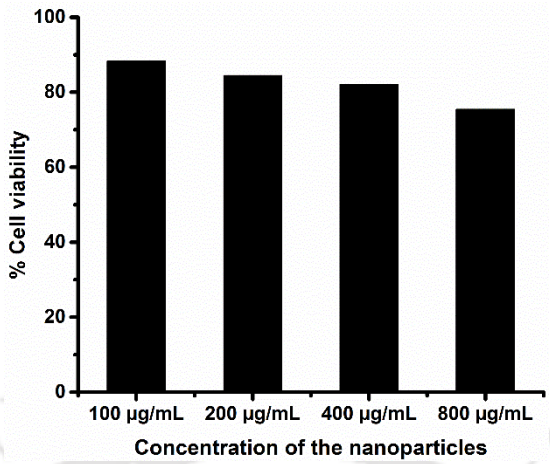

Figure 4.10 Cytotoxicity profile of blank 5-Fu palmitic acid conjugate nanoparticles.

4.3 Experimental section

4.3.1 Synthesis of compounds (2a-4c).

A. Synthesis of Prodrug (4-((5-fluoro-2,4-dioxo-3,4-dihydropyrimidin-1(2*H*)-yl) methyl)-3-nitrobenzoic acid) (2a): The prodrug was synthesized according to the procedure described in section 2.4.1A.[32]

B. Synthesis of *N*-(2-((2-aminoethyl)disulfanyl)ethyl)palmitamide (4b): To prepare compound **4b** similar protocol was followed as reported earlier by Kim and his group.[22-23] First palmitoyl chloride was prepared by reacting palmitic acid (200 mg, 0.7813 mmol) with thionyl chloride (372 mg, 3.13 mmol) in reflux condition for 4 hours. After that, the excess thionyl chloride was removed in a rotary evaporator and finally by high vacuum pump to yield a light yellow oil (compound **4a**).[22] The obtained compound **4a** was used without further purification. For the preparation of *N*-(2-((2-aminoethyl)disulfanyl)ethyl)palmitamide, cystamine dihydrochloride (200 mg, 0.89 mmol) was mixed with pyridine (104 mg, 1.31mole) in dry DMF and stirred for 10 minutes. The reaction mixture then transferred to an ice bath and palmitoyl chloride (360 mg, 1.31 mmol) was added dropwise to that. The temperature of the reaction mixture was kept within 5ºC during the addition of compound **4a**. The resulting reaction mixture was then transferred to room temperature and stirred for 10 hours. After completion of the reaction, the reaction mixture was poured in ice water in order to remove the pyridine

salts. The solid white precipitate was filtered and washed several times with cold water and finally dried under vacuum to obtain compound **4b** (483 mg, 94.2%). The compound was characterized by matching with literature.[23] HRMS (ESI) *m/z* $[M + H]^+$calcd. for $C_{20}H_{42}N_2OS_2$: 390.2811, found: 390.2811.

C. Synthesis of 4-((5-fluoro-2,4-dioxo-3,4-dihydropyrimidin-1(2*H*)-yl)methyl)-3-nitro-*N*-(2-((2-palmitamidoethyl)disulfanyl)ethyl)benzamide (4c): Compound **4c** was synthesized by amide coupling reaction between compound **2a** and **4b**. Briefly, compound **2a** (300 mg, 0.971 mmol) was reacted with compound **4b** (379 mg, 0.971 mmol) in an HBTU (478 mg, 1.26 mmol) assisted coupling procedure using DIPEA (253 µL, 1.46 mmol) and DMF (2 mL) as base and solvent respectively. After completion of the reaction, the reaction mixture was extracted with ethyl acetate and the organic layer was dried over sodium sulfate to get the crude. The crude was further purified by silica gel column chromatography using 9:1 chloroform/ methanol solvent system. Compound **4c** was obtained as a light yellow powder in 51.3% yield (339 mg). ^{1}H NMR (400 MHz, DMSO-d_6) δ_{ppm} 12.01 (d, J = 5.1 Hz, 1H), 9.09 (t, J = 5.5 Hz, 1H), 8.63 (d, J = 1.7 Hz, 1H), 8.23 – 8.13 (m, 2H), 8.02 (t, J = 5.6 Hz, 1H), 7.57 (d, J = 8.2 Hz, 1H), 5.27 (s, 2H), 3.63 (dd, J = 12.6, 6.4 Hz, 2H), 3.40 – 3.35 (m, 2H), 2.97 (t, J = 6.8 Hz, 2H), 2.84 (t, J = 6.7 Hz, 2H), 2.10 (t, J = 7.4 Hz, 2H), 1.57 – 1.46 (m, 2H), 1.27 (s, 24H), 0.90 (t, J = 6.8 Hz, 3H); ^{13}C NMR (100 MHz, DMSO-d_6) δ_{ppm} 172.8, 164.4, 158.2 (d, C-4, $J_{C\text{-}F}$ = 26 Hz), 150.3, 147.9, 141.8 (s, C-5, $J_{C\text{-}F}$ = 229 Hz), 139.5, 135.3, 134.9, 133, 130.5 (d, C-6, $J_{C\text{-}F}$ = 34 Hz), 130.2, 129.1, 124.1, 48.9, 40.6, 40.4, 40.2, 39.9, 39.7, 39.5, 39.3, 38.3, 37.8, 37.3, 35.8, 31.8, 29.5, 29.5, 29.4, 29.2, 29.2, 29.1, 25.7, 22.6, 14.4. HRMS (ESI) *m/z* $[M + H]^+$calcd. for $C_{32}H_{48}FN_5O_6S_2$: 682.3103, found: 682.3103.

4.3.2 Determination of CAC of nanoparticles

Different concentrations of compound **4c** were made in phosphate buffer (PBS, pH 7.4) starting from 0 to 200 µg/mL. 2µL of pyrene in ethanol solution was added to 1 mL of compound **4c** nanoparticle solution in various concentrations so that the final concentration of pyrene in each solution became 2 µM. After that, the resulting solution was kept in the dark for 1 hour prior to the experiment. Finally, the fluorescence emission of pyrene in different solution was measured with the excitation wavelength of

336 nm. The I_3/I_1 values were plotted against concentration and the CAC was calculated from the intersection of the tangents drawn to the two linear portions of the plot.

4.3.3 ^{1}H NMR Experiment

5 mg of compound **4c** was dissolved in 1:15 DMSO-d_6 / acetonitrile-d_3 solvent mixture. The sample was subjected to irradiation under 365 nm UV light and the course of photocleavage was monitored for 6 hours by acquiring ^{1}H NMR after each 2 hours interval.

4.3.4 Preparation of blank nanoparticles from compound 4c

In this case, nanoprecipitation method was employed to prepare the nanoparticles. Typically 1 mg of compound **4c** was dissolved in 4:1 acetone/DMSO mixture and added dropwise, with continuous stirring, to the aqueous solution of 0.05% PEG 6000 (w/v). PEG 6000 was used as the stabilizing agent for the nanoparticles. Then the mixture was stirred for 4 hours for complete evaporation of the organic solvent. After 4 hours, the nanoparticles were collected by centrifugation and washed with fresh distilled water three times to remove the excess stabilizing agent. The collected nanoparticles were resuspended in distilled water and lyophilized to obtain powdered nanoparticles, which was kept at -20˚C for further analysis.

4.3.5 Preparation of CPT loaded nanoparticles from compound 4c

To prepare CPT loaded nanoparticles, similar method was followed as the blank nanoparticles. But for efficient loading, the DMSO solution of CPT was mixed with the acetone solution of compound **4c** and kept in stirring for 30 minutes for proper mixing. This solution was added dropwise to the aqueous solution of the stabilizer, PEG 6000 (0.05% w/v). After 4 hours, the unloaded drug was removed by centrifugation at 2000 rpm, containing the CPT loaded nanoparticles. The supernatant was then filtered through a 0.45 µm syringe filter to remove aggregated particles and some remaining drug molecules. Finally, the CPT loaded nanoparticles were collected by centrifugation at a speed of 15000 rpm. at 10ºC. Obtained nanoparticles were resuspended in distilled water and lyophilized to get the powdered nanoparticles and stored at -20˚C.

4.3.6 Drug loading and entrapment efficiency

For measuring the drug loading and encapsulation efficiency, the lyophilized nanoparticles were dissolved in 1:1 acetonitrile/DMSO solution. The CPT concentration was evaluated by measuring UV absorbance at 365 nm and comparing with a standard curve of CPT in the same solvent.

4.3.7 Characterization of nanoparticles

DLS measurements were done at 25˚C with Malvern Zetasizer Nano ZS90 using appropriate viscosity and refractive index.

4.3.8 Field emission scanning electron microscope (FESEM)

1 mg of nanoparticles were first dispersed in 1 mL water. 5µL of this dispersion was placed on an alumina foil-covered glass plate. The samples were coated with gold prior to the analysis with SIGMA ZEISS FESEM instrument.

4.3.9 GSH responsive i*n vitro* release of CPT from the nanoparticles

The *in vitro* release of CPT in presence and absence of GSH was monitored by dialysis. 2 mg of CPT loaded nanoparticles was suspended in 1 mL PBS buffer (pH=7.4) and dialysed against 30 mL release media (10 mM GSH in PBS buffer, pH=7.4) under very slow stirring. 1 mL aliquot was withdrawn from the release media after certain intervals and was also replaced by 1 mL fresh PBS buffer (pH=7.4) to maintain the sink condition. The CPT concentration in the collected aliquots was measured by fluorescence with an excitation wavelength of 370 nm and emission at 435 nm. The concentration of the released CPT at different time intervals was calculated by comparing with a standard curve of CPT in PBS (7.4). Similarly, the amount of CPT released in the absence of GSH was determined by using only PBS buffer as the release media instead of GSH solution.

4.3.10 Cytotoxicity of Nanoparticles

The evaluation of cytotoxicity of the nanoparticles was estimated by MTT assay in human cervical HeLa cell lines, obtained from National Centre for Cell Sciences

(NCCS), Pune, India, following previously demonstrated procedure.[33] $5x10^3$ cells were seeded into 96-well microplate in 90 µL Dulbecco's modified Eagle's medium (DMEM) and were incubated for 24 hours at 37˚C in presence of 5% CO_2. After the incubation period cells were then treated with varying concentrations of the blank (5-Fu-palmitic acid) nanoparticles (100, 200, 400, 800 µg/mL) and again kept in incubation. After 48 hours MTT was added. After the addition of MTT, each plate was incubated for 2 hours at 37˚C. The medium was then removed and 60 µL of DMSO was added to produce formazan that showed absorption (A) at 570 nm. The optical density (OD) of each well-plate was measured with the background reference at 690 nm. All the tests were performed in triplicates. The control experiment was also carried out in a similar way but without the addition of nanoparticles. The percentage cell viability with respect to the control was calculated by using the standard formula as given below.

$$\%\ of\ cell\ viability = \frac{(A_{570} - A_{690})\ of\ treated\ cells}{(A_{570} - A_{690})\ of\ control\ cells} \times 100\ \%$$

4.4 Conclusion

A designer amphiphile, with a covalently attached 5-Fu, has been synthesized. The self-assembled amphiphile has been shown to act as a dual-responsive, dual-drug nanocarrier. The fibrillar morphology of the amphiphile was further modulated, by nanoprecipitation method, to promote the formation of nanoparticles having the size in the range of 180.5±3.01. The amphiphile was also found to be nontoxic up to a very high concentration of 800 µg/mL as seen in HeLa cells. Apart from the photocleavable 5-Fu, the nanoparticles exhibited exceptional efficiency to physically entrap another drug CPT, a hydrophobic anti-tumor agent, inside its hydrophobic region. The CPT encapsulation efficiency of the nanoparticles was found to be quite high as 32.7%. The release of CPT was controlled by GSH as the nanoparticles were designed in such a way that its self-assembly can be disrupted by cleaving the disulfide bond in presence of glutathione (GSH). Controlled release of both the drugs from the nanoparticles were demonstrated by various studies. So this system provides a way of designing versatile amphiphilic molecules as well as modulation of their self-assembly property to generate various nanostructures and using them for the controlled delivery of two drugs at a time.

4.5 References

1. Rosen, H.; Abribat, T., The rise and rise of drug delivery. *Nat. Rev. Drug Discovery* **2005,** *4* (5), 381-385.

2. Allen, T. M.; Cullis, P. R., Drug delivery systems: entering the mainstream. *Science* **2004,** *303* (5665), 1818-1822.

3. Park, K., Controlled drug delivery systems: past forward and future back. *J. Control. Release* **2014,** *190*, 3-8.

4. Dai, L.; Liu, J.; Luo, Z.; Li, M.; Cai, K., Tumor therapy: targeted drug delivery systems. *J. Mater. Chem. B* **2016,** *4* (42), 6758-6772.

5. Patra, J. K.; Das, G.; Fraceto, L. F.; Campos, E. V. R.; del Pilar Rodriguez-Torres, M.; Acosta-Torres, L. S.; Diaz-Torres, L. A.; Grillo, R.; Swamy, M. K.; Sharma, S., Nano based drug delivery systems: recent developments and future prospects. *J. Nanobiotechnol.* **2018,** *16* (1), 71.

6. Peer, D.; Karp, J. M.; Hong, S.; Farokhzad, O. C.; Margalit, R.; Langer, R., Nanocarriers as an emerging platform for cancer therapy. *Nat. Nanotechnol.* **2007,** *2* (12), 751-760.

7. Sharma, A.; Sharma, U. S., Liposomes in drug delivery: progress and limitations. *Int. J. Pharm.* **1997,** *154* (2), 123-140.

8. Moghassemi, S.; Hadjizadeh, A., Nano-niosomes as nanoscale drug delivery systems: an illustrated review. *J. Control. Release* **2014,** *185*, 22-36.

9. Wissing, S.; Kayser, O.; Müller, R., Solid lipid nanoparticles for parenteral drug delivery. *Adv. Drug Delivery Rev.* **2004,** *56* (9), 1257-1272.

10. Kataoka, K.; Harada, A.; Nagasaki, Y., Block copolymer micelles for drug delivery: design, characterization and biological significance. *Adv. Drug Delivery Rev.* **2012,** *64*, 37-48.

11. Gillies, E. R.; Frechet, J. M., Dendrimers and dendritic polymers in drug delivery. *Drug Discov. Today* **2005,** *10* (1), 35-43.

12. Slowing, I. I.; Vivero-Escoto, J. L.; Wu, C.-W.; Lin, V. S.-Y., Mesoporous silica nanoparticles as controlled release drug delivery and gene transfection carriers. *Adv. Drug Delivery Rev.* **2008,** *60* (11), 1278-1288.

13. Liu, D.; Yang, F.; Xiong, F.; Gu, N., The smart drug delivery system and its clinical potential. *Theranostics* **2016,** *6* (9), 1306-1323.

14. Manzoor, A. A.; Lindner, L. H.; Landon, C. D.; Park, J.-Y.; Simnick, A. J.; Dreher, M. R.; Das, S.; Hanna, G.; Park, W.; Chilkoti, A., Overcoming limitations in nanoparticle drug delivery: triggered, intravascular release to improve drug penetration into tumors. *Cancer Res.* **2012,** *72* (21), 5566-5575.

15. Li, F.; Mahato, R. I., Bioconjugate Therapeutics: Current Progress and Future Perspective. *Mol. Pharmaceutics* **2017**, *14* (5), 1321-1324.

16. Riley, T. N., The prodrug concept and new drug design and development. *J. Chem. Educ.* **1988,** *65* (11), 947-953.

17. Luo, C.; Sun, J.; Sun, B.; He, Z., Prodrug-based nanoparticulate drug delivery strategies for cancer therapy. *Trends Pharmacol. Sci.* **2014,** *35* (11), 556-566.

18. Cheetham, A. G.; Zhang, P.; Lin, Y.-a.; Lock, L. L.; Cui, H., Supramolecular nanostructures formed by anticancer drug assembly. *J. Am. Chem. Soc.* **2013,** *135* (8), 2907-2910.

19. Patchornik, A.; Amit, B.; Woodward, R., Photosensitive protecting groups. *J. Am. Chem. Soc.* **1970,** *92* (21), 6333-6335.

20. Kar, M.; Shih, Y.-R. V.; Velez, D. O.; Cabrales, P.; Varghese, S., Poly (ethylene glycol) hydrogels with cell cleavable groups for autonomous cell delivery. *Biomaterials* **2016,** *77*, 186-197.

21. Batist, G.; Tulpule, A.; Sinha, B.; Katki, A.; Myers, C.; Cowan, K. H., Overexpression of a novel anionic glutathione transferase in multidrug-resistant human breast cancer cells. *J. Biol. Chem.* **1986,** *261* (33), 15544-15549.

22. Anderson, M.; Afewerki, S.; Berglund, P.; Córdova, A., Total Synthesis of Capsaicin Analogues from Lignin-Derived Compounds by Combined Heterogeneous Metal, Organocatalytic and Enzymatic Cascades in One Pot. *Adv. Synth. Catal.* **2014,** *356* (9), 2113-2118.

23. Zhang, L.; Li, H.; Ha, C. S.; Suh, H.; Kim, I., Fabrication of nanotubules and microspheres from the self-assembly of amphiphilic monochain stearic acid derivatives. *Langmuir* **2010,** *26* (23), 17890-17895.

24. Leyva, V.; Corral, I.; Schmierer, T.; Gilch, P.; Gonzalez, L., A comparative analysis of the UV/Vis absorption spectra of nitrobenzaldehydes. *Phys. Chem. Chem. Phys.* **2011,** *13* (10), 4269-4278.

25. Nagavarma, B.; Yadav, H. K.; Ayaz, A.; Vasudha, L.; Shivakumar, H., Different techniques for preparation of polymeric nanoparticles-a review. *Asian J. Pharm. Clin. Res* **2012,** *5* (3), 16-23.

26. Govender, T.; Stolnik, S.; Garnett, M. C.; Illum, L.; Davis, S. S., PLGA nanoparticles prepared by nanoprecipitation: drug loading and release studies of a water soluble drug. *J. Control. Release* **1999,** *57* (2), 171-185.

27. Torchilin, V. P., Structure and design of polymeric surfactant-based drug delivery systems. *J. Control. Release* **2001,** *73* (2-3), 137-172.

28. Cragg, G. M.; Newman, D. J., Plants as a source of anti-cancer agents. *J. Ethnopharmacol.* **2005,** *100* (1-2), 72-79.

29. Concellón, A.; Clavería-Gimeno, R.; Velázquez-Campoy, A.; Abian, O.; Piñol, M.; Oriol, L., Polymeric micelles from block copolymers containing 2, 6-diacylaminopyridine units for encapsulation of hydrophobic drugs. *RSC Adv.* **2016,** *6* (29), 24066-24075.

30. Yang, A.; Liu, Z.; Yan, B.; Zhou, M.; Xiong, X., Preparation of camptothecin-loaded targeting nanoparticles and their antitumor effects on hepatocellular carcinoma cell line H22. *Drug Delivery* **2016,** *23* (5), 1699-1706.

31. Alqahtani, M. S.; Alqahtani, A.; Syed, R.; Thabit, A.; Roni, M., Novel lignin nanoparticles for oral drug delivery. *J. Mater. Chem. B* **2019**, *7*, 4461-4473.

32. Zhang, Z.; Hatta, H.; Ito, T.; Nishimoto, S.-i., Synthesis and photochemical properties of photoactivated antitumor prodrugs releasing 5-fluorouracil. *Org. Bimol. Chem.* **2005,** *3* (4), 592-596.

33. Ghosh, R.; Goswami, U.; Ghosh, S. S.; Paul, A.; Chattopadhyay, A., Synergistic anticancer activity of fluorescent copper nanoclusters and cisplatin delivered through a hydrogel nanocarrier. *ACS Appl. Mater. Interfaces* **2014,** *7* (1), 209-222.

4.6 NMR and HRMS spectra of synthesized compounds

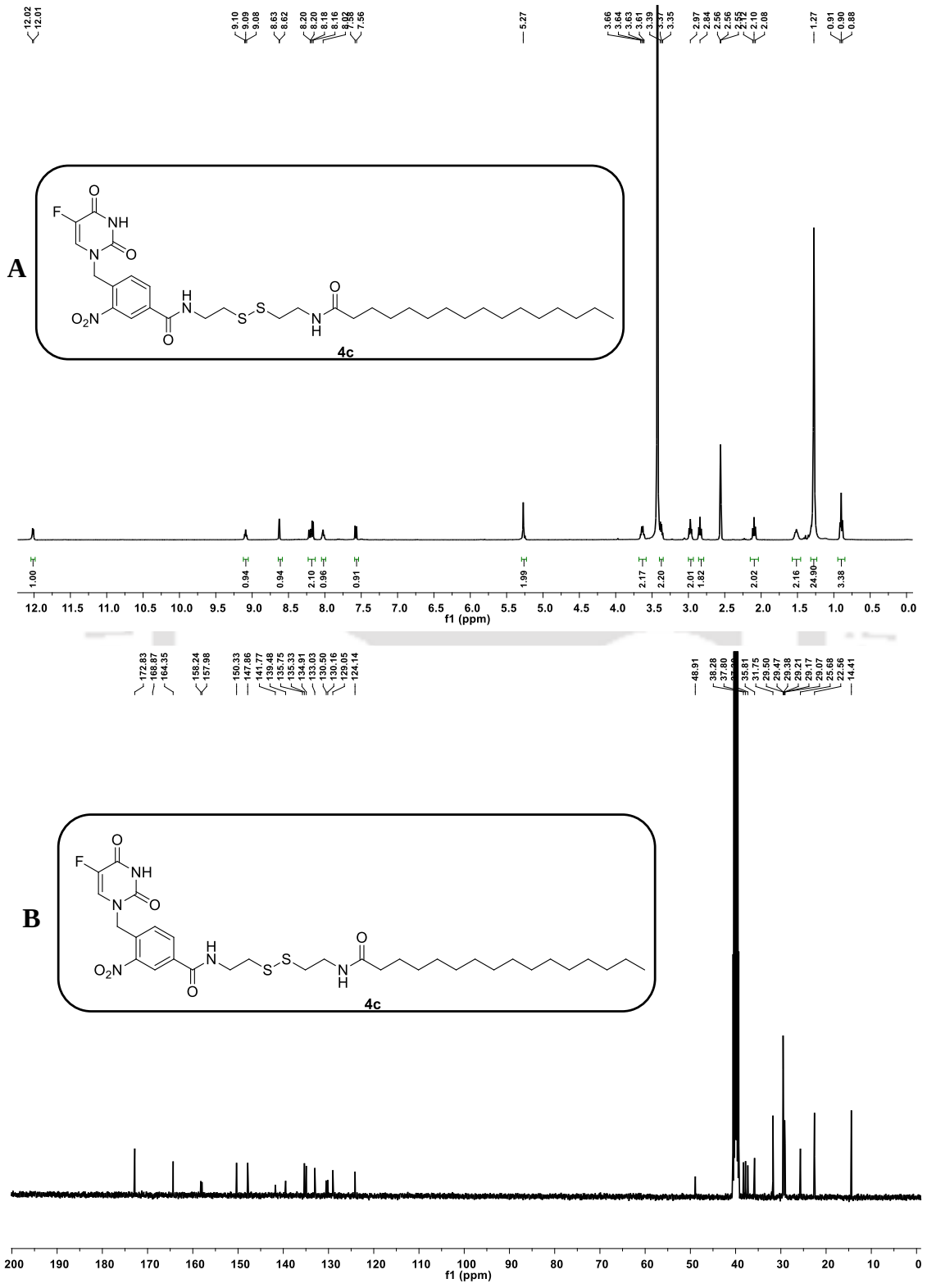

^{1}H (A) and ^{13}C (B) spectra of compound **4c.**

^{1}H NMR Spectra during irradiation of compounds 4c.

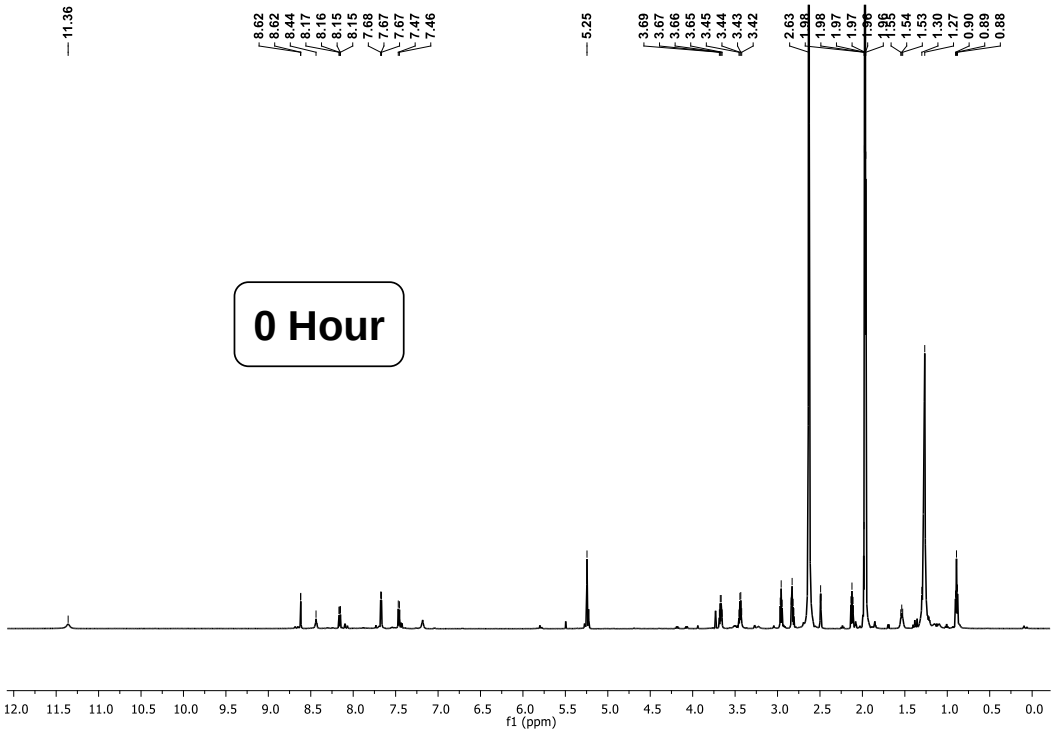

^{1}H NMR spectra of compound **4c** in acetonitrile-d_3 without irradiation.

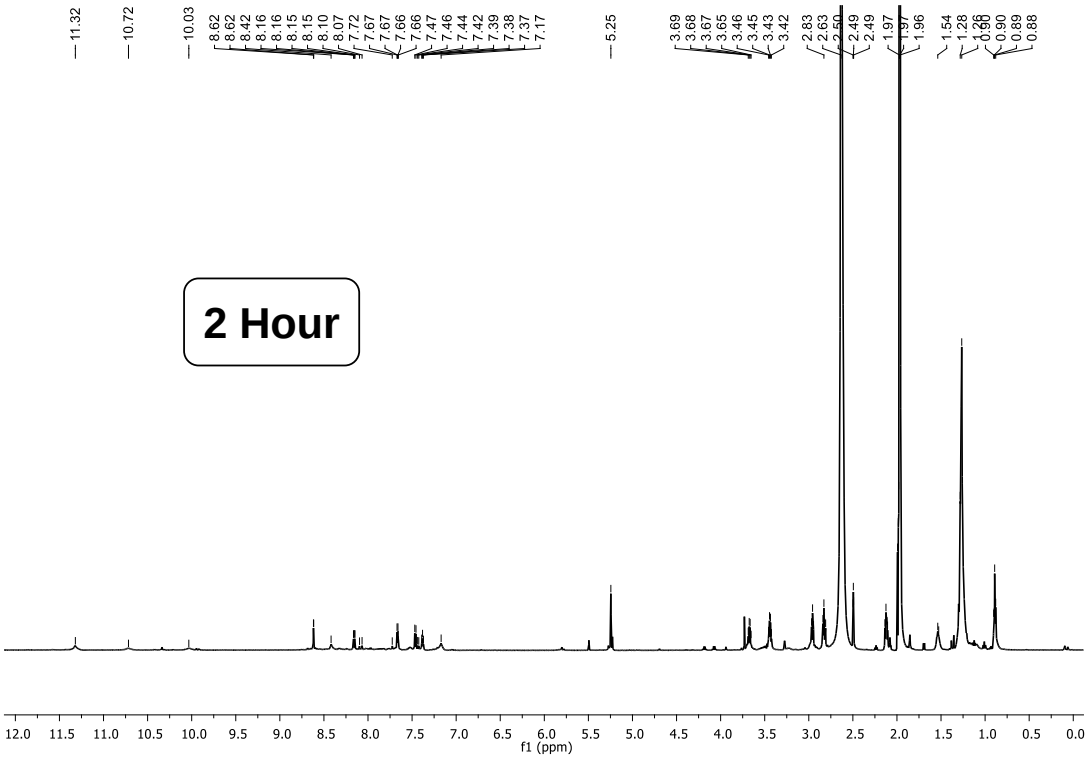

^{1}H NMR spectra of compound **4c** in acetonitrile-d_3 after 2 hours of irradiation.

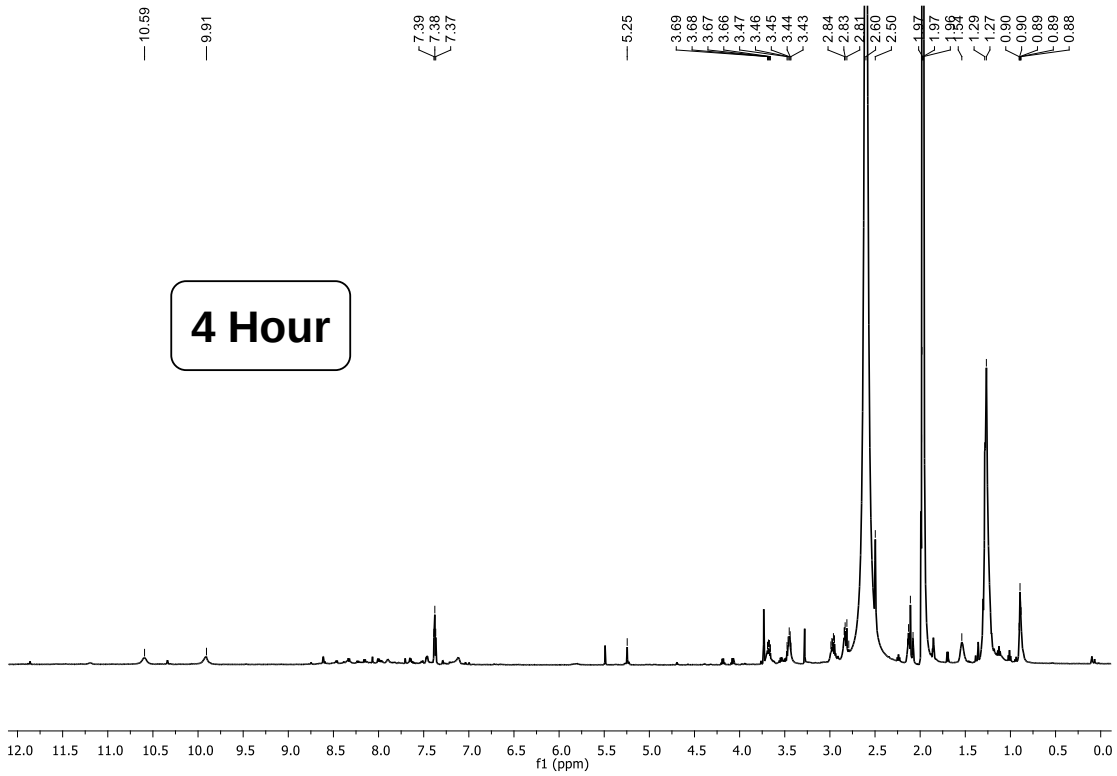

^{1}H NMR spectra of compound **4c** in acetonitrile-d_3 after 4 hours of irradiation.

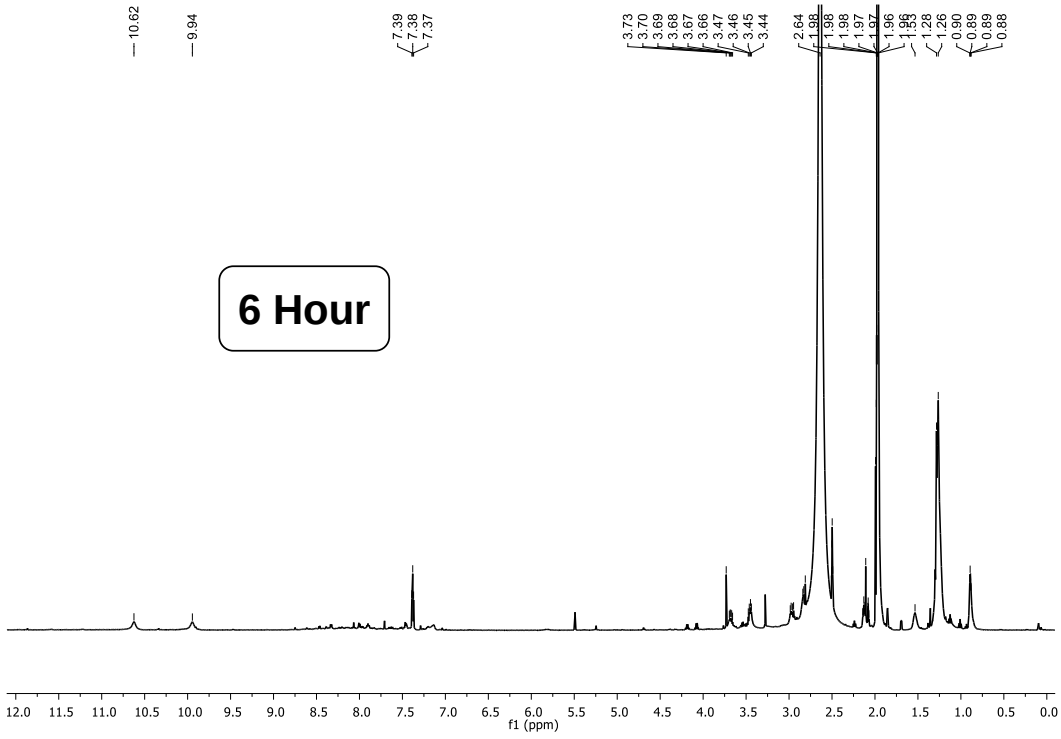

^{1}H NMR spectra of compound **4c** in acetonitrile-d_3 after 6 hours of irradiation.

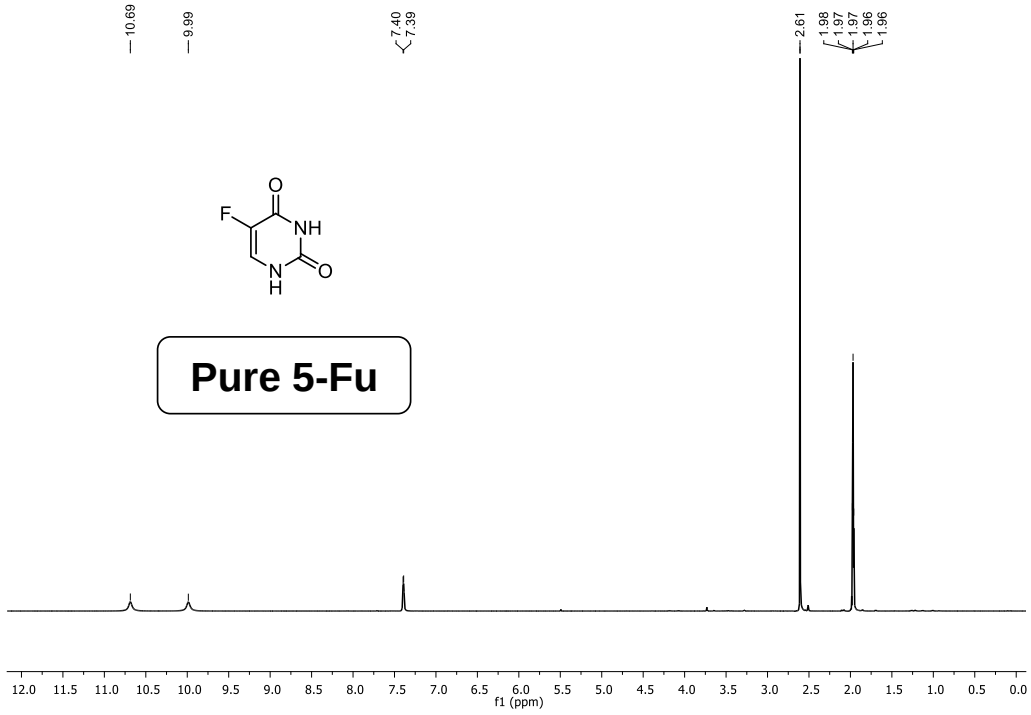

^{1}H NMR spectra of pure 5-Fu in acetonitrile-d_3.

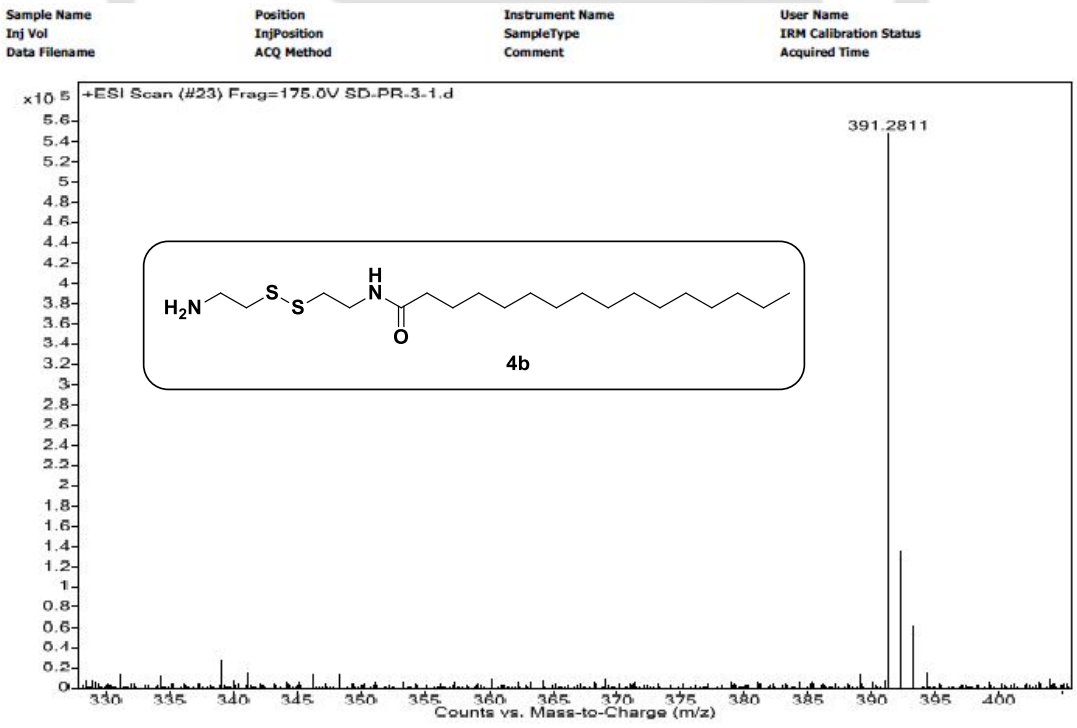

HRMS spectra of compound **4b**

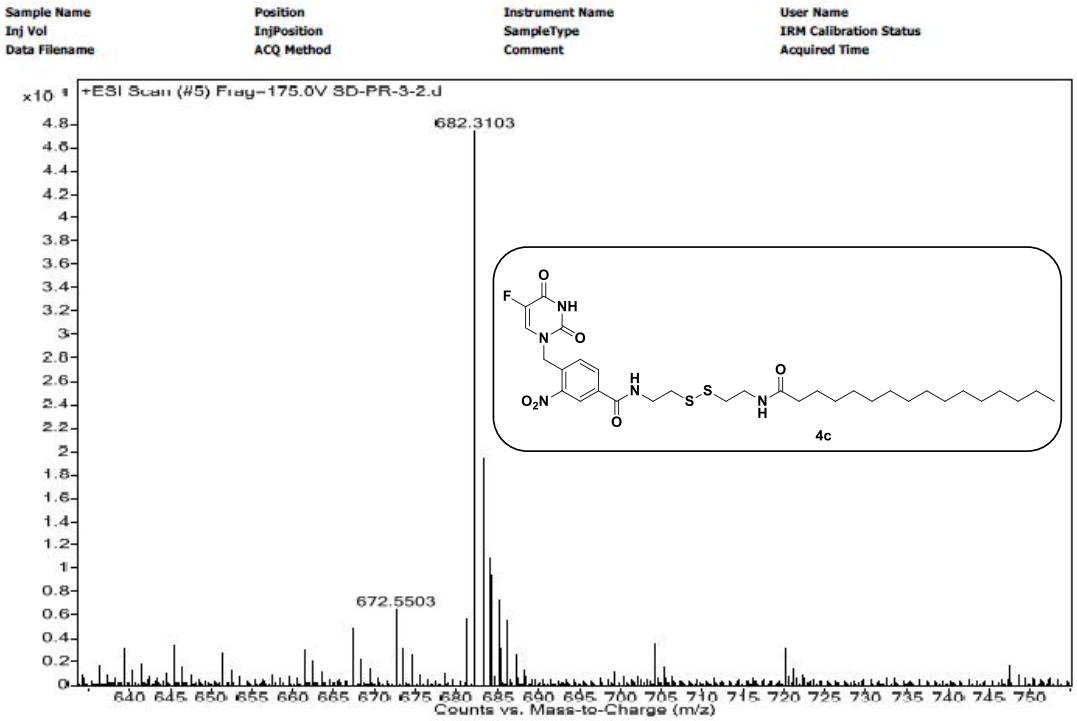

HRMS spectra of compound **4c**

Chapter 5

Development of Hydrogelator for the Targeted and Controlled Delivery of 5-Fluorouracil

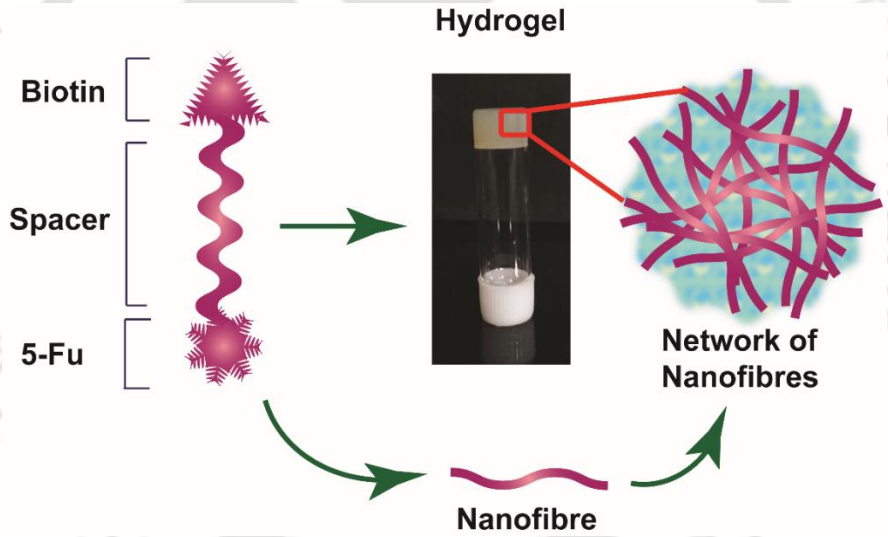

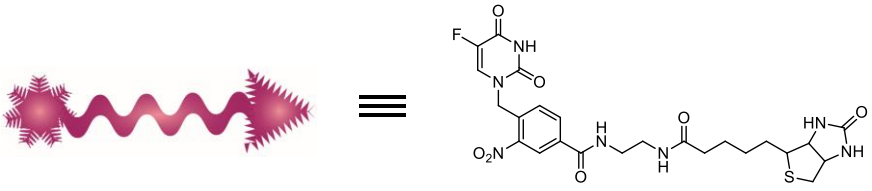

5.1 Introduction

Hydrogels are a highly promising platform for drug delivery applications.[1] The applicability of hydrogels in various branches of medicines such as tissue engineering,[2] wound healing,[3] ophthalmology,[4] cardiology,[5] anticancer therapy[6] is noteworthy. Hydrogels are actually three-dimensional network formed mostly by components having hydrophilic domains such as –OH, -COOH, -CONH, $-SO_3H$, $-CONH_2$ etc. which can imbibe a large amount of water. The high water content of hydrogel provides a soft consistency which resembles with living tissues and also lowers the interfacial tension with aqueous media.[7] All these properties make them highly biocompatible for biomedical applications.

Initially, polymer-based hydrogels have gained immense importance. However, recently peptides, proteins and other biomolecular hydrogels have found extensive application in drug delivery, due to their significant biocompatibility. Hydrogels were formed by the supramolecular self-assembly of the biomolecules. For the last few years, a great effort has been employed to understand this self-assembly process of molecules, resulting in the innovation of low molecular weight hydrogelators (LMWG) which is advantageous in terms of their synthesis, purification and the opportunity for facile modulation of the properties. Several LMWG were designed specifically for drug delivery purpose, along with other application.[8-9] Most of them have used peptide and polymers to prepare the hydrogel and entrap the drug inside the hydrogel network. However recently a smart strategy has been invented where the hydrogelator consists of the drug itself as a building block.[10-12] Xu and his group have prepared D-glucosamine hydrogelator by attaching Nap-L-phenylalanine or Nap-D-phenylalanine with D-glucosamine which was used for mild osteoarthritis.[13] Our group has also reported an LMWG consisting of 5-Fu and diphenylalanine peptide for the photo-responsive delivery of 5-Fu.[14]

Herein, we are reporting another design of LMWG for the photoresponsive delivery of 5-Fu. In this report, the hydrogelator is prepared by conjugating photoresponsive prodrug of 5-Fu with biotin *via* an ethylenediamine spacer as shown in scheme 1. Previously, biotin was utilized to design hydrogelator by attaching different amino acids with it.[15] The minimum gelation concentration (MGC) was found to be 0.3

wt% for biotin-L-norleucine. Such hydrogels were shown to be useful for drug delivery by entrapping a hydrophilic drug inside the hydrogel network. However, in our work biotin was directly conjugated with the hydrophilic anticancer drug 5-Fu, producing the hydrogelator where the drug itself was used as a building block for the formation of supramolecular architecture. Such kind of one component nanomedicines was also previously reported, but in most of the cases, the designs relied on attaching a hydrophilic drug with a hydrophobic segment (peptide, polymers and sometimes the drug itself) and vice versa.[16-17] In the present report, biotin was not only chosen for its hydrogen bond-forming ability but also to target the cancer cells. It is now well documented that some of the cancer cells are overexpressed with biotin receptors.[18] Thus the hydrogel formed by this 5-Fu biotin conjugate can be used as a controlled and targeted delivery system of 5-Fu for the localized lesion.

5.2 Results and discussion

5.2.1 Design and synthesis of 5-Fu-biotin conjugate

Herein we have demonstrated a design of a hydrogelator. The design consists of 5-Fu, an anticancer agents and biotin (vitamin H). Biotin is already well known to display self-assembly characteristics in water, forming nanofibers.[19] Self-assembly of the molecules mostly governed by non-covalent forces such as hydrogen bonding, hydrophobic interaction, π-π interaction, Van der Wall forces etc. Among them, hydrogen bonding interaction was frequently been used in inducing self-assembly between the interacting molecules. The ureido group of biotin is known to have extensive hydrogen bond formation ability in the water, procuring self-assembly and thus generating nanofibers. Utilizing this information, we have covalently attached biotin with the hydrophilic anticancer drug, 5-Fu which also possess hydrogen bond donor and acceptor site. Ethylenediamine was used as a small spacer between biotin and the 5-Fu.

The target molecule was prepared by convergent method of synthesis using amide coupling procedure (Scheme 5.1). At first, 5-Fu was tethered with the photo-removable *o*-nitrobenzyl moiety to prepare the 5-Fu prodrug following a previously discussed procedure (2.4.1A). Biotin was conjugated with ethylenediamine in a separate reaction.

Finally, these two fragments were coupled to each other by HBTU assisted amide coupling procedure to generate the 5-Fu biotin molecule.

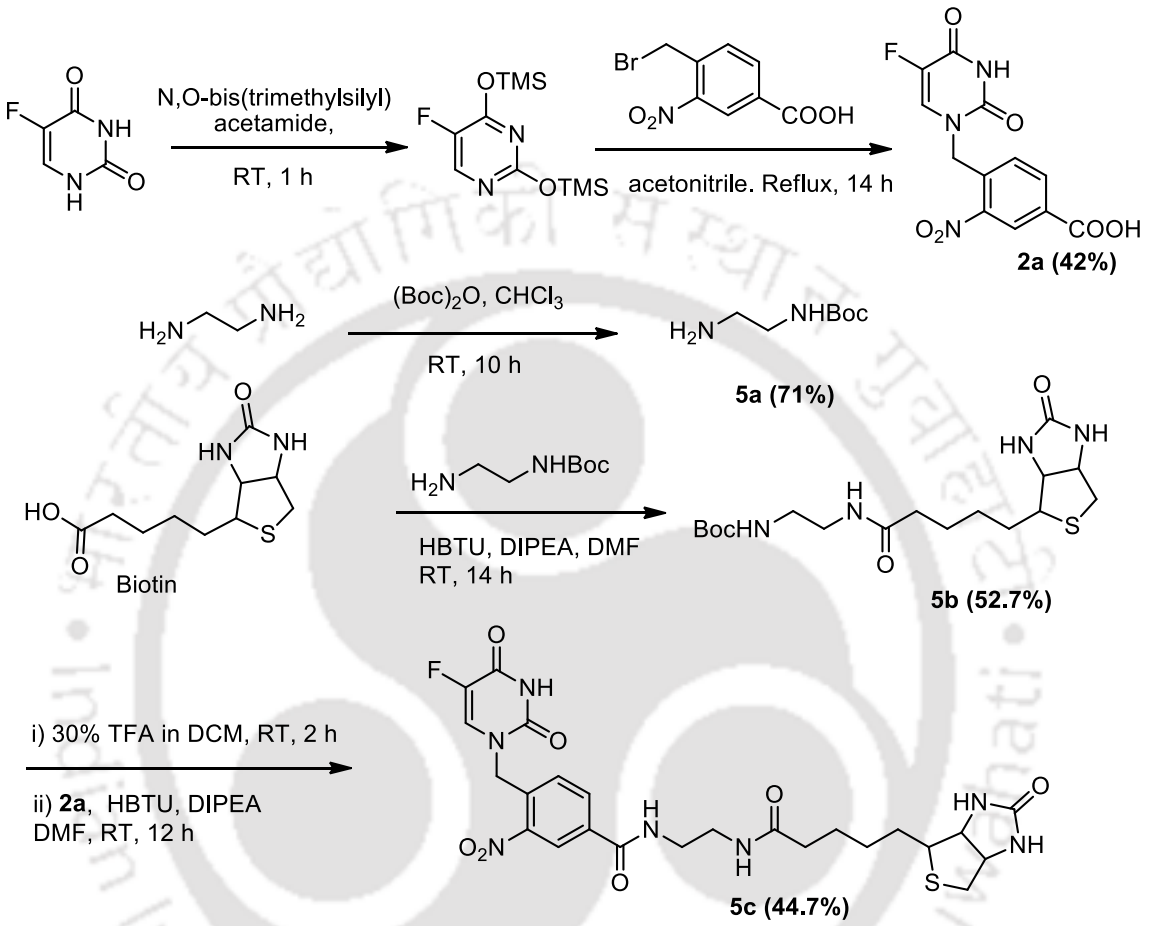

Scheme 5.1 Schematic presentation for the synthesis of 5-Fu-biotin conjugate.

5.2.2 Preparation of gels from 5c

The self-assembly characteristic of the molecule **5c** in water was investigated thoroughly by varying pH and weight of **5c**. It was able to form hydrogel at pH 7 and at a minimum concentration of 2 wt%. Although compound **5c** displayed self-assembly property at a much lower concentration, it was able to entrap water by forming the hydrogel only at 2 wt% concentration. The formation of hydrogel was confirmed by vial inversion test (Figure 5.1). The sol-gel transition temperature (T_g) was evaluated as 52°C (Figure 5.1a). The value of T_g was also found to depend on the concentration of the gelator and with increase in concentration T_g also increased.

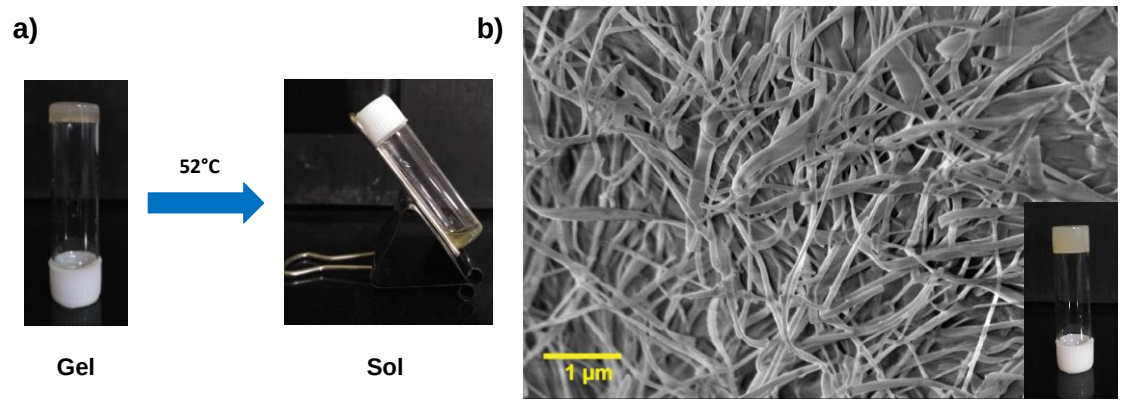

Figure 5.1 a) Gel to sol conversion of the hydrogel, b) FESEM image (scale bar 1µm) of xerogel (2 wt%).

5.2.3 Morphological analysis of the hydrogel

The morphology of the hydrogel was analyzed by field emission scanning electron microscope (FESEM). The xerogel was subjected to FESEM analysis and the images revealed a fibrous structure having a range of diameters from 70 to 120 nm (Figure 5.1b). Fibers were found to be several micrometers long. The varying width of the fibers indicates about an extensive aggregation tendency among them.

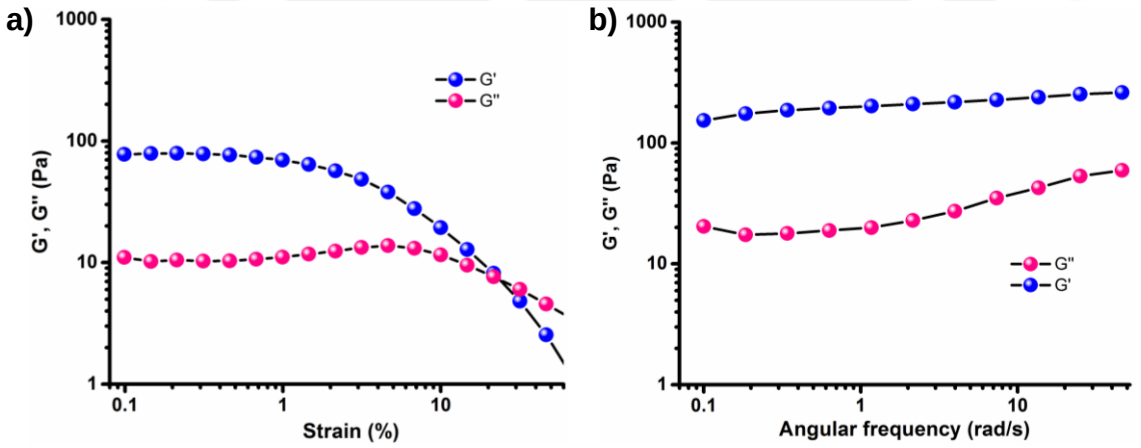

Figure 5.2 Rheological study of the hydrogel c) Strain sweep, d) amplitude sweep.

5.2.4 Rheological measurement of the hydrogel

The mechanical strength of the hydrogel was measured by rheological studies at 25 ºC using Anton-Paar MCR 102 rheometer with 20 mm parallel plate. The linear viscoelastic region (LVR) was determined by frequency sweep test. From the strain sweep graph, it can be observed that the storage modulus *G´* is larger compared to the loss modulus *G´´* and up to a strain of 10%, the difference between them remained almost constant (Figure 5.2a). Frequency sweep study was performed at a constant strain of 0.1% (obtained as LVR from strain sweep graph). A frequency-independent behavior was noticed for the hydrogel within the range of 0.1-50 rad/s (Figure 5.2b). A comparatively high storage (*G´*) and loss modulus (*G´´*) of the hydrogel obtained from the rheology indicate about a rather stiff hydrogel.

5.2.5 Driving forces behind self-assembly

The driving forces behind the self-assembly behavior of **5c** were investigated by FTIR and ^{1}H NMR analysis. A significant shifting of carbonyl stretching bands of the amide groups from 1711 and 1651 to 1692 and 1642, respectively, were observed in the gel state compared to the powdered state (Figure 5.3a). This shift of stretching frequencies suggested about the extensive amount of hydrogen bonding interaction provided by the amide bonds to initiate the self-assembly process.[20-21] Apart from the shifting of peaks, broadening of all the amide peaks (3433, 1692, and 1642) also indicated about the strong hydrogen bonding by the amides.

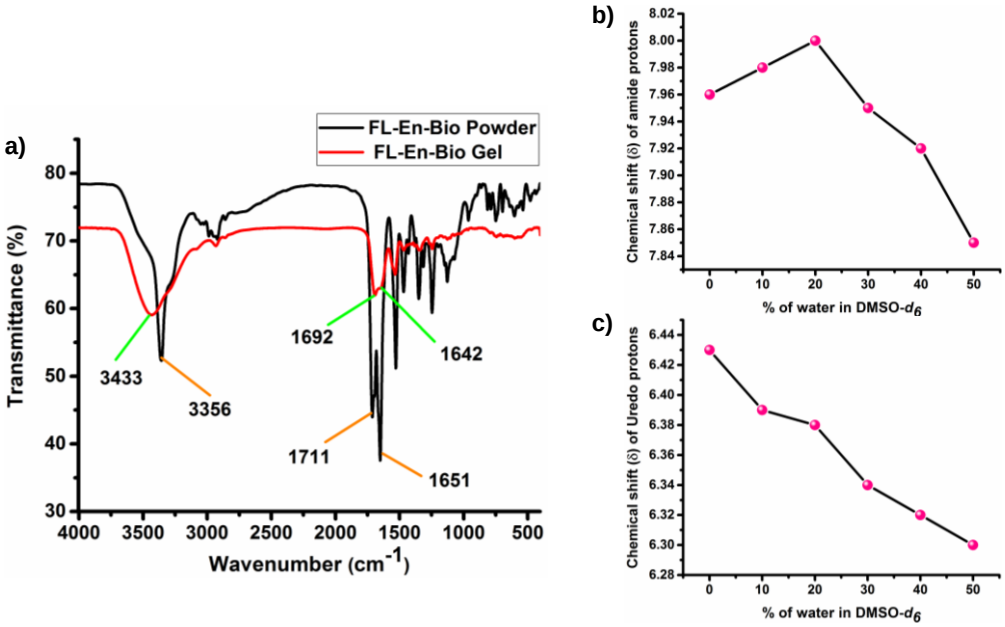

Figure 5.3 a) Comparison of FTIR spectra of compound **5c** in powder and gel state. b) Changes in chemical shift of the amide protons of compound **5c** with increase in % of water in DMSO-d_6. c) Changes in chemical shift of the uredo protons of compound **5c** with increase in % of water in DMSO-d_6. The changes in chemical shifts and FTIR peaks indicates about intermolecular hydrogen bonding.

The hydrogen bonding during the hydrogelation was also observed in ^{1}H NMR experiment where a change in chemical shift of the peaks occurred with the change in the ratio of DMSO-d_6/water. An immediate change in chemical shift for the amide protons can be noticed (Figure 5.3b) with the addition of only 10% water in the DMSO-d_6 solution of compound **5c**. As the amount of water increased, the amide protons were shifted to the lower field up to 30% of water but then they shifted upfield (>30% water). The initial lower field shifting was possibly due to the change in hydrogen bonding from $(CD_3)_3SO$---H-N to H_2O---H-N.[15, 22] However, with more than 30% water the upfield shifting of the amide protons indicates about the intermolecular hydrogen bonding among the molecules.[23-24] It has already been reported that amide units usually start intermolecular hydrogen bonding at ca. 20-30% water.[25] Comparatively the shift for the ureido group was observed towards upfield from the beginning at only 10% of water concentration (Figure 5.3c). Thus, the role of uredo group in intermolecular hydrogen bonding at a very low concentration of water was very much evident.[24] Thus both the uredo and amide groups

were responsible for the self-assembly process of compound **5c** resulting in hydrogelation. However, the tendency of participating in intermolecular hydrogen bonding of the ureido group was much quicker than the amide groups.

5.2.6 Photo-controlled release of 5-Fu

The photo-controlled release of 5-Fu was investigated by irradiation under 365 nm and was monitored by UV-Vis spectrophotometry and ^{1}H NMR. Under UV irradiation with 365 nm light, compound **5c** undergone photo-cleavage reaction as the reaction progressed, a new broad peak at 325 nm appeared (Figure 5.4a). The broad peak corresponds to *o*-nitrosobenzaldehyde, which is a photo product of the reaction.[26] As the reaction progressed, the absorption of the characteristic peak also increased, indicating the occurrence and furtherance of the photo-cleavage reaction. Along with the spectral changes, the color of the solution also changes from colorless to yellow.

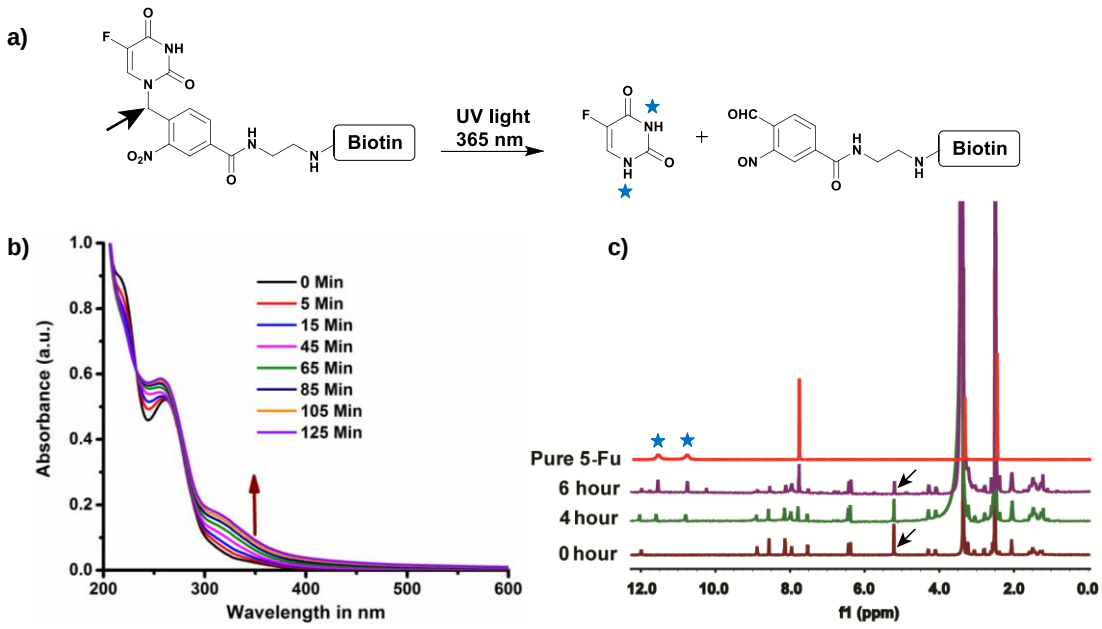

Figure 5.4 a) Photo-cleavage reaction compound **5c**, b) UV-Vis spectra of 5-Fu release experiment of compound **5c** (50 µM) in acetonitrile, c) ^{1}H NMR spectra of drug release experiment of compound **5c** in DMSO-d_6.

Although the photo-cleavage phenomenon was evidenced by UV-Vis spectroscopy, the release of 5-Fu was clearly visible in ^{1}H NMR of the irradiated compound **5c** (Figure 5.4b).

All the characteristics peaks of pure active 5-Fu (11.54, 10.77 and 7.79 for the N3, N1 and C6 protons respectively) appeared gradually with increasing time of irradiation. Also, the peak at 5.19 ppm which corresponds to the-CH_2, adjoining 5-Fu with the photolinker, got diminished over time.

5.2.7 Loading of DOX in the hydrogel

Not only as a self-delivery vehicle for 5-Fu, the hydrogel was also found to be able to load another water-soluble drug effectively. As a model water-soluble drug, we have used doxorubicin hydrochloride (DOX) for loading inside the hydrogel network. For this, compound **5c** was allowed to form hydrogel in a 20 µM solution of DOX (0.5 mL). The morphology of the hydrogel after DOX entrapment revealed a denser network of fibers compared to only hydrogel (Figure 5.5a). The slow and sustained release of DOX was also observed from the hydrogel into PBS (7.4) buffer (Figure 5.5b). The release of Dox from gel phase to buffer was investigated by measuring the fluorescence emission intensity of DOX at 590 nm with an excitation wavelength of 488 nm.[27] The amount of released DOX was calculated from the obtained emission intensity by using a standard curve of DOX, also prepared in PBS (7.4). It has been found that only ca. 13% DOX was released after 2 days.

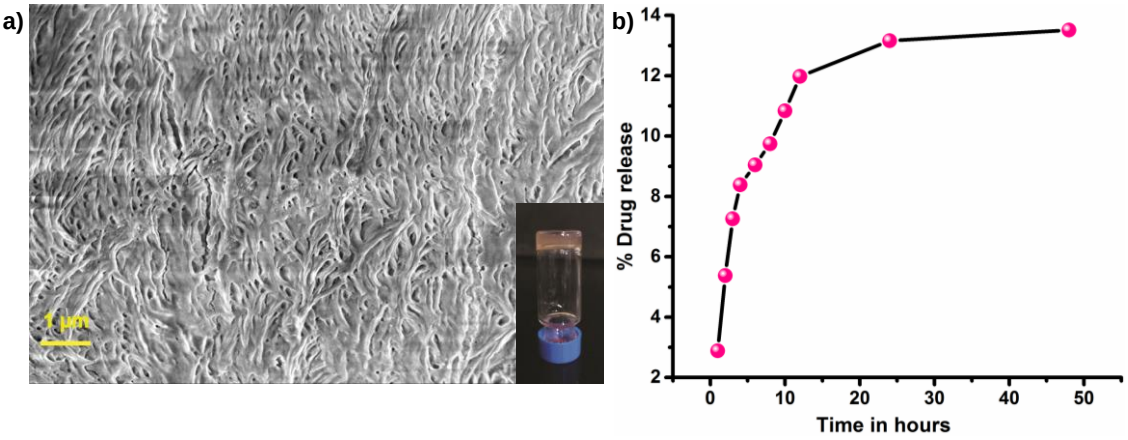

Figure 5.5 a) FESEM image of DOX loaded hydrogel (scale bar 1µm) and pictorial representation of DOX loaded hydrogel (inset), b) release profile of DOX from the hydrogel for 48 hours, measured in fluorescence.

5.2.8 Cytotoxicity measurement of compound 5c

To investigate the potential of the synthesized compound **5c** as a drug delivery vehicle, its cytotoxicity was measured by MTT assay on A-549 cell lines. Different concentrations of compound **5c** were added to A-549 cells and incubated for 48 hours. The IC_{50} value of 5-Fu, a constituent of the molecule **5c** was found to be 8 µM for A-549 cell lines after 48 hours. However, **5c** showed almost no toxicity towards the cells after 48 hours, up to a very high concentration such as 80 µM (Figure 5.6). This result indeed proved that **5c** does not have any inherent toxicity.

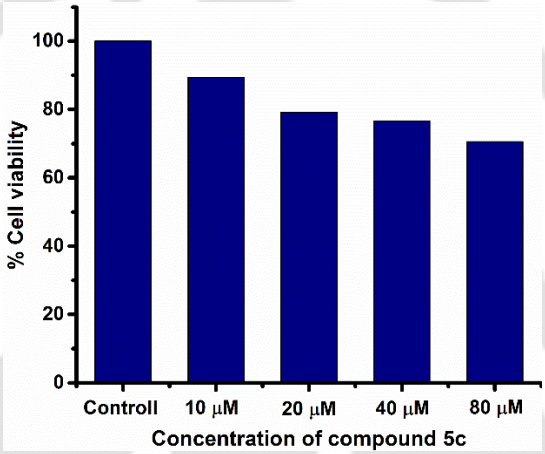

Figure 5.6 Cytotoxicity of compound **5c** to A-549 cell lines.

5.3 Experimental section

5.3.1 Instrumentation and characterization

All chemicals were purchased commercially from reputed sources and used directly. All synthesized compounds were purified via column chromatography by using silica gel (60-120 mesh). The reactions were monitored, by thin-layer chromatography (TLC) using silica gel 60 F254 (0.25 mm) precoated glass-backed TLC plates. All the ^{1}H NMR and ^{13}C NMR spectra were recorded with Brucker spectrometer by 600 and 150 MHz, respectively. $CDCl_3$, DMSO-d_6 and were utilized as solvents for recording NMR spectra with tetramethysilane (TMS) as an internal standard. The chemical shifts (δppm) and coupling constants (*J*) were presented in parts per million (ppm) and Hertz (Hz), respectively. The abbreviations, used for designating the peak multiplicities, were as

follows: s (singlet), d (doublet), t (triplet), m (multiplet) and br (broadened). Agilent Q-TOF mass spectrometer with Z-spray source was employed for the acquisition of high-resolution mass spectra (HRMS). The obtained HRMS data was analyzed by built-in software. For all the experiments of hydrogel preparation, Millipore water was used. FESEM was carried out in a SIGMA 300 instrument. UV-Vis and fluorescence experiments were done by using Perkin Elmer UV-Vis spectrophotometer and Horiba scientific Fluoromax-4 spectrofluorometer, respectively.

5.3.2 Synthetic procedure of compounds 2a-5c

A. Synthesis of prodrug (4-((5-fluoro-2,4-dioxo-3,4-dihydropyrimidin-1(2H)-yl) methyl)-3-nitrobenzoic acid) (2a): The prodrug of 5-Fu (**2a**) according to the protocol described in section 2.4.1A.[14]

B. Synthesis of *tert*-butyl (2-aminoethyl)carbamate (5a): The synthesis of compound **5a** was achieved by reported procedure.[28] Briefly, ethylenediamine (963 mg, 16 mmol) was reacted with di-*tert*-butyl dicarbonate (500 mg, 2.3 mmol) using chloroform as solvent. Di-*tert*-butyl dicarbonate was dissolved in chloroform and added slowly to the ethylenediamine solution in the same solvent under cold condition. After the addition, the mixture was brought into room temperature and kept under stirring, overnight. The progression of the reaction was checked by TLC and after completion of the reaction, the solvent was evaporated in rotavapor and the crude mixture was further purified by column chromatography using 1:10 MeOH/ $CHCl_3$. The product was obtained as a light yellow liquid (1.8 g, 71%). ^{1}H NMR (600 MHz, $CDCl_3$) δ 4.99 (s, 2H), 3.17 (d, J = 5.1 Hz, 5H), 2.79 (t, J = 5.7 Hz, 4H), 1.60 (s, 5H), 1.44 (s, 22H); ^{13}C NMR (150 MHz, $CDCl_3$) δ 156.2, 77.2, 77.0, 76.8, 41.9, 28.4, 28.4. HRMS (ESI) calc. for $C_7H16N_2O_2$ $[M + H]^+$: 161.1285, found: 161.1291.

C. Synthesis of *tert*-butyl (2-(5-(2-oxohexahydro-1H-thieno[3,4-d]imidazol-4-yl)pentanamido)ethyl)carbamate (5b): Compound **5b** was synthesized from compound **5a** (200 mg, 1.25 mmol) and biotin (305 mg, 1.25 mmol) utilizing amide coupling method. *N*,*N*,*N*′,*N*′-Tetramethyl-*O*-(1*H*-benzotriazol-1-yl)uronium hexafluorophosphate (HBTU, 616 mg, 1.62 mmole) and *N*, *N*-Diisopropylethylamine (DIPEA, 242 mg, 1.87 mmole)

was used as coupling reagent and base respectivly. The reaction mixture was stirred overnight in room temperature. After completion of the reaction, the crude reaction mixture was purified by column chromatography by using 1:10 MeOH/$CHCl_3$ solvent system. The product was obtained as white powder (255 mg, 52.7%). ^{1}H NMR (400 MHz, DMSO-d_6) δ 7.79 (s, 1H), 6.78 (s, 1H), 6.43 (s, 1H), 6.36 (s, 1H), 4.34 – 4.26 (m, 1H), 4.17 – 4.09 (m, 1H), 3.13 – 3.01 (m, 3H), 3.01 – 2.92 (m, 2H), 2.82 (dd, *J* = 12.4, 5.1 Hz, 1H), 2.58 (d, *J* = 12.4 Hz, 1H), 2.04 (t, *J* = 7.4 Hz, 2H), 1.66 – 1.57 (m, 1H), 1.49 (dd, *J* = 14.4, 6.4 Hz, 3H), 1.38 (s, 9H), 1.29 (dd, *J* = 14.0, 7.6 Hz, 2H); ^{13}C NMR (150 MHz, DMSO-d_6) δ 172.7, 163.2, 156.1, 78.1, 61.5, 59.7, 55.9, 40.5, 40.4, 40.3, 40.2, 40.1, 40.0, 39.8, 39.7, 39.5, 39.1, 35.7, 28.7, 28.5, 25.7. HRMS (ESI) calcd. for $C_{17}H_{30}N_4O_4S$ $[M + H]^+$: 387.2061, found: 387.2061.

D. Synthesis of 4-((5-fluoro-2,4-dioxo-3,4-dihydropyrimidin-1(2*H*)-yl)methyl)-3-nitro-*N*-(2-(5-(2-oxohexahydro-1*H*-thieno[3,4-d]imidazol-4-yl)pentanamido)ethyl)benzamide (5c): For preparing compound **5c**, first compound **5b** was deprotected by using 30% TFA in dichloromethane (DCM) to make free the amine group for further coupling reaction. After that, the deprotected compound (100 mg, 0.35 mmol) was coupled with compound **2a** (108 mg, 0.35 mmol) by using HBTU (172 mg, 0.45 mmol) and DIPEA (68 mg, 0.52 mmol) assisted standard coupling reaction. The reaction was completed after stirring the reaction mixture for 12 hours at room temperature. The reaction mixture was then extracted with ethyl acetate and the organic layer was dried over sodium sulfate. The obtained crude product was further purified by column chromatography using 1:10 MeOH/ $CHCl_3$ solvent system producing a pale yellow colored compound **5c** (90 mg, 44.7%). ^{1}H NMR (600 MHz, DMSO-d_6) δ 11.99 (s, 1H), 8.89 (s, 1H), 8.56 (s, 1H), 8.17 – 8.11 (m, 2H), 7.96 (t, *J* = 5.5 Hz, 1H), 7.53 (d, *J* = 8.1 Hz, 1H), 6.44 (s, 1H), 6.38 (s, 1H), 5.22 (s, 2H), 4.32 – 4.27 (m, 1H), 4.10 (s, 1H), 3.33 (d, *J* = 6.1 Hz, 2H), 3.23 (d, *J* = 6.0 Hz, 2H), 3.06 (s, 1H), 2.80 (dd, *J* = 12.4, 5.0 Hz, 1H), 2.56 (d, *J* = 12.4 Hz, 1H), 2.06 (t, *J* = 7.2 Hz, 2H), 1.62 – 1.54 (m, 1H), 1.54 – 1.47 (m, 2H), 1.47 – 1.40 (m, 1H), 1.31 – 1.25 (m, 2H); ^{13}C NMR (150 MHz, DMSO-d_6) δ 172.9, 164.4, 163.2, 158.2 (d, C-4, $J_{C\text{-}F}$ = 27 Hz), 150.3, 147.8, 141.4 (s, C-5, $J_{C\text{-}F}$ = 228 Hz), 135.2, 133, 130.5 (d, C-6, $J_{C\text{-}F}$ = 34 Hz), 129, 124.2, 61.4, 59.6, 55.8, 49, 40.5, 38.4,

35.7, 28.6, 28.5, 25.7. For confirming the mass of the compound matrix-assisted laser desorption/ionization-time of flight (MALDI-TOF) mass spectrometry (Autoflex speed, Bruker, Germany) was used. Compound **5c** was dissolved in a solvent mixture of acetonitrile: water (7:3) with 0.1% formic acid for the MALDI-TOF analysis. The analysis was carried out without using a matrix.

5.3.3 Preparation of hydrogel

The hydrogel was prepared from compound **5c** in a pH-dependent manner. 20 mg of compound **5c** was kept in 5 mL glass vial and 500 µL distilled water was added to that. Then the compound was made soluble in water by adding 120 µL of 2(N) NaOH. Finally, the pH of the solution was adjusted to 7.0 by adding 62 µL of 4(N) HCl slowly and the volume of the total solution was made 1 mL by adding distilled water. The solution was heated and vortexed to dissolve the compound completely and then cooled down to room temperature slowly. After 3 hours, the formation of the gel was confirmed by vial inversion test.

5.3.4 FESEM Analysis

The hydrogel was lyophilized and the dried gel was employed for FESEM analysis. A small amount of the xerogel was placed on carbon tape and coated with gold before the analysis.

5.3.5 The Molecular Orientation by FTIR and ^{1}H NMR Analysis

To explore the molecular orientation of compound **5c** during hydrogel formation, the xerogel was further utilized for FTIR analysis and it was compared with the FTIR of the compound in powder form. The ^{1}H NMR experiment was carried out with preparing different samples by dissolving compound **5c** in different ratios of DMSO-d_6 and water. The samples contained 10%, 20%, 30%, 40%, 50% water respectively. The change in chemical shifts of the characteristic protons was evaluated by recording ^{1}H NMR of all the samples and comparing them.

5.3.6 Irradiation experiment of 5-Fu-biotin

To examine the 5-Fu release from compound **5c** irradiation experiment was carried out and monitored by UV-Vis spectrometry and ^{1}H NMR. For both occasion 365 nm, LED light of 24 W was used. The UV-Vis experiment was performed by irradiating a 50 µM of compound **5c** solution in acetonitrile and measuring the change in absorption after certain intervals of 5, 15, 45, 65, 85, 105, 125 minutes by a Perkin Elmer UV-Vis spectrophotometer. For the ^{1}H NMR experiment, 3 mg of compound **5c** was dissolved in 600 µL of DMSO-d_6 and the solution was subjected to irradiation under 365 nm light. The change in chemical structure and uncaging of active 5-Fu was monitored by taking ^{1}H NMR of the solution after 4 and 6 hours of irradiation.

5.3.7 Doxorubicin loading and release study

In 0.5 mL of 20 µM aqueous solution of doxorubicin hydrochloride (DOX), the hydrogelator **5c** was allowed to form gel. The obtained gel was subjected for investigation of DOX release study by placing 0.5 mL of PBS (7.4) above the gel. The water, above the gel, was monitored by fluorescence with an excitation wavelength of 488 nm and collecting the emission at 590 nm for the estimation of released DOX. After recording the fluorescence, the same water was again placed over the gel. This process was continued for 2 days.

5.3.8 Measurement of Cytotoxicity by MTT assay

The cytotoxicity of compound **5c** was measured by MTT assay in A-549 cell lines, obtained from National Centre for Cell Sciences (NCCS), Pune, India. In a 96-well microplate, 5x10^3 cells were seeded using 90 µL Dulbecco's modified Eagle's medium (DMEM) and were incubated for 24 hours at 37˚C in presence of 5% CO_2. After that cells were treated with different concentrations of compound **5c** (10, 20, 40, 80 µM) and again kept in incubation. After 48 hours MTT was added to the wells and kept in incubation for 2 hours at 37˚C. Then after removing the medium, 60 µL of DMSO was added to produce formazan that showed absorption (A) at 570 nm. The optical density (OD) of each well-plate was measured with the background reference at 690 nm. All the tests were performed in sextets. The control experiment was also carried out similarly but without the addition

of **5c**. The percentage cell viability with respect to the control was calculated by using the standard formula as given below.

$$\%\ of\ cell\ viability = \frac{(A_{570} - A_{690})\ of\ treated\ cells}{(A_{570} - A_{690})\ of\ control\ cells} \times 100\ \%$$

5.4 Conclusion

In conclusion, this report provides the design and synthesis of a target-specific self-delivery hydrogel, consisting of the drug (5-Fu) itself tethered with the targeting agent, biotin. The conjugation of biotin and 5-Fu was achieved by using ethylenediamine and a photocleavable *o*-nitrobenzyl moiety which allowed the photo-responsive release of 5-Fu. The hydrogel was also shown to entrap another water-soluble drug DOX. The results demonstrated the photo-controlled release of 5-Fu from the synthesized compound as well as sustained release of DOX from the hydrogel. Thus, this system can be useful for drug delivery purpose as a stimuli-responsive dual drug carrier.

5.5 References

1. Hoare, T. R.; Kohane, D. S., Hydrogels in drug delivery: Progress and challenges. *Polymer* **2008,** *49* (8), 1993-2007.

2. Lee, K. Y.; Mooney, D. J., Hydrogels for tissue engineering. *Chem. Rev.* **2001,** *101* (7), 1869-1880.

3. Obara, K.; Ishihara, M.; Ishizuka, T.; Fujita, M.; Ozeki, Y.; Maehara, T.; Saito, Y.; Yura, H.; Matsui, T.; Hattori, H., Photocrosslinkable chitosan hydrogel containing fibroblast growth factor-2 stimulates wound healing in healing-impaired db/db mice. *Biomaterials* **2003,** *24* (20), 3437-3444.

4. Stapleton, F.; Stretton, S.; Papas, E.; Skotnitsky, C.; Sweeney, D. F., Silicone hydrogel contact lenses and the ocular surface. *Ocul Surf.* **2006,** *4* (1), 24-43.

5. Wang, T.; Wu, D. Q.; Jiang, X. J.; Zhang, X. Z.; Li, X. Y.; Zhang, J. F.; Zheng, Z. B.; Zhuo, R.; Jiang, H.; Huang, C., Novel thermosensitive hydrogel injection inhibits post-infarct ventricle remodelling. *Eur. J. Heart Fail.* **2009,** *11* (1), 14-19.

6. Tian, R.; Chen, J.; Niu, R., The development of low-molecular weight hydrogels for applications in cancer therapy. *Nanoscale* **2014,** *6* (7), 3474-3482.

7. Peppas, N.; Bures, P.; Leobandung, W.; Ichikawa, H., Hydrogels in pharmaceutical formulations. *Eur. J. Pharm. Biopharm.* **2000,** *50* (1), 27-46.

8. Latxague, L.; Ramin, M. A.; Appavoo, A.; Berto, P.; Maisani, M.; Ehret, C.; Chassande, O.; Barthélémy, P., Control of stem-cell behavior by fine tuning the supramolecular assemblies of low-molecular-weight gelators. *Angew. Chem. Int. Ed.* **2015,** *54* (15), 4517-4521.

9. Vemula, P. K.; Cruikshank, G. A.; Karp, J. M.; John, G., Self-assembled prodrugs: An enzymatically triggered drug-delivery platform. *Biomaterials* **2009,** *30* (3), 383-393.

10. Yang, X.; Zhang, G.; Zhang, D., Stimuli responsive gels based on low molecular weight gelators. *J. Mater. Chem.* **2012,** *22* (1), 38-50.

11. Wang, H.; Yang, Z., Molecular hydrogels of hydrophobic compounds: a novel self-delivery system for anti-cancer drugs. *Soft Matter* **2012,** *8* (8), 2344-2347.

12. Zhao, F.; Ma, M. L.; Xu, B., Molecular hydrogels of therapeutic agents. *Chem. Soc. Rev.* **2009,** *38* (4), 883-891.

13. SunnyáAbbah, A.; WilliamáLu, W., D-glucosamine-based supramolecular hydrogels to improve wound healing. *Chem. Commun.* **2007,** (8), 843-845.

14. Das, S.; Horo, H.; Goswami, U.; Kundu, L. M., Synthesis of a Peptide Conjugated 5-Fluorouracil Gelator Prodrug for Photo-Controlled Release of the Antitumor Agent. *ChemistrySelect* **2019,** *4* (22), 6778-6783.

15. Bhuniya, S.; Park, S. M.; Kim, B. H., Biotin− Amino Acid Conjugates: An Approach Toward Self-Assembled Hydrogelation. *Org. Lett.* **2005,** *7* (9), 1741-1744.

16. Huang, P.; Wang, D.; Su, Y.; Huang, W.; Zhou, Y.; Cui, D.; Zhu, X.; Yan, D., Combination of small molecule prodrug and nanodrug delivery: amphiphilic drug–drug conjugate for cancer therapy. *J. Am. Chem. Soc.* **2014,** *136* (33), 11748-11756.

17. Wang, Y.; Cheetham, A. G.; Angacian, G.; Su, H.; Xie, L.; Cui, H., Peptide–drug conjugates as effective prodrug strategies for targeted delivery. *Adv. Drug Deliv. Rev.* **2017,** *110*, 112-126.

18. Ren, W. X.; Han, J.; Uhm, S.; Jang, Y. J.; Kang, C.; Kim, J.-H.; Kim, J. S., Recent development of biotin conjugation in biological imaging, sensing, and target delivery. *Chem. Commun.* **2015,** *51* (52), 10403-10418.

19. Joshi, K. e. B.; Verma, S., Ditryptophan conjugation triggers conversion of biotin fibers into soft spherical structures. *Angew. Chem. Int. Ed.* **2008,** *47* (15), 2860-2863.

20. Ye, X.; Li, X.; Shen, Y.; Chang, G.; Yang, J.; Gu, Z., Self-healing pH-sensitive cytosine-and guanosine-modified hyaluronic acid hydrogels via hydrogen bonding. *Polymer* **2017,** *108*, 348-360.

21. Sivakova, S.; Rowan, S. J., Nucleobases as supramolecular motifs. *Chem. Soc. Rev.* **2005,** *34* (1), 9-21.

22. Suzuki, M.; Yumoto, M.; Kimura, M.; Shirai, H.; Hanabusa, K., A Family of Low-Molecular-Weight Hydrogelators Based on L-Lysine Derivatives with a Positively Charged Terminal Group. *Chem. Eur. J.* **2003,** *9* (1), 348-354.

23. Rabenstein, D. L., Nuclear magnetic resonance studies of the acid-base chemistry of amino acids and peptides. I. Microscopic ionization constants of glutathione and methylmercury-complexed glutathione. *J. Am. Chem. Soc.* **1973,** *95* (9), 2797-2803.

24. Berl, V.; Huc, I.; Khoury, R. G.; Krische, M. J.; Lehn, J.-M., Interconversion of single and double helices formed from synthetic molecular strands. *Nature* **2000,** *407* (6805), 720-723.

25. Suzuki, M.; Yumoto, M.; Kimura, M.; Shirai, H.; Hanabusa, K., Hydrogel Formation Using New L-Lysine-Based Low-Molecular-Weight Compounds with Positively Charged Pendant Chains. *Helv. Chim. Acta* **2003,** *86* (6), 2228-2238.

26. Il'ichev, Y. V.; Schwörer, M. A.; Wirz, J., Photochemical reaction mechanisms of 2-nitrobenzyl compounds: methyl ethers and caged ATP. *J. Am. Chem. Soc.* **2004,** *126* (14), 4581-4595.

27. Suarasan, S.; Craciun, A.-M.; Licarete, E.; Focsan, M.; Magyari, K.; Astilean, S., Intracellular Dynamic Disentangling of Doxorubicin Release from Luminescent Nanogold Carriers by Fluorescence Lifetime Imaging Microscopy (FLIM) under Two-Photon Excitation. *ACS Appl. Mater. Interfaces* **2019,** *11* (8), 7812-7822.

28. Komiyama, M.; Aiba, Y.; Ishizuka, T.; Sumaoka, J., Solid-phase synthesis of pseudo-complementary peptide nucleic acids. *Nat. Protoc.* **2008,** *3* (4), 646-654.

5.6 NMR and HRMS spectra of synthesized compounds.

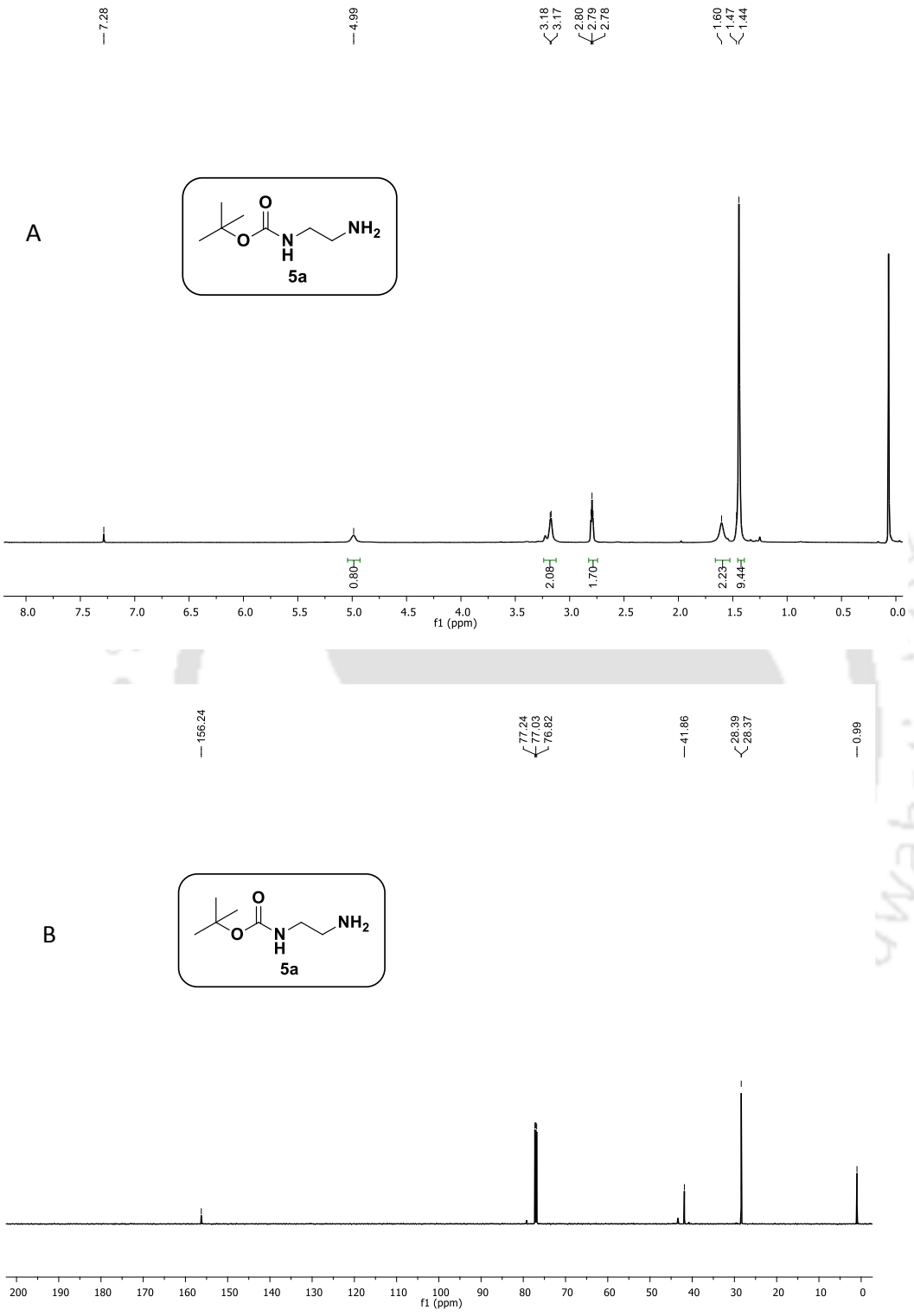

^{1}H (A) and ^{13}C (B) spectra of compound **5a.**

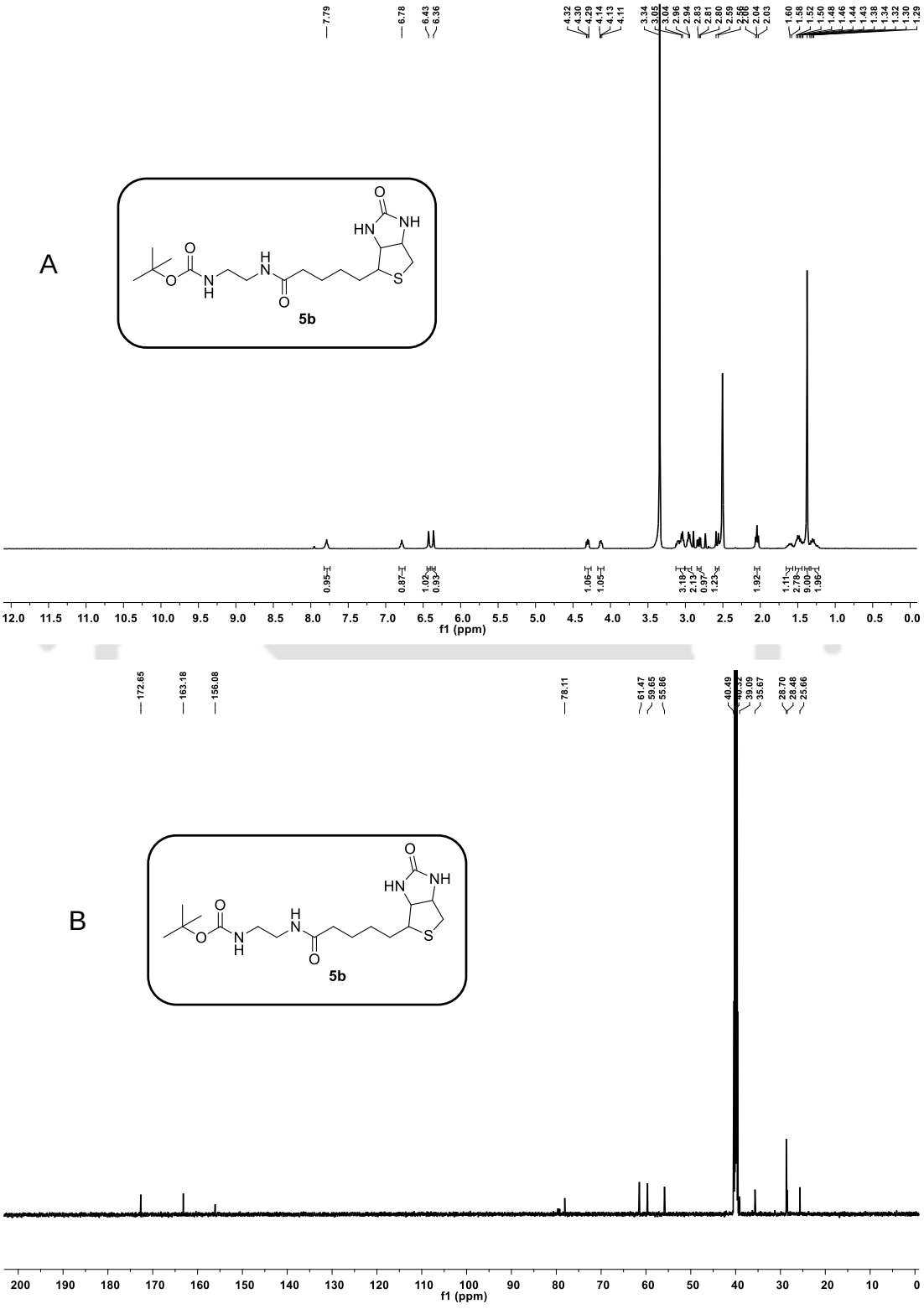

^{1}H (A) and ^{13}C (B) spectra of compound **5b.**

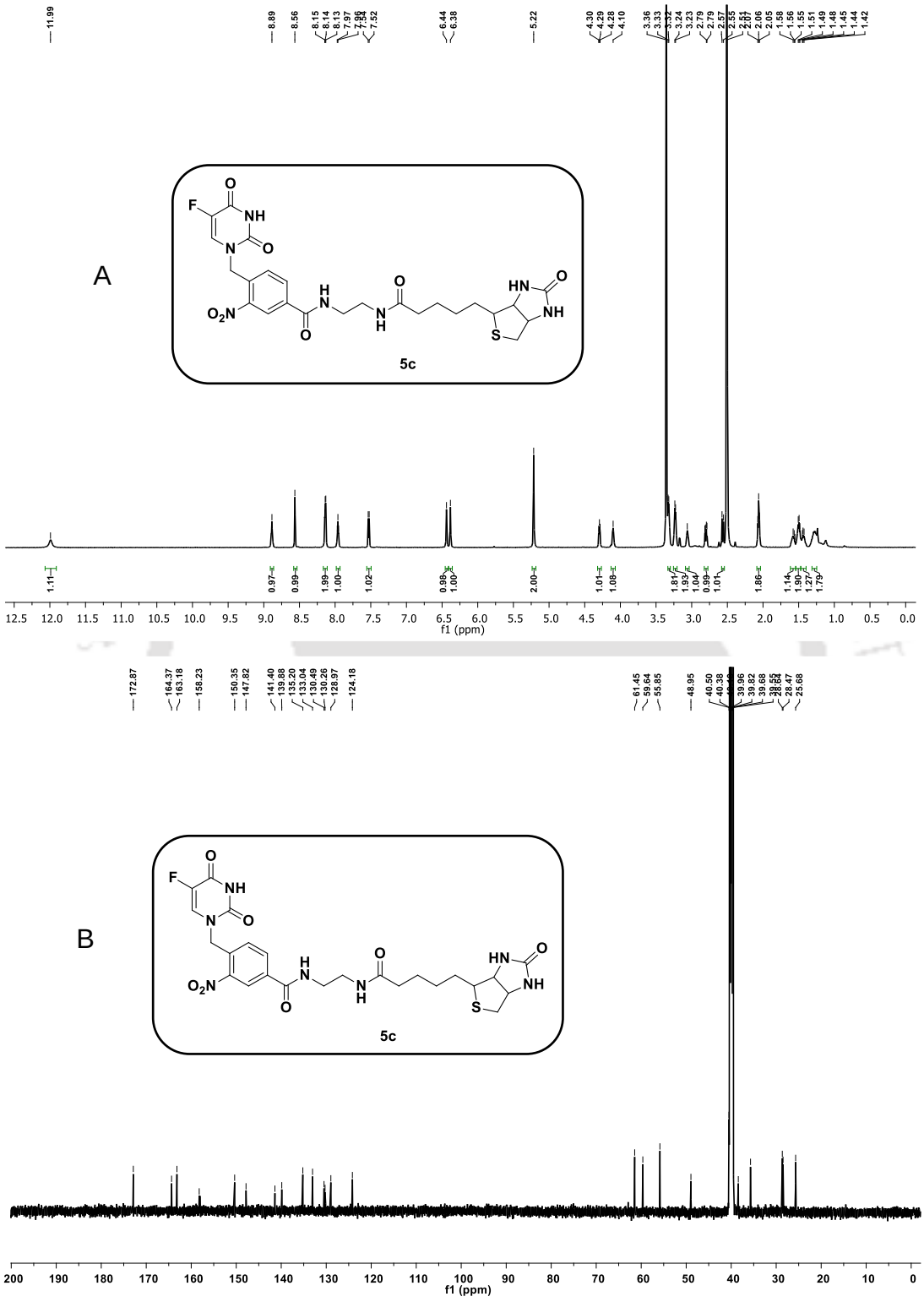

^{1}H (A) and ^{13}C (B) spectra of compound **5c.**

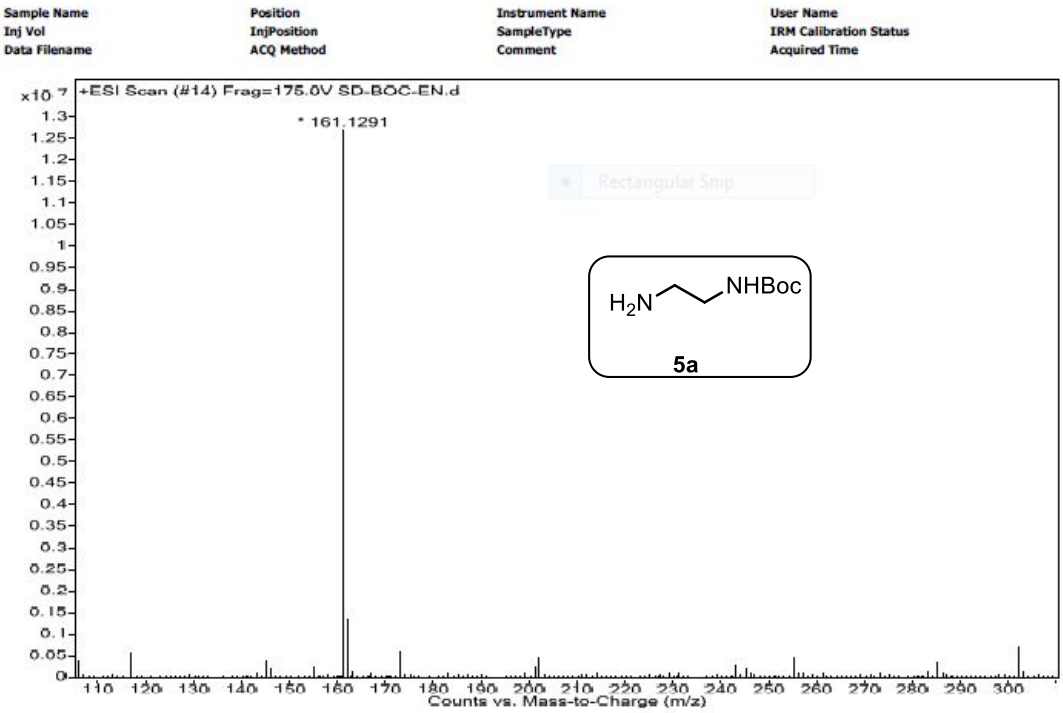

HRMS spectra of compound **5a**

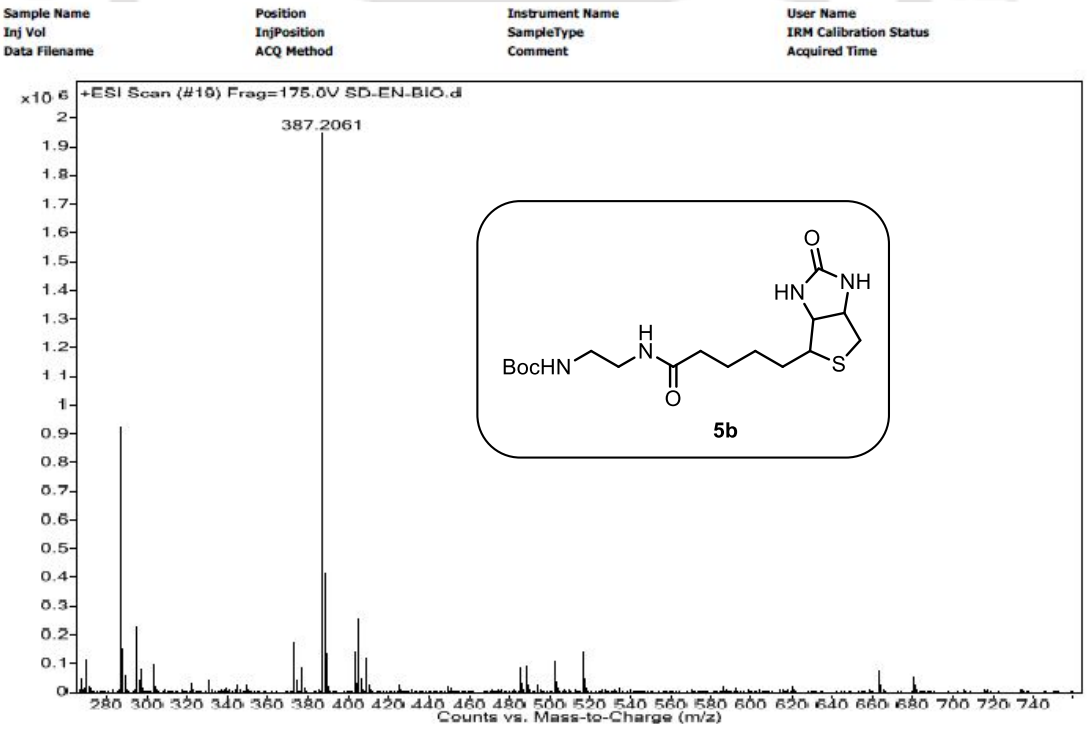

HRMS spectra of compound **5b.**

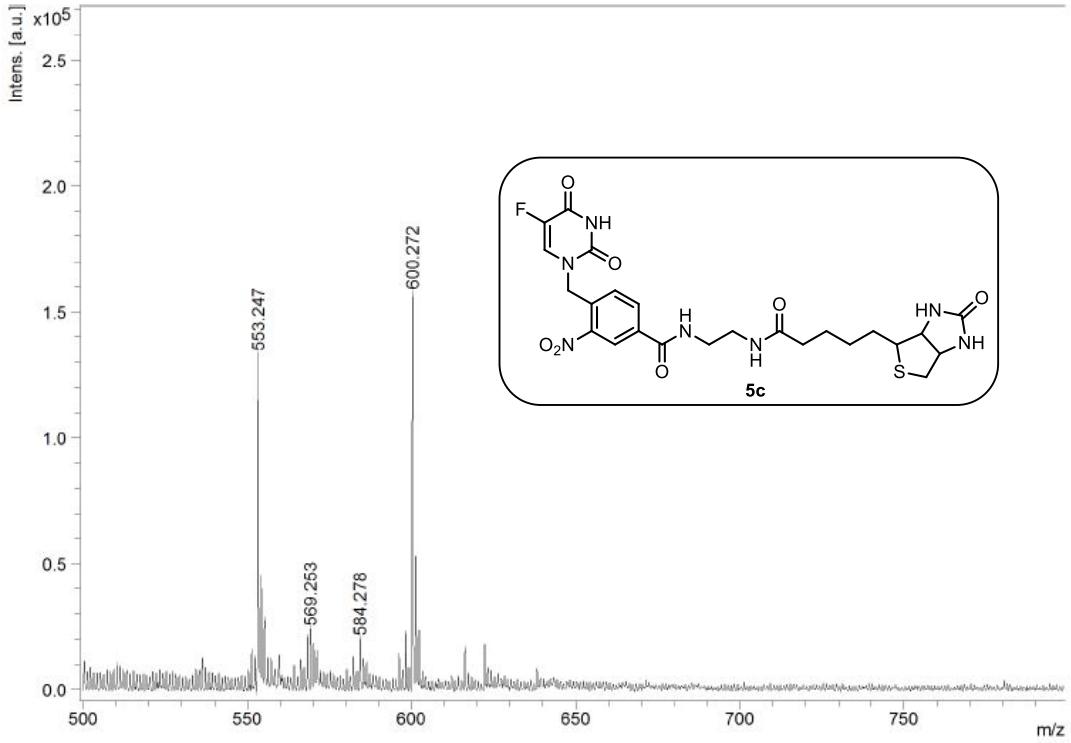

Mass spectra of compound **5c.**

^{1}H NMR Spectra of Hydrogen Bonding Experiment

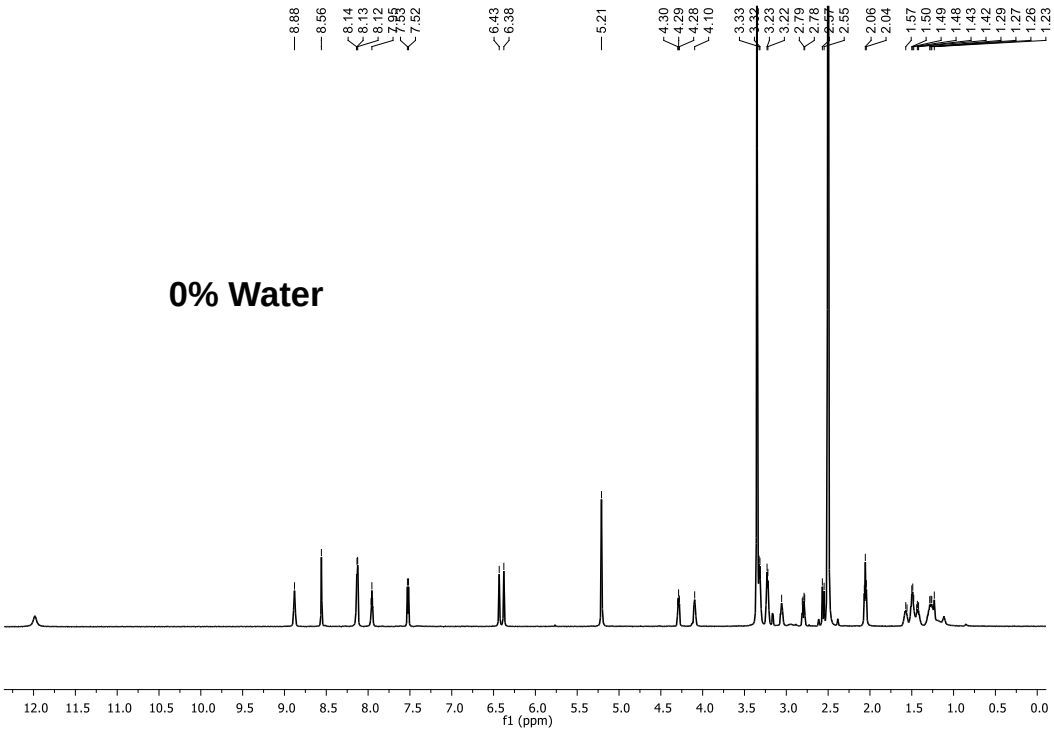

^{1}H NMR spectra of compound **5c** in 0% water in DMSO-d_6.

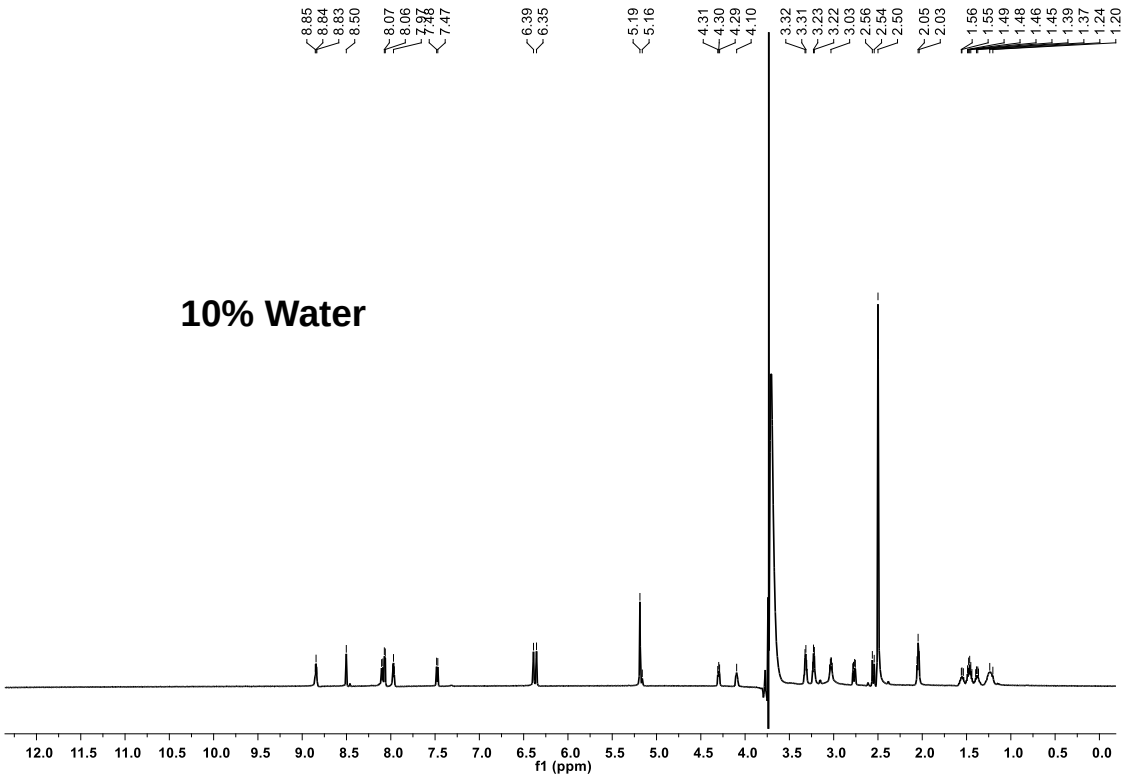

^{1}H NMR spectra of compound **5c** in 10% water in DMSO-d_{6}.

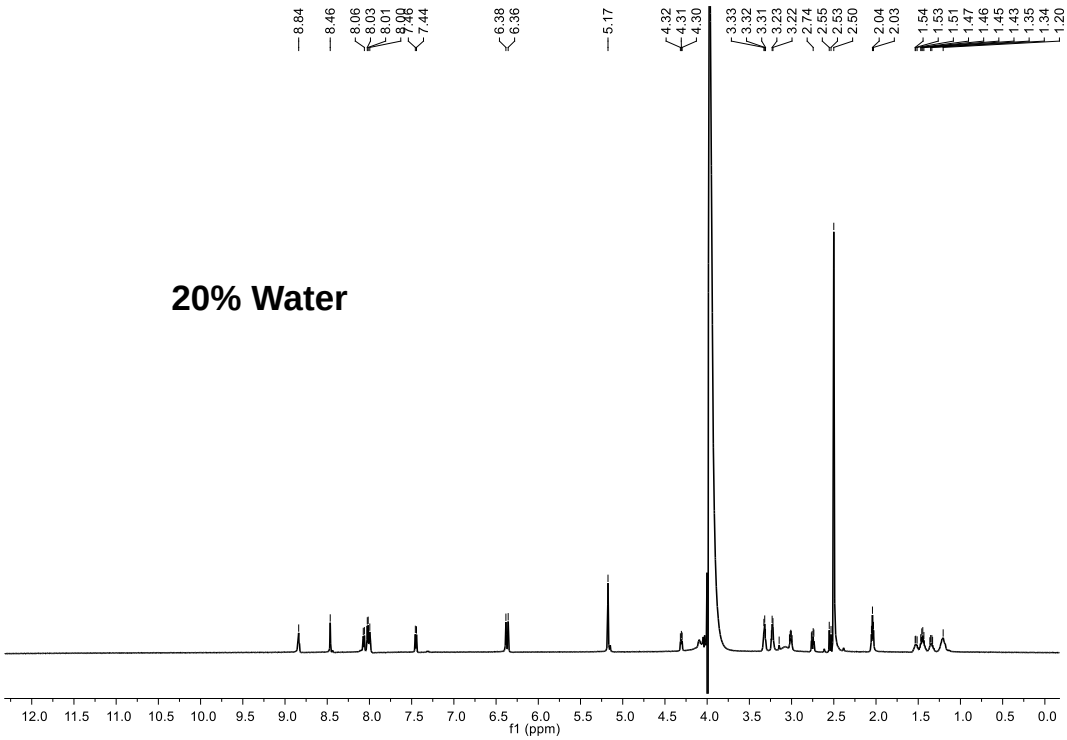

^{1}H NMR spectra of compound **5c** in 20% water in DMSO-d_{6}.

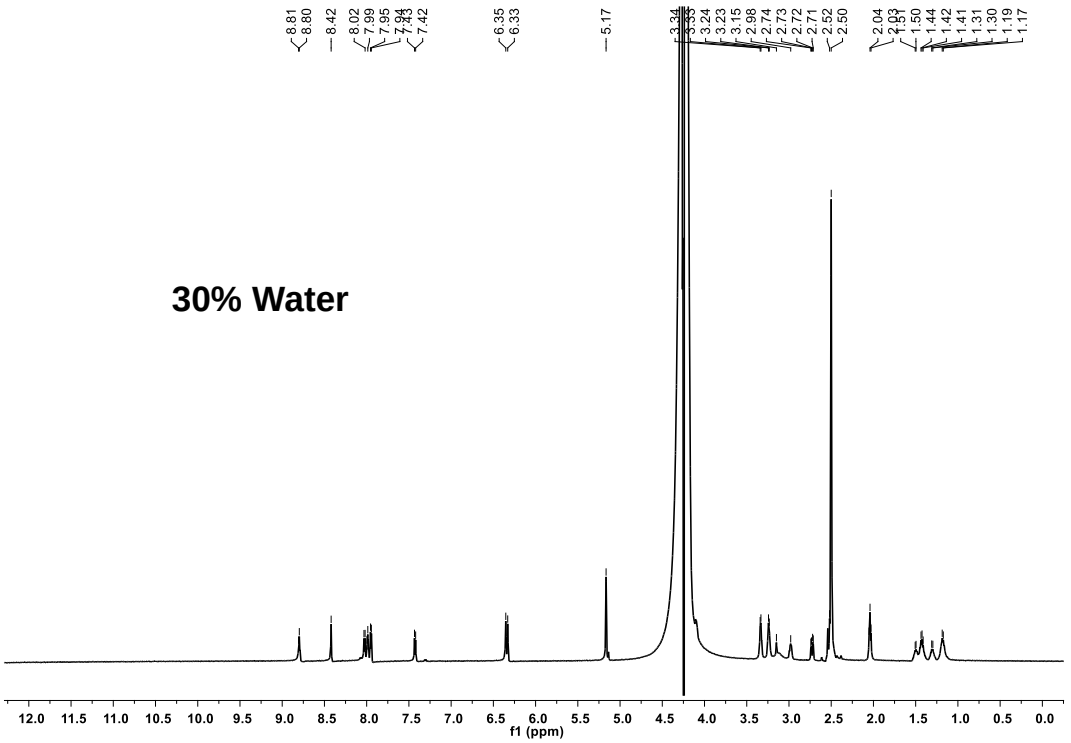

^{1}H NMR spectra of compound **5c** in 30% water in DMSO-d_6.

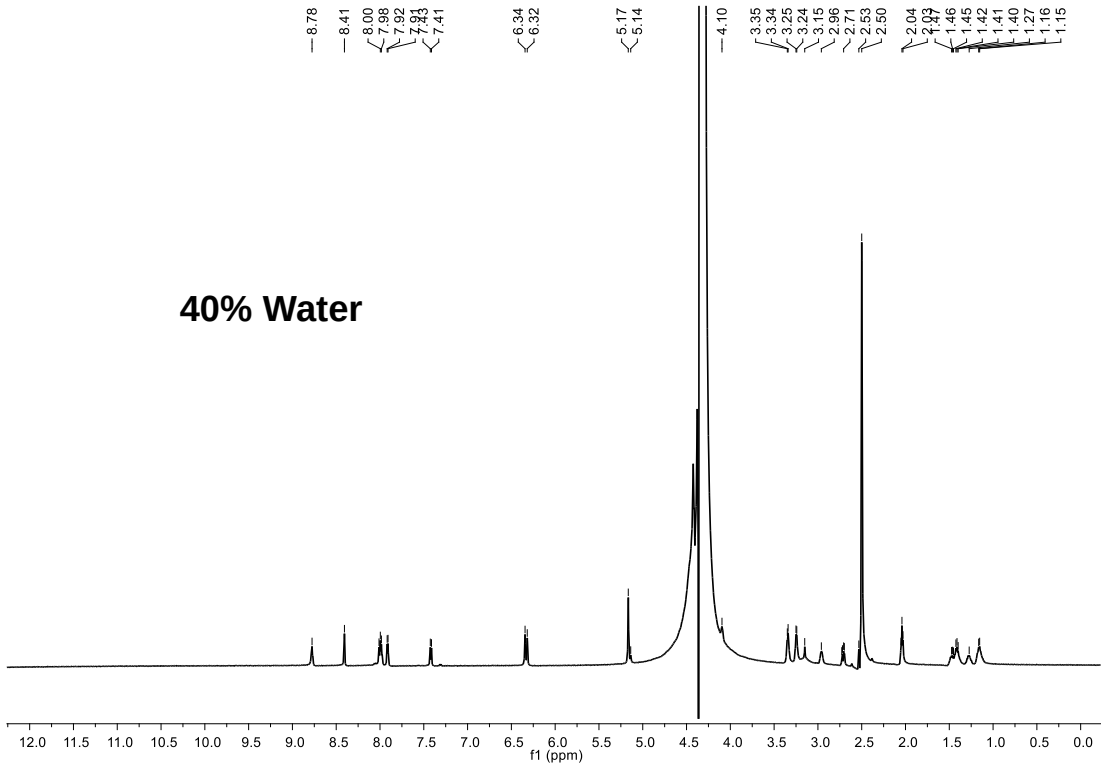

^{1}H NMR spectra of compound **5c** in 40% water in DMSO-d_6.

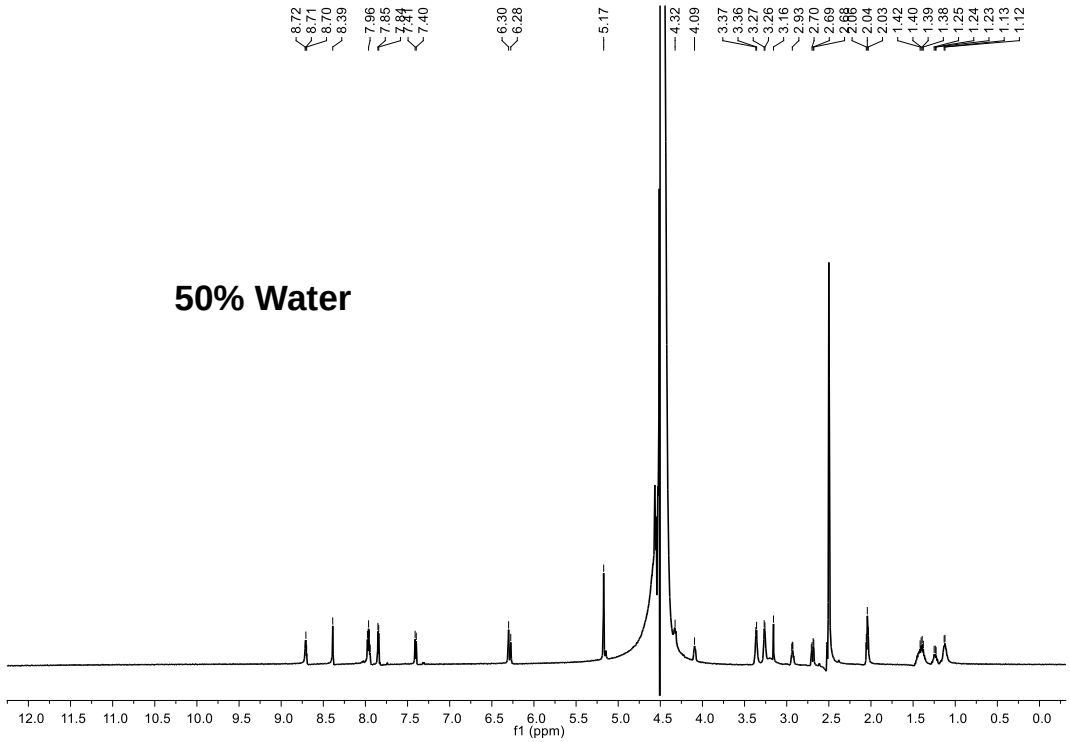

^{1}H NMR spectra of compound **5c** in 50% water in DMSO-d_6.

^{1}H NMR Spectra During Irradiation Experiment

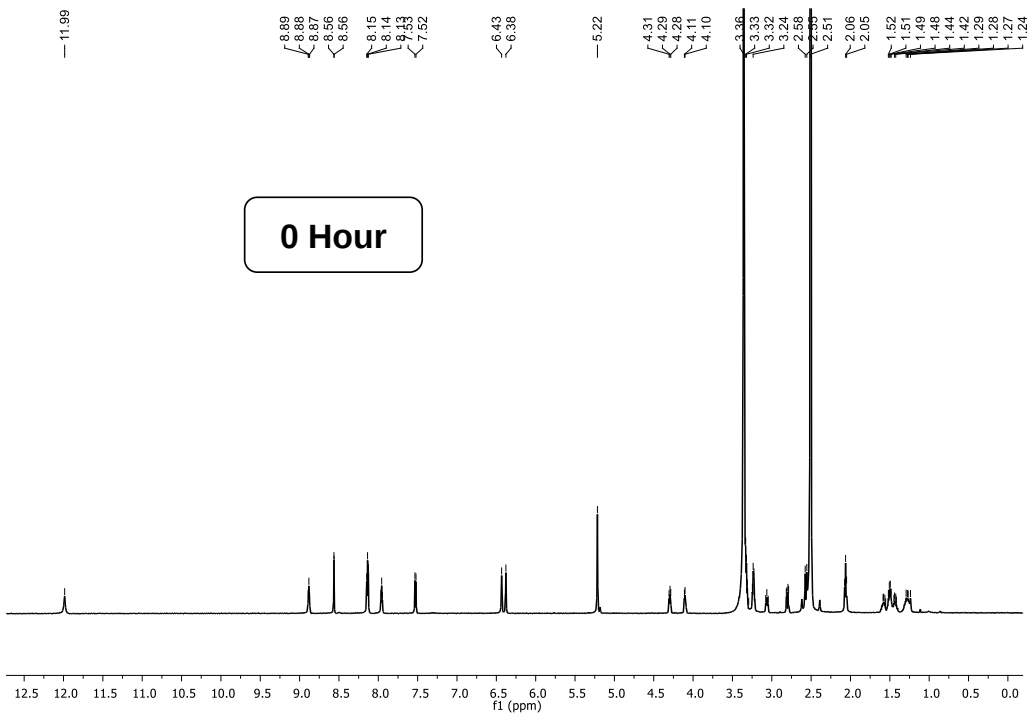

^{1}H NMR spectra of compound **5c** before irradiation.

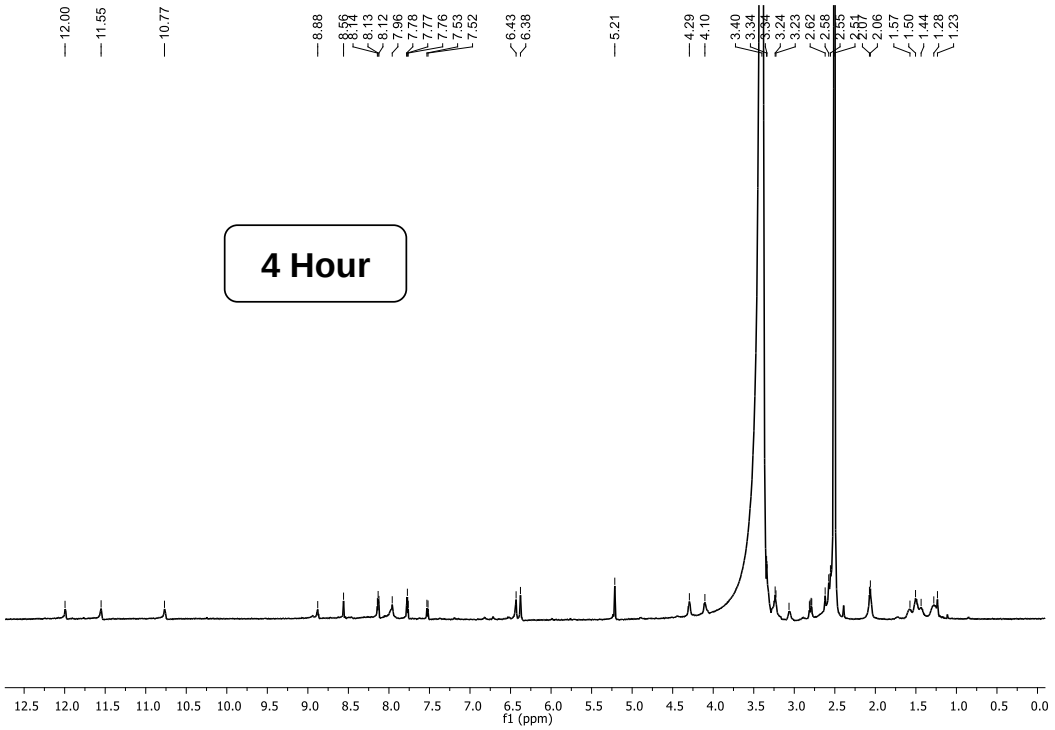

^{1}H NMR spectra of compound **5c** after 4 hours of irradiation.

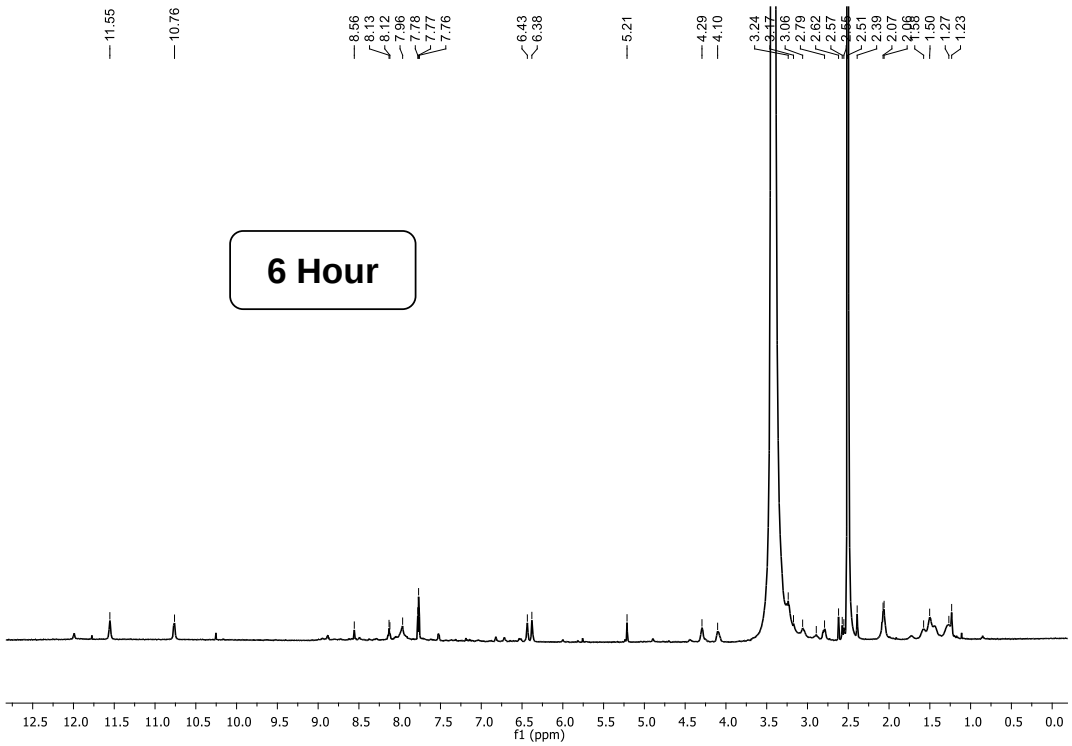

^{1}H NMR spectra of compound **5c** after 6 hours of irradiation.

Chapter 6: Summary and Future Prospects

6.1 Research Summary

This report provides a detailed description of the DDS developed for anticancer treatment. Most of the existed anticancer drugs have severe side effects due to their lack of nonspecific absorption and many other factors. DDS was introduced to achieve the optimum potency of these drugs by reducing all these problems. With the evolution of drug delivery research, nanomedicines have gained ardent recognition. Several nanomaterial-based chemotherapeutics have already found its utilization in clinical purposes. Recently, one component nanomedicines constructed with self-assembling drug conjugates have emerged as exceptionally beneficial to be used in chemotherapy for their better stability, drug release profile and a lot more advantages.

In this report, we have developed peptide and small molecule-based drug conjugate amphiphiles. We have successfully synthesized them mostly by convergent method of synthesis. The self-assembly properties of the synthesized conjugates were also investigated extensively. Furthermore, we have developed procedure to modulate the self-assembly of the molecules to generate various nanostructures such as fibers, nanoparticles etc. Most of the prepared nanomaterials were designed in such a way that they were capable of acting as a dual drug carrier. The successful release of the active drugs from the conjugates was also studied minutely in *in vivo* and *in vitro* condition. Additionally, the non-toxic nature of our synthesized molecules in the absence of the stimulation was studied in cancer cell lines. Overall, our experimental results propose that the synthesized amphiphiles can be of importance to study activities of potential therapeutic agents. However, further modifications can be done to improve their targeting efficiency and more extensive biological studies are also required for their fruitful clinical use.

6.2 Future prospects

This report provides the primary investigation of a few models of drug conjugates based small molecular DDS. However, various detailed biological studies would be essential for their effective use in therapeutic purpose for cancer treatment. More improvement

will be required for these molecules in terms of their targeting efficiency and drug loading capability.

List of Publications

1. **Soumi Das**, Krishan Kumar Thakur, Ajaikumar B Kunnumakkara and Lal Mohan Kundu*, "Development of a biotin-drug conjugate hydrogelator for the targeted and controlled delivery of 5-Fluorouracil." submitted.
2. **Soumi Das**, Kamlesh Verma, Vikash Kumar Dubey and Lal Mohan Kundu*, "Synthesis and fabrication of nanoparticles from an enzyme-cleavable, palmitic acid 5-Fluorouracil conjugate for dual responsive dual drug delivery" submitted.
3. **Soumi Das**, Kamlesh Verma, Vikash Kumar Dubey and Lal Mohan Kundu*, "Fabrication of a 5-Fluorouracil conjugated peptide nanoparticles as a versatile, stimuli-responsive dual drug carrier with high antiproliferation activity" *Biorg. Chem*. **2019**, just accepted.
4. **Soumi Das**, Himali Horo, Upasi Goswami and Lal Mohan Kundu*, "Synthesis of a peptide conjugated 5- Fluorouracil gelator prodrug for photo- controlled release of the antitumor agent" *ChemistrySelect* **2019**, *4*, 6778 –6783.
5. Himali Horo, **Soumi Das**, Bishnupada Mandal and Lal Mohan Kundu*, "Development of a photoresponsive chitosan conjugated prodrug nano-carrier for controlled delivery of antitumor drug 5-fluorouracil" *Int.J.Biol.Macromol.* **2019**, *121*, 1070-1076.
6. **Soumi Das**, Himali Horo and Lal Mohan Kundu*, "Biopolymers and peptide based materials for targeted antitumor drug delivery: an overview" *Nov Appro Drug Des Dev* **2018**, *4*(4),555643.
7. K Radhakrishnan, **Soumi Das** and Lal Mohan Kundu*, "Synthesis of size-expanded nucleobase analogues for artificial base-pairing using a ligand-free, microwave-assisted copper(I)-catalyzed reaction" *ChemistrySelect* **2018**, *3*(46), 13098-13102.

List of Poster Presentations

1. S. Das, L. M. Kundu "Fatty acid based Drug Conjugate: A Potent Drug Delivery System" *Frontiers in Chemical Sciences*, 6-8th December, **2018**, IIT Guwahati, Assam, India.
2. S. Das, L. M. Kundu "Dual Drug Delivery by a Lipid Drug Conjugate Nanoparticle" International Conference on *Emerging Trends in Chemical Sciences*, 26-28th February, **2018**, Department of Chemistry, Dibrugarh University, Assam, India.
3. S. Das, K. Gogoi, L. M. Kundu "Synthesis of photo activated antitumor prodrug containing 5-Fluorouracil for controlled drug delivery" *Research Conclave*, 16-19th March, **2017**, IIT Guwahati, Assam, India.
4. S. Das, L. M. Kundu "Development of a peptide hydrogelator covalently conjugated to a prodrug for controlled release of 5-Fluorouracil" *19th CRSI National Symposium in Chemistry*, 14-16th July, **2016**, North Bengal University (NBU), India.
5. S. Das, L. M. Kundu "Synthesis of photo activated antitumor prodrug containing 5-fluorouracil for targeted drug delivery" *ChemConvene*, 8th April, **2015**, Department of Chemistry, IIT Guwahati.